2009

Mechanistic and Physiological Studies of the Insulin-Dependent Regulation of FOXA2

Jessica Jean Howell

MECHANISTIC AND PHYSIOLOGICAL STUDIES OF THE INSULIN-DEPENDENT REGULATION OF FOXA2

A Thesis Presented to the Faculty of

The Rockefeller University

in Partial Fulfillment of the Requirements for

the degree of Doctor of Philosophy

by

Jessica Jean Howell

June 2009

MECHANISTIC AND PHYSIOLOGICAL STUDIES OF THE INSULIN-DEPENDENT REGULATION OF FOXA2

Jessica Jean Howell, Ph.D.
The Rockefeller University 2009

The Forkhead box A2 transcription factor (Foxa2/HNF-3β) has been shown to be a key regulator of genes involved in the maintenance of glucose and lipid homeostasis in the liver, and is constitutively inactivated in several hyperinsulinemic/obese mouse models, thereby enhancing their metabolic phenotypes. Foxa2 is activated under fasting conditions, but is inhibited by insulin signaling via PI3K/Akt in a phosphorylation-dependent manner, which results in its nuclear exclusion. However, the mechanism and relative importance of nuclear export have not yet been elucidated. In addition, the existence and potential role of insulin-dependent regulation of Foxa2 have not been studied in other tissues where it is expressed, such as the gut, lung, and hypothalamus.

Here we further investigate the regulation of Foxa2 by insulin and the mechanism and relevance of its nuclear exclusion. We demonstrate that differential regulation of Foxa2 exists in different mouse models, that this variability is dependent on circulating insulin levels, and that Foxa2 activity correlates with metabolic function. We further show that Foxa2 contains a functional nuclear export signal and is excluded from the nucleus via a CRM1-

dependent pathway in response to insulin signaling. Our data provide direct evidence that nuclear export-defective Foxa2 is phosphorylated and inactivated by insulin both *in vitro* and *in vivo*, suggesting that phosphorylation itself is the main regulatory event regulating the activity of Foxa2, and not nuclear exclusion *per se*. Finally, we provide evidence for and physiological consequences of insulin-dependent inactivation of Foxa2 in two other metabolic organs: the hypothalamus and the lung.

ACKNOWLEDGMENTS

If I have learned one thing from my time in graduate school (which is not really a fair statement since I have of course learned many things) it is to always expect the unexpected. In life, as in science, one can play the game of forming hypotheses and trying to predict outcomes, but in the end it is the questions asked and the experimental design that determine the value of the undertaking. And, quite often, it is the unexpected results that are the most valuable and the most rewarding.

When I joined the Stoffel lab and prepared my original thesis proposal I had very definite plans for where my life and science was going. Suffice it to say (five years later) that everything, most definitely, did not go according to plan. (The move to Switzerland, of course, epitomizes this finding.) This is not to say that everything went wrong, however. Quite the contrary. I am happy to say that everything turned out very well in the end, and now I have many people to thank.

First and foremost, I would like to thank Markus, not only for keeping my life interesting, but for providing me with a very supportive and educational atmosphere in which to do my PhD. Manuela Hitz provided superb technical assistance, and many helpful mouse training sessions. Additionally she has been a great friend and translator, and has made my time in Switzerland much more enjoyable. I would also like to thank Christian Wolfrum for his expert

advice, patience and unfailing (often irrational) optimism. His scientific guidance and support, coupled with the occasional WCIII game, was invaluable. I'm also very grateful for the support of all of the members of the Stoffel lab who I've had the pleasure of working with over the past several years.

Honorable mention for the role of scientific mentors goes to Celeste Simon and Brian Keith for providing me with the opportunity to work in their lab as an undergraduate, despite my inexperience. They provided a stimulating, instructive and enjoyable environment for my first foray into science, even driving me from Bryn Mawr to Philadelphia so that I could work in the lab on Saturdays. Oh, and for always bringing bagels…

On the same note, I would like to thank Andrew M Arsham (whose middle name is really just M, or so he claims) who had the pleasure of putting up with me in the Simon lab. He taught me most everything I didn't know, (which was most anything) and his advice still haunts me to this day ("Go to law school.").

Last, but not least, I would like to thank my family and friends for their constant love and support, and for putting up with me living 4,000 miles and 6 hours time difference away. I would especially like to thank my parents, Lenard and Nancy Howell, my grandparents, Robert and Virginia Bauer, my sister, Kim and brother, Dustin, and my best friend, and fiancé, Karl Schmitz.

TABLE OF CONTENTS

LIST OF FIGURES

LIST OF TABLES

INTRODUCTION

Globally, diabetes is ranked by the world health organization as the fifth leading cause of death (1). Using data from 2003, the international diabetes foundation estimated that 194 million people, ages 20-79 (roughly 5% of the world's population) have diabetes. An additional 8% show signs of impaired glucose tolerance, a high risk factor for the development of type 2 diabetes (2). With the death rate from diabetes mellitus having increased by 45% from 1987-2002, it is imperative that we understand the underlying causes of this complex disorder (3).

Originally described as nonketotic, or non-insulin-dependent diabetes, type 2 diabetes mellitus is a complex disease characterized by abnormal glucose tolerance and hyperglycemia due to increased insulin resistance in combination with relative insulin deficiency (4). While it has become clear that obesity (5, 6), fat distribution (5), and physical inactivity (6) are all risk factors correlated with the development of type 2 diabetes, the molecular mechanisms connecting these risk factors to the onset of insulin resistance and relative insulin deficiency resulting in type 2 diabetes remain unclear.

Understanding the pathology of diabetes requires an intricate knowledge of the cellular signaling associated with insulin. In mammals, insulin is the main hormone regulating the maintenance of glucose homeostasis. In fasting states there exists a balance between glucose production and tissue uptake and

utilization, such that blood glucose levels are maintained within a narrow range. In response to increased glucose levels, such as after a meal, insulin secreted from pancreatic beta cells induces the uptake of glucose into peripheral tissues and inhibits endogenous glucose production, thus restoring and maintaining normoglycemia. Conversely, in fasting states when glucose and insulin levels are low, and glucagon levels are increased, this suppression is relieved. (7)

The liver plays an essential role in this process of glucose homeostasis and is a main target of insulin action. When insulin levels are high, hepatic programs of gluconeogenesis, glycogenolysis and fatty acid beta oxidation are suppressed (8). Though the effects of insulin are pleitropic and complex, this suppression occurs in large part through the transcriptional inhibition of key rate limiting enzymes in these pathways (9). To this end, the forkhead box A2 transcription factor (Foxa2/HNF3β) has been shown to be a key regulator of genes involved in the maintenance of glucose and lipid homeostasis in the liver (10, 11).

The forkhead superfamily of transcription factors, of which Foxa2 is a member, is defined by a conserved, 110-amino acid winged-helix DNA binding domain (12). Currently more than 100 members have been assigned to this gene family in species ranging from yeast to humans (13). However, there is very little sequence conservation outside of the winged helix domain in many

of these genes, where even subtle changes have been seen to affect DNA binding (13, 14). Consequently the different forkhead family members have been found to affect a varied array of target genes with functions ranging from regulation of development in a wide variety of tissues (15, 16), to DNA repair (17), and apoptosis (18). Some forkhead proteins have been shown to act as transcriptional activators while others act as repressors.

The hepatocyte nuclear factor 3 (HNF-3)/forkhead family of transcription factors in mammals includes three genes designated *Foxa1* (*HNF-3α*), *Foxa2* (*HNF-3β*) and *Foxa3* (*HNF-3γ*), which have overlapping patterns of tissue expression, including gut, central nervous system, neuroendocrine cells, and lung (14, 19). Originally identified as liver-enriched proteins that bind to specific sequences in the transthyretin (TTR) and alpha1-antitrypsin (α1-AT) promoters and activate their transcription (20), the HNF-3 (Foxa) proteins are generally considered to be the founders of the forkhead family (identified at the same time as the drosophila fork head protein) (14).

Foxa proteins have subsequently been shown to be critical regulators of development, growth and metabolism in worms, flies and mammals. Reduced levels of pha-4, the Foxa homologue in worms, leads to developmental arrest and, post-embryonically, inhibits the ability of the organism to respond to dietary manipulations (21). Simultaneous knock-down of daf-16, the Foxo

homologue, had an additive effect on dauer recovery in worms, suggesting that these two factors function in parallel pathways. Furthermore, dietary restriction leads to increased expression of pha-4, which activates genes that protect against oxidative damage (e.g. superoxide dismutase) (22).

Mouse genetic studies have also revealed important roles for murine Foxa genes in development and metabolism. In livers of adult mice, Foxa2 activity has been shown to mediate fasting responses, including fatty acid oxidation, ketogenesis, and increased VLDL and HDL secretion, by activating gene expression of key enzymes of these pathways (10, 23, 24).

The DNA-binding domain of Foxa3 has been crystallized bound to its target DNA sequence, revealing monomeric DNA-binding and a novel "winged helix" motif (25). The extent and pattern of sequence conservation in the DNA-binding regions of known members of the forkhead family indicates that all forkhead family members share this basic structural domain. In particular, this is assumed to be the case for Foxa1 and Foxa2 which share 95% and 90% sequence identity in this region, respectively.

Interestingly, it was also observed that this Foxa DNA binding domain is similar in structure to that of the linker histone H5 (25). However, in contrast to linker histones that compact DNA in chromatin and repress gene expression, FoxA proteins are associated with transcriptionally active chromatin and may decompact DNA from the nucleosome (26, 27).

Additionally, this high affinity DNA-binding site in combination with C-terminal regions mediating interaction with histones H3 and H4 have been shown to enable Foxas to act as pioneer transcription factors, which are able to decompact DNA from nucleosomes without ATP-dependent enzymes (26).

While Foxa proteins share very high sequence homology within the DNA binding domain (as well as a suggested common consensus sequence for DNA binding (28)), Foxa proteins are not entirely redundant in function. Outside of this conserved region, Foxa1 and Foxa2 are only 39% identical, with Foxa3 being even more distinct (14). Accordingly, these differences are reflected in phenotypes of knock-out mice. Mice homozygous for a null mutation in Foxa2 exhibit an embryonic lethal phenotype, lack a notochord and exhibit defects in foregut and neural tube development, while Foxa3-deficient mice develop normally (29-31). Mice lacking Foxa1 expression develop neonatal persistent hypoglycemia, hormonal insufficiencies, pancreatic alpha- and beta-cell dysfunction and die between postnatal days 2 and 14 (32, 33).

The sequence divergence among the Foxa proteins also allows for unique posttranslational modifications and differential DNA and protein interactions. Previous work in our lab has shown that Foxa2, but not Foxa1 or Foxa3, is negatively regulated by insulin in the liver. In unstimulated, or fasting states, Foxa2 is consistently observed in the nucleus, and only extensive

mutation of the DNA-binding/nuclear localization domains alters this cellular distribution (10, 11, 19, 20, 34, 35). However, in response to increasing concentrations of insulin *in vitro* and *in vivo* in perfused mouse liver, Foxa2 shows dose-dependent nuclear exclusion, which corresponds with its phosphorylation (10, 36). This phosphorylation has been mapped to threonine 156 in a conserved AKT site, and a single point mutation of T156 to alanine (T156A) alone abolishes insulin-induced nuclear exclusion. Insulin has also been shown to inhibit transactivation by Foxa2, both in reporter assays, as well as in *ad libitum* fed and hyperinsulinemic mice. Likewise, this transcriptional inactivation is completely alleviated by T156A mutation. Thus, Foxa2T156A is a constitutively active, constitutively nuclear Foxa2 variant.

Cotransfection of wildtype or constitutively active (but not dominant negative) AKT in reporter assays was shown to mimic the effects of insulin on Foxa2 transactivation, while inhibition of PI3-kinase signaling repressed the effects of insulin. Direct phosphorylation of Foxa2 by AKT was further supported by *in vitro* kinase assays, in addition to coimmunoprecipitation experiments, in which wildtype Foxa2, but not Foxa2 T156A or R153A (a Foxa2 mutant that is unable to bind AKT) can be immunoprecipitated with and phosphorylated by AKT (36, 37). Together these data have led to the model proposed in Figure 1.

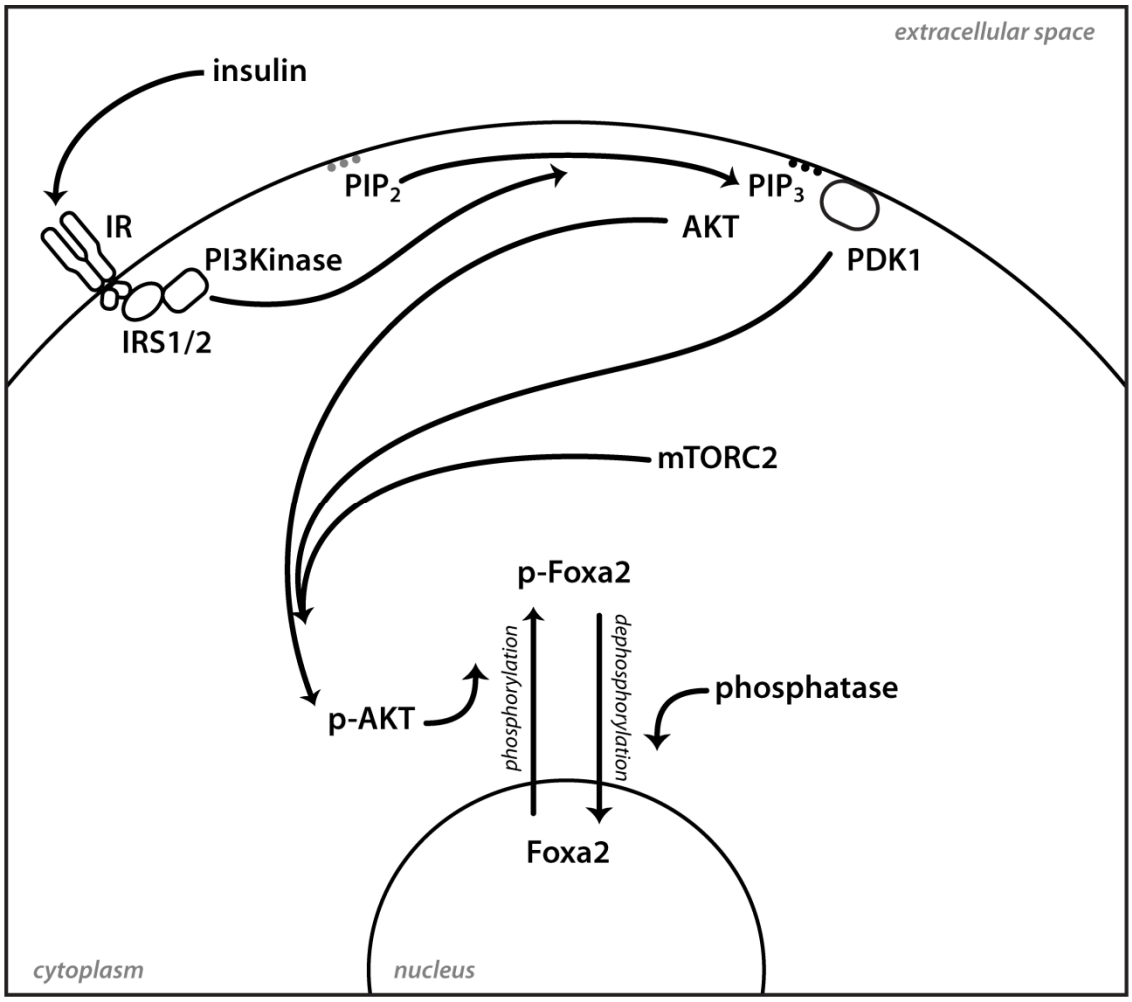

Figure 1. Model illustrating the regulation of Foxa2 by insulin. Insulin binds to and activates the insulin receptor (IR), which triggers autophosphorylation and the recruitment and phosphorylation of insulin receptor substrate (IRS) adaptor proteins. These proteins transmit the insulin signal by activating PI3-kinase, which phosphorylates phosphatidylinositol (4,5) bisphosphate (PIP_2) and catalyzes the formation of PIP_3. This leads to the phosphorylation and activation of protein kinase B (AKT) by PDK1 and the mTORC2 complex. AKT, which has been found in the nucleus upon activation, phosphorylates Foxa2 at T156, which is then excluded from the nucleus and thus inactivate. Insulin withdrawal allows reentry of Foxa2 into the nucleus, presumably through regulation of a phosphatase.

Several studies have been carried out to elucidate the function of different domains of Foxa2, and are summarized in Figure 2. In addition to its winged helix DNA-binding domain, the regions flanking the C-terminal, and partially overlapping the N-terminal end of this domain have been shown to be

required for nuclear localization. Four additional conserved regions have been identified and together form two transactivation domains (at the amino and carboxy terminal), which are important for target gene discrimination and activation (34, 38). More recently the AKT phosphorylation site and a PGC1β-interaction domain have been described (24, 36).

Figure 2. Schematic depiction of Foxa2 showing known domains. II-V, transactivation domains; p, phosphorylation site; NLS, nuclear localization signal (N- or C-terminal of the DNA binding domain); DBD, DNA binding domain; PGC1β, PGC1β interaction domain.

The importance of the phosphorylation site has been further analyzed in mouse models of type 2 diabetes. In hyperinsulinemic/obese mice, Foxa2 (but not Foxo1) is permanently excluded from the nucleus and its inactivation contributes to the development of hepatic steatosis and insulin resistance. This has been demonstrated by re-expression of constitutive active Foxa2 (Foxa2T156A) in livers of obese mouse models that led to increased Fatty acid oxidation, increased VLDL secretion, reduced hepatic TAG content and increased insulin sensitivity and normalization of blood glucose levels (10).

The differential regulation of Foxo1 and Foxa2 in insulin resistant states is somewhat counterintuitive, since both have been shown to be inhibited by insulin signaling through the PI3-kinase pathway. However, this can be explained by increased sensitivity of Foxa2. Knockdown of IRS2 alone was

able to abolish nuclear export of Foxo1, however knockdown of both IRS1 and IRS2 was required for inhibition of nuclear export of Foxa2 (10). It has been shown that there is decreased expression of IRS2 in insulin-resistance states, while IRS1 levels remain unchanged (39). This provides an enticing explanation for the mixed insulin resistance observed in many models of type 2 diabetes, and suggests a mechanism whereby the inhibition of gluoconeogenesis is lost, but the inhibition of fatty acid oxidation is not.

As evidenced by Foxo1, the negative regulation of forkhead transcription factors by nutritional or stress signals is not unique to Foxa proteins. PI3-kinase/Akt signaling in the nematode *Caenorhabditis elegans,* suppresses the function of DAF-16*,* a transcription factor that belongs to the Foxo branch of the forkhead/winged-helix family (40). Mutations in the insulin/Igf-1 receptor homologue (*daf-2*) (41, 42), the catalytic subunit of PI3-kinase (*age-1*) (43), or Akt (*akt1* and *akt2*) (44), result in increased longevity and constitutive *dauer* formation, a stage of developmental arrest and reduced metabolic activity that enhances survival during periods of food deprivation and other environmental stresses. In each case, mutation of *daf-16* restored normal life span and prevented entry into *dauer* stage.

In mammals, this regulation has also been described for Fkhr (Foxo1), Fkhrl1 (Foxo3), and AFX (Foxo4) (18, 45-47). Foxo-1 can be phosphorylated by Pkb/Akt at multiple sites causing repression of transcriptional activity of

target genes such as insulin growth factor binding protein 1 (Igfbp-1), glucose-6-phospatase and phosphoenolpyruvate carboxykinase (48, 49). Similar to Foxa2, this regulation has been shown to occur, at least in part, by nuclear exclusion, although recent findings suggest that additional mechanisms are involved (50). At the moment it is unclear whether nuclear export is the key mechanism regulating Foxo transcription factors or whether other nucleus specific regulatory pathways are involved in the regulation of this factor as well.

The constitutive inactivation of Foxa2 by insulin, in addition to the beneficial effects of constitutively active Foxa2 in mouse models of obesity make understanding the molecular mechanisms of its regulation of great scientific and potentially therapeutic interest. While it is clear that phosphorylation is necessary for nuclear exclusion of Foxa2, the mechanism and importance of nuclear exclusion in the inactivation of Foxa2 by insulin has not previously been investigated. Here, we explore the molecular mechanisms controlling nuclear exclusion of Foxa2 in response to insulin signaling, and its physiological impact in the liver, lung and hypothalamus.

CHAPTER 1: Genetic Strain variations modulate Foxa2 activity

1.1 Effect of insulin on Foxa2 in hepatocytes from diabetic mice

We have shown that nuclear exclusion of Foxa2 closely correlates with insulin levels, both in wild-type C57Bl/6 and in hyperinsulinemic mouse models. Nonetheless, there was initially some disagreement in the literature over this point (11). While wildtype C57Bl/6 mice have fasting glucose levels around 0.3 ng/mL (going up to ~3 ng/mL in fed mice) *ob/ob, db/db* and HF mice are all hyperinsulinemic even after a fast, with plasma insulin concentrations ranging from ~5-80 ng/mL. To directly analyze the effects of insulin on the nuclear exclusion of Foxa2, we isolated primary hepatocytes from these mice and subjected them to controlled amounts of insulin.

As evidenced by quantitation of nuclear and cytoplasmic extracts, an overnight "fast" (serum withdrawal) is sufficient to restore Foxa2 to the nucleus of primary hepatocytes derived from different hyperinsulinemic mouse models, when left untreated (Figure 3). This demonstrates that there is no inherent/irreversible defect in these cells that results in nuclear exclusion of Foxa2. Furthermore, Foxa2 is excluded from the nucleus and localizes to the cytosol in a dose-dependent manner in response to insulin in all hepatocytes. Thus, alterations in the insulin levels alone are sufficient to induce nuclear inclusion or exclusion of Foxa2.

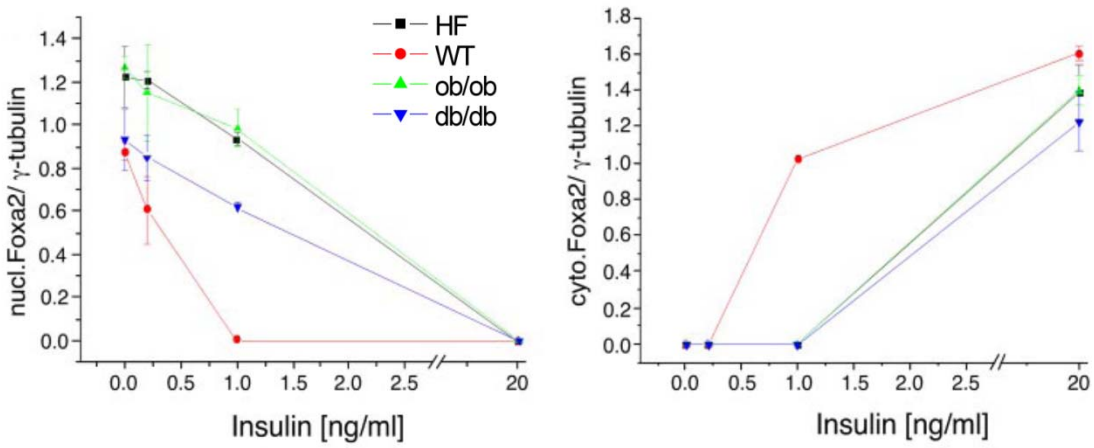

Figure 3. Insulin-dependent Foxa2 localization in primary hepatocytes. Nuclear and cytoplasmic extracts were prepared from primary hepatocytes of wild-type *C57Bl*/6, *ob/ob*, *db/db*, and HF diet-induced obese mice, which were incubated for 6 h in the presence of varying amounts of insulin. Foxa2 was detected by immunoblotting, quantified by densitometry and normalized to γ-Tubulin. Data are means ± SD, n=2.

Notably, while insulin removal completely restored Foxa2 to the nucleus in hepatocytes of *ob/ob*, *db/db* and HF diet mice, higher concentrations of insulin were needed to re-induce nuclear exclusion. In hepatocytes from wildtype C57Bl/6 mice, Foxa2 was already cytoplasmic at 1 ng/mL insulin. However, this concentration of insulin results in only ~20-25% nuclear exclusion in *ob/ob*, *db/db* and HF hepatocytes, demonstrating that their hepatocytes do retain a low level of insulin resistance in culture.

1.2 Genetic strain variations affect metabolic parameters

Diabetic mouse models represent an extreme metabolic phenotype. However, even wild-type strains have been shown to display differing propensities for weight gain and development of features of the metabolic

syndrome. C57Bl/6 mice, for example, are more obese, glucose intolerant, hyperinsulinemic, and hyperletpinemic than Sv129 mice on either regular chow or a high-fat diet, and are more susceptible to the development of insulin resistance and diabetes (51, 52). While these genetic discrepancies cannot be traced to single genetic alterations, it has subsequently been found that different strains have varying levels of circulating hormones such as insulin, and exhibit different metabolic parameters (51-54).

	Sv129 fasted	**Sv129 fed**	**CD1 fasted**	**CD1 fed**	**DBA fasted**	**DBA fed**	**C57Bl/6 fasted**	**C57Bl/6 fed**
Glucose (mg/dL)	83 ± 9	164 ± 11	90 ± 10	171 ± 21	81 ± 7	199 ± 21	100 ± 10	255 ± 31
Insulin (ng/mL)	0.14 ± 0.04	0.31 ± 0.06	0.22 ± 0.05	0.48 ± 0.07	0.25 ± 0.04	0.63 ± 0.1	0.31 ± 0.05	1.7 ± 0.12
Cholseterol	104 ± 10	103 ± 13	106 ± 11	104 ± 13	94 ± 13	90 ± 11	92 ± 10	80 ± 9
Triglycerides	104 ± 12	102 ± 34	101 ± 11	100 ± 33	99 ± 14	99 ± 27	87 ± 13	84 ± 31
Ketone bodies	2.6 ± 0.2	2.5 ± 0.2	2.4 ± 0.2	2.6 ± 0.3	2.6 ± 0.2	1.9 ± 0.2	2.5 ± 0.3	1.3 ± 0.2
Liver triglycerides	19 ± 3	20 ± 2	20 ± 2	20 ± 2	22 ± 3	25 ± 2	24 ± 2	30 ± 2
Glycogen	n.d	3.1 ± 0.4	n.d	3.5 ± .5	n.d	3.5 ± .6	n.d	3.3 ± .5

Table 1. Metabolic parameters of different mouse strains. Fasting and fed blood glucose, plasma insulin, cholesterol, triglycerides and ketone bodies, liver triglycerides and glycogen were measured from 6 male mice age 10-14 weeks. Data are means ± SD.

Initially we chose to investigate four different mouse strains: Sv129 (129), CD1, DBA, and C57Bl/6 (B6). As shown in Table 1, these mice exhibit striking differences in their metabolic parameters, with 129 mice having the lowest insulin levels, and B6 mice the highest. While B6 mice tended to have lower circulating cholesterol and triglyceride levels in fasting and fed states, these differences were not significant. However, circulating ketone body concentrations were significantly decreased in fed DBA and B6 mice, inversely correlated to plasma insulin levels. Additionally, circulating ketone bodies were significantly decreased in the fed state compared to the fasted state in DBA and

B6 mice, while no significant differences between fed and fasted states were observed in 129 or CD1 mice. We analyzed the rate of β-oxidation in livers of these mice in fasted and fed states, and observed similar results. Both in the fed and fasted state, DBA and B6 mice had the lowest rates of mitochondrial β-oxidation, while 129 and CD1 animals exhibited the highest rates (Figure 4). Furthermore, no change in rate was observed between fed and fasting states in the latter two strains, while increased β-oxidation was observed in the fasted, compared to the fed state of the DBA and B6 mice.

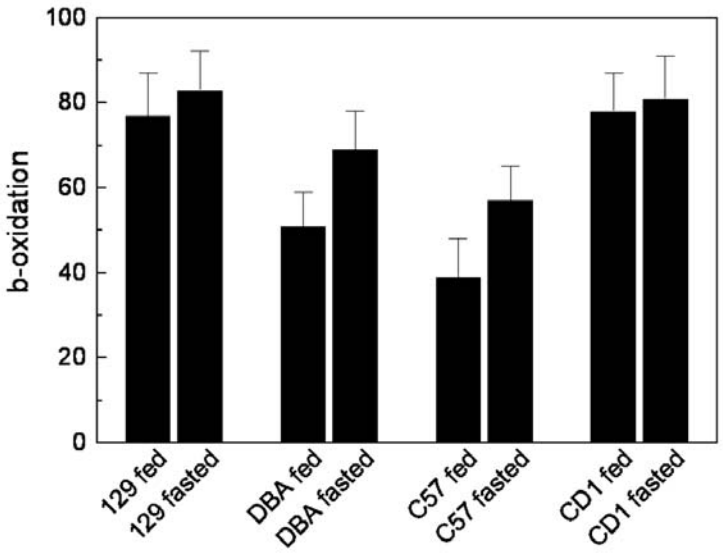

Figure 4. Fasting and fed β-oxidation rates varies between strains. Mitochondrial β-oxidation was measured from livers as a function of $^{14}CO_2$ production from [1-^{14}]C-palmitic acid. n≥4.

1.3 Foxa2 and Foxo1 localization in different mouse strains

The differences in insulin levels, as well as the observed correlation with the downstream regulation of β-oxidation and ketone body metabolism,

encouraged us to analyze the nuclear localization of Foxo1 and Foxa2. These two transcription factors have been shown to regulate metabolic genes and are inhibited by insulin signaling in the liver. Foxa2, in particular, has been shown to increase fatty acid oxidation and ketone body production, while Foxo1 is preferentially involved in the activation of gluconeogenesis (10, 55).

Nuclear extracts were prepared from livers of mice from all four strains (129, CD1, DBA, and B6), which were either *ad libitum* fed, fasted, or injected with 10 ng/mL insulin through the portal vein. Western blotting of nuclear fractions revealed that both Foxo1 and Foxa2 remain nuclear in fed and fasted Sv129 and CD1 mice, while both are excluded from the nucleus in fed DBA and B6 mice (Figure 5).

Furthermore, we could show that this is not an inherent defect in the signaling ability or nuclear export mechanism in the livers of these mice, since a bolus injection of insulin restored nuclear export of both Foxo1 and Foxa2. Thus, insulin is able to enact nuclear exclusion of Foxo1 and Foxa2 to a similar extent in livers of all four strains. This suggests that the differential regulation observed in *ad libitum* fed states is a function of plasma insulin levels, which are below the necessary threshold to achieve this effect, even in a fed state, in 129 and CD1 mice.

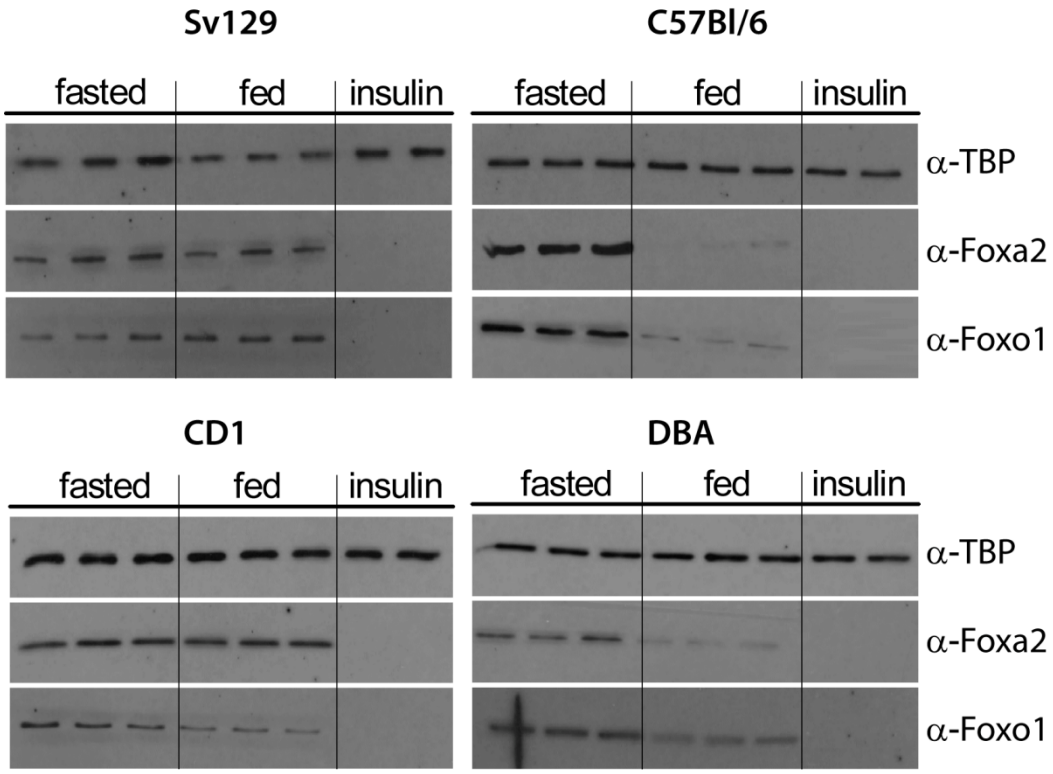

Figure 5. Strain variation in nuclear localization of Foxa2 and Foxo1. Immunoblots of nuclear extracts from livers of fasted, fed and fasted, insulin-injected Sv129, C57Bl/6, CD1, and DBA mice.

1.4 Decreased insulin signaling, but increased sensitivity in Sv129 and CD1 mice

To determine the more general hepatic effects of different circulating concentrations of insulin in these strains, we perfused livers with increasing amounts of insulin and analyzed insulin signaling pathways by western blotting and RT-PCR. Total levels of insulin receptor (IR), insulin receptor stubstrates 1 and 2 (Irs-1, Irs-2) and Akt expression remained unchanged in all strains during insulin perfusion, however we observed an increase in Akt phosphorylation, as well as Mapk phosphorylation, in response to increasing insulin concentration in the perfusate (Figure 6). Accordingly, decreased levels

of nuclear Foxa2 and Foxo1 were observed in all strains with increasing concentrations of insulin. RT-PCR analysis revealed that the expression of downstream target genes of Foxa2 and Foxo1 is also inhibited by insulin (Figure 7).

As a functional readout we measured β-oxidation and ketone body production in the livers of these mice. Again, insulin resulted in decreased β-oxidation and ketone body production in all strains in a dose-dependent manner (Figure 8). Notably, 129 and CD1 strains were even more insulin sensitive, showing earlier activation of insulin signaling pathways and greater levels of target gene suppression at lower concentrations of insulin. This suggests that the altered metabolic rates observed between these strains are directly correlated to plasma insulin levels, insulin signaling and Foxa2 and Foxo1 localization.

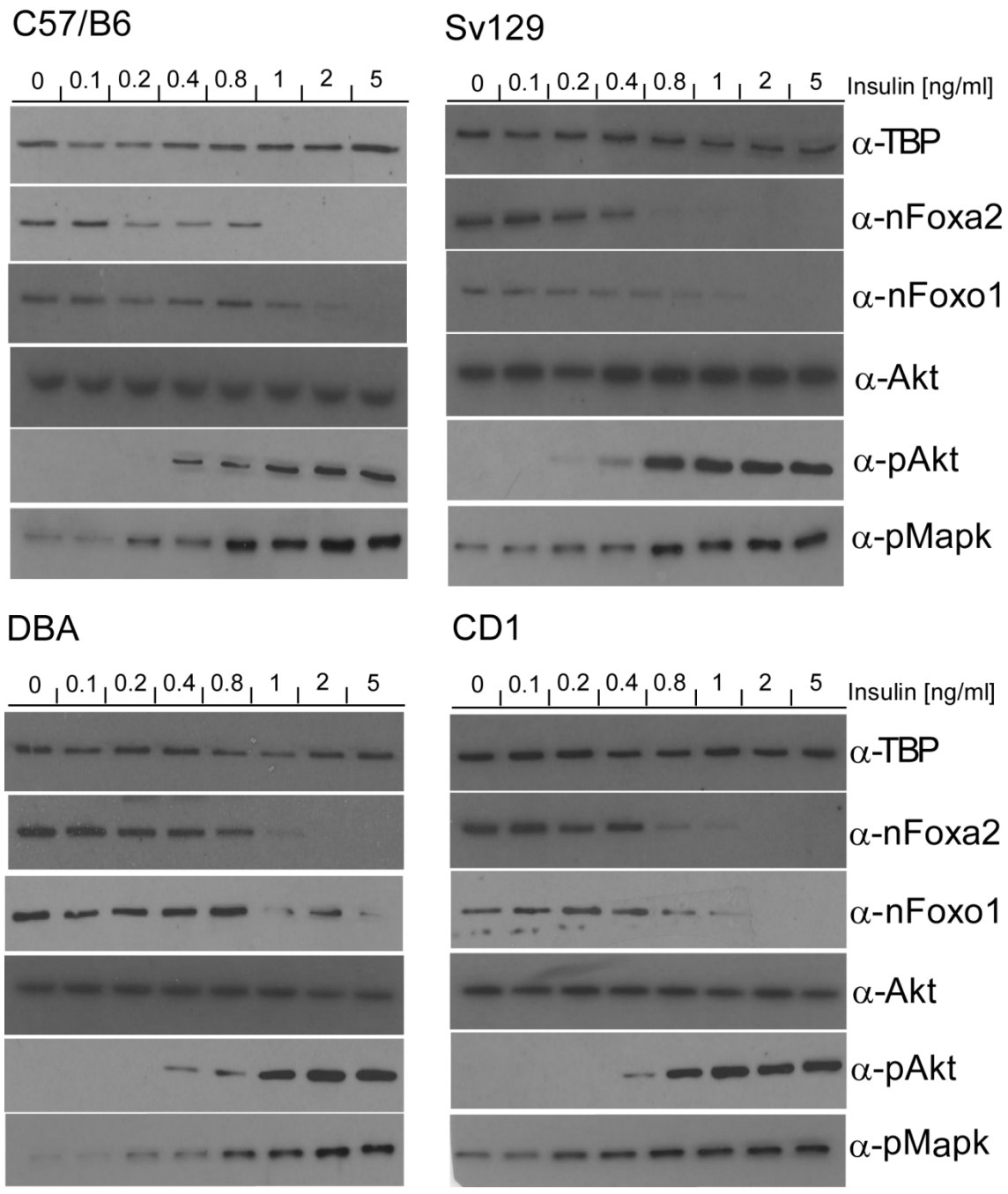

Figure 6. Insulin perfusion shows strain variations in insulin signaling. Livers from B6, 129, DBA and CD1 mice were perfused with increasing concentrations of insulin and activation of insulin signaling pathways was analyzed by immunoblotting whole cell or nuclear (n) lysates. TBP, Tata-binding protein; p, phopsho.

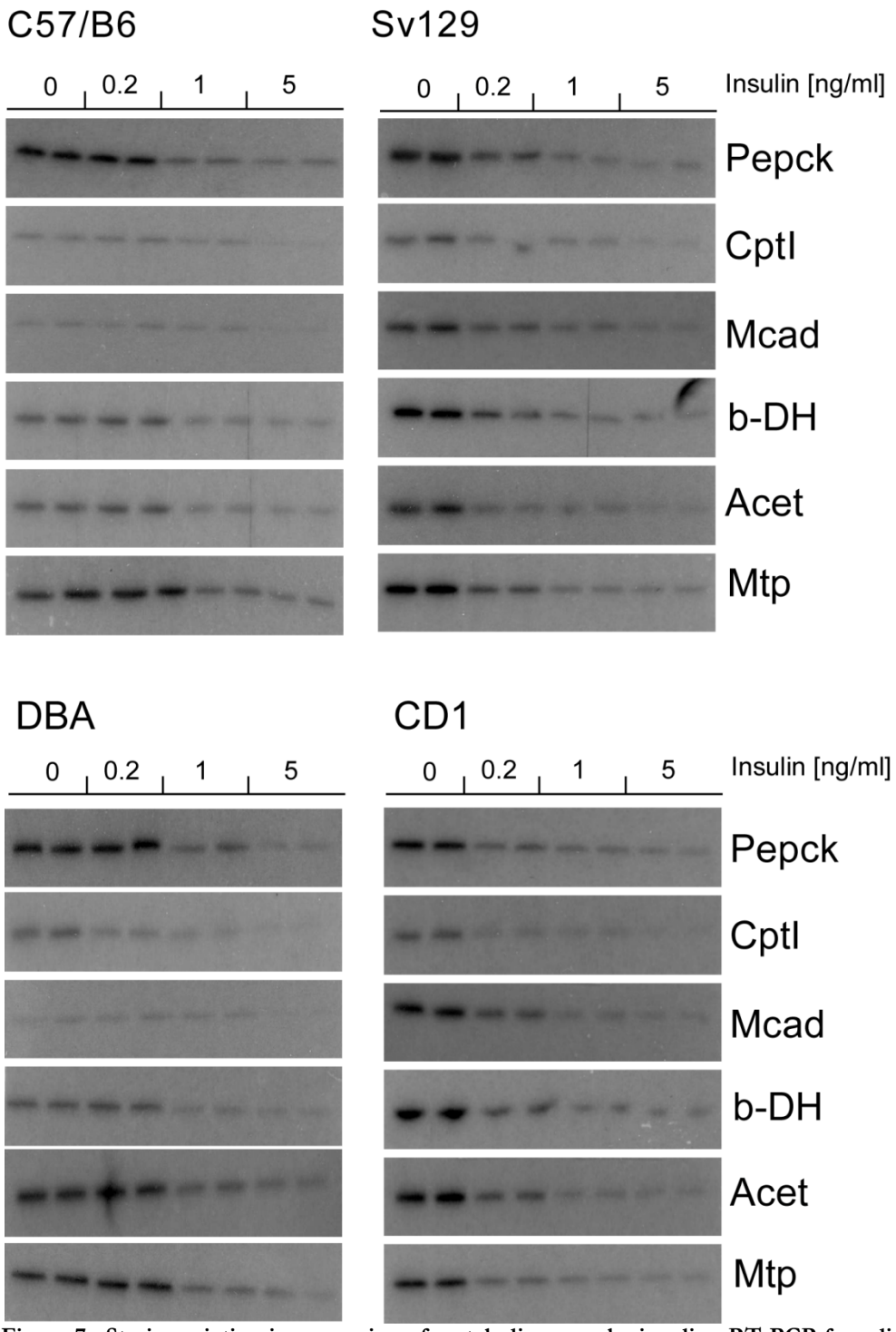

Figure 7. Strain variation in repression of metabolic genes by insulin. RT-PCR from livers of B6, 129, DBA and CD1 mice perfused with increasing concentrations of insulin. Pepck, Phosphoenolpyruvate carboxykinase; CptI, Carnitine palmitoyltransferase 1; Mcad, Medium chain acetyl-coA dehydrogenase; b-DH, 3-Hydroxybutyrate dehydrogenase; Acet, Acetyl-CoA Synthase; Mtp, Microsomal triglcyeride transfer protein.

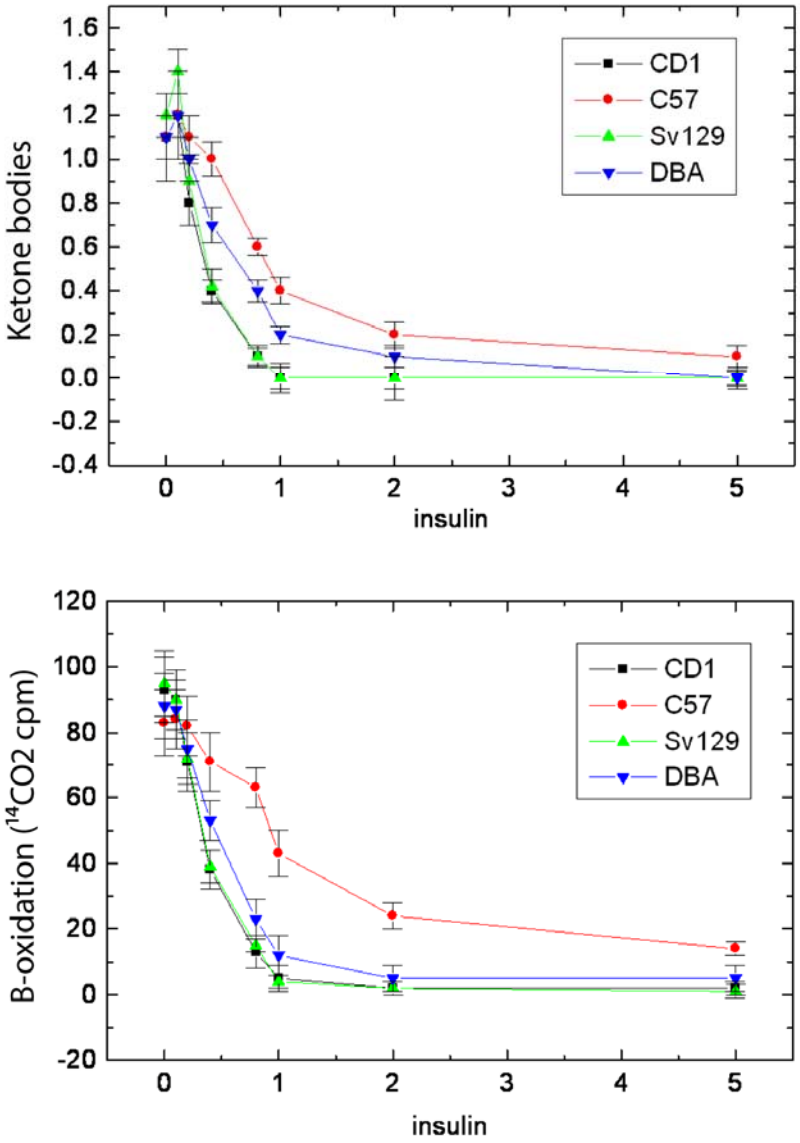

Figure 8. Strain variations in ketone body production and β-oxidation in response to insulin. Ketone body production and mitochondrial β-oxidation were measured from livers as a function of $^{14}CO_2$ production and ^{14}C- acid-soluble products, respectively, from [1-^{14}]C-palmitic acid. n≥4.

1.5 Constitutive activation of Foxa2 increases hepatic lipid metabolism in livers of Fed C57Bl/6 mice

To more directly determine what effect the amount of active/nuclear Foxa2 has on the observed metabolic discrepancies in these mouse strains, we injected *ad libitum* fed Sv129 and C57Bl/6 mice with constitutively active Foxa2

(T156A) adenovirus. As shown in Figure 9, cellular fractionation confirmed that endogenous Foxa2 is nuclear in livers of 129 mice, but cytoplasmic in livers of B6 control mice injected with GFP adenovirus. Adenovirally expressed Foxa2-T156A is constitutively nuclear in livers of both strains.

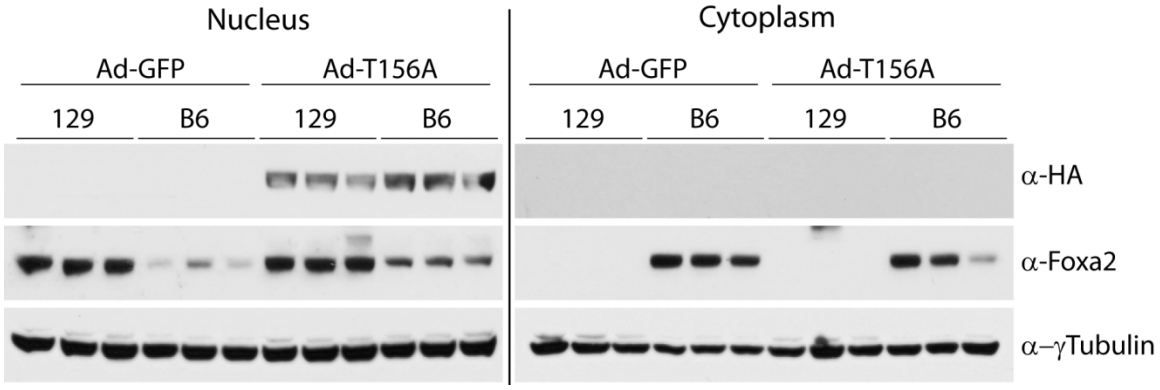

Figure 9. Localization of Foxa2 and Foxa2-T156A in livers of 129 and B6 mice. 129 and B6 were injected with 1E9 PFU of GFP or Foxa2-T156A adenovirus. Six days post injection, mice were sacrificed, livers were fractionated, and nuclear and cytoplasmic extracts were analyzed for Foxa2 localization by western blotting.

As shown in (Figure 10), expression of constitutive active Foxa2 leads to a significant increase in mitochondrial β-oxidation in B6 mice, where endogenous Foxa2 is inactive. Conversely, the effect of Foxa2-T156A is not significant in 129 animals, which already have active Foxa2 in the nucleus.

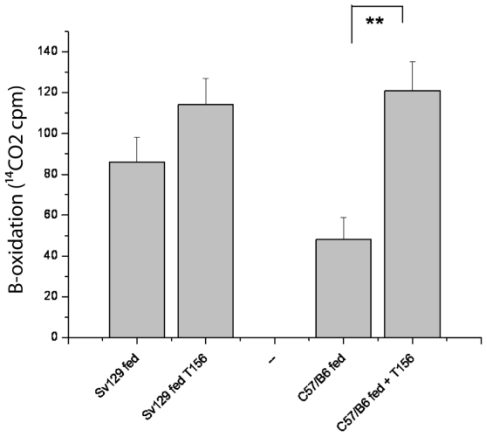

Figure 10. Activation of Foxa2 restores β-oxidation in livers of Fed B6 mice. Mitochondrial β-oxidation measured in 129 and B6 mice six days post injection with either Ad-GFP or constitutively active (Ad-T156A) Foxa2. Data are means ± SD, n≥4. ** , p<0.01 by students t-test.

RT-PCR reveals a similar trend in expression of genes involved in β-oxidation and ketone body synthesis. Foxa2-T156A results in significant upregulation of CptI, Mcad, Vlcad, and b-DH in B6 mice, compared to GFP controls, while Pepck gene expression (encoding the rate-limiting enzyme for heptatic gluconeogenesis) is unchanged (Figure 11). Foxa2-T156A also increases expression of these genes in Sv129 mice, however to a lesser extent, and only Cpt is significantly upregulated.

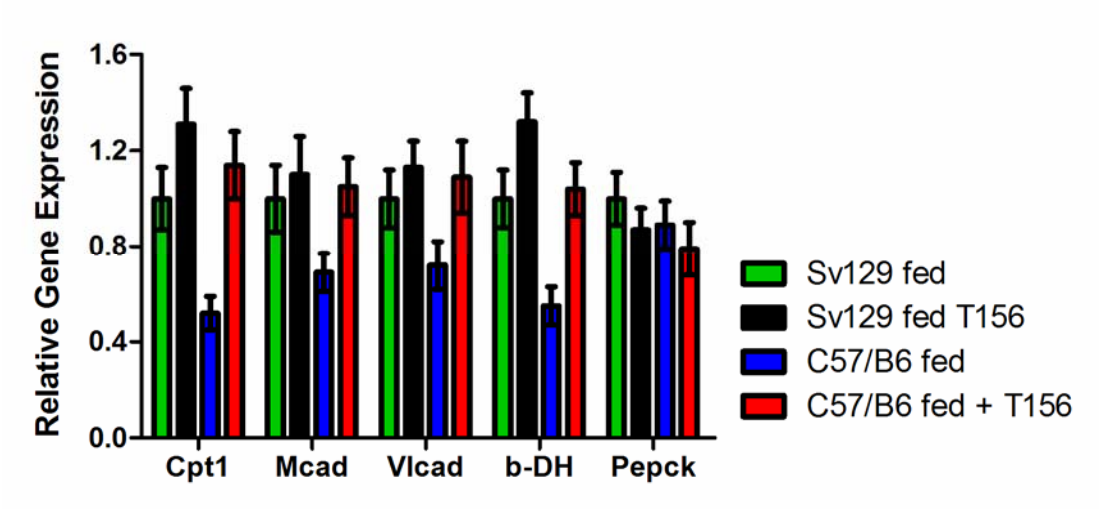

Figure 11. T156A-Foxa2 re-activates expression of B-oxidation genes in the liver. Relative expression levels of genes involved in B-oxidation, ketone body synthesis and gluconeogenesis were analyzed by real time PCR from livers of 129 or B6 mice adenovirally expressing GFP or Foxa2-T156A (T156). Data are means ± SD, n≥4.

1.6 Summary

These studies demonstrate that genetic strain variations, in mice as in humans, play an important role in determining metabolic phenotypes. Here we show that nuclear localization of Foxa2 (and Foxo1) correlates with physiological insulin levels in four different mouse strains. Sv129 and CD1

mice, which have low physiological levels of insulin, retain Foxa2 in the nucleus even in fed states. DBA and C57Bl/6 mice have higher insulin levels, which are sufficient to induce nuclear export and inactivation of Foxa2 in the fed state. This data also provides a possible explanation for the lack of Foxa2 shuttling observed by Zhang and colleagues (11). Interestingly, constitutive activation of Foxa2 in livers of fed B6 mice is sufficient to restore mitochondrial β-oxidation to fasting levels, similar to fed Sv129 mice, and suggests that the differential regulation of Foxa2 plays a major role in liver lipid metabolism, and the metabolic phenotype.

CHAPTER 2: Shuttling of Tagged Foxa2

2.1 Functional analysis of the Foxa2 Akt phosphorylation site

We have shown that Akt phosphorylation of Foxa2 at T165 mediates its nuclear exclusion and transcriptional inactivation in response to insulin; however the mechanisms involved in this regulation remain unclear. It has been observed that the Foxa2 Akt site (RRSYTH) does not perfectly match the canonical Akt recognition motif (RARSYS/TH), yet it is evolutionarily conserved in Foxa2. To attempt to address whether this imperfection has some additional significance in the regulation of Foxa2, we generated two variants with canonical Akt sites: Foxa2-pAins was generated by inserting an additional alanine after R152, while Foxa2-pMut was generated by mutating Y151R and R152A. In reporter assays both Foxa2-pAins, and Foxa2-pMut showed similar transactivation levels to wildtype Foxa2 under basal conditions,

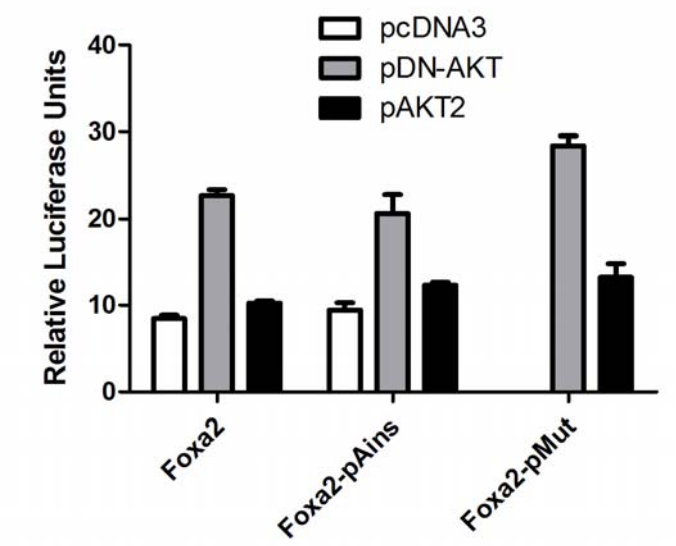

Figure 12. Transactivation of Foxa2 Akt site variants. HepG2 cells were transfected with expression vectors containing Foxa2 or variants, alone or in combination with DN-Akt or Akt2. p6xCdx-TkLuc was used as a reporter gene, normalized to renilla luciferase, and shown relative to vector only controls. Experiments were performed in triplicate and are representative of 2 independent experiments.

similar increases when coexpressed with dominant negative Akt (DN-Akt), and all were repressed to a similar degree by coexpression of wildtype Akt (Figure 12). Thus, it appears that the exact sequence of this Akt site is not essential for the regulation of Foxa2 by Akt. Nonetheless, we cannot rule out that alteration of this site might have a more subtle effect *in vivo* that was not observed in an *in vitro* analysis requiring cellular manipulation and overexpression.

To further investigate the importance of this phosphorylation site we took advantage of the fact that Foxa1, a highly homologous member of the Foxa family, does not shuttle in response to insulin. Additionally, sequence alignment of these two proteins revealed that Foxa1 has a T->P substitution in the region corresponding to the Akt phosphorylation site in Foxa2 (alignment of this region is shown in Figure 13.)

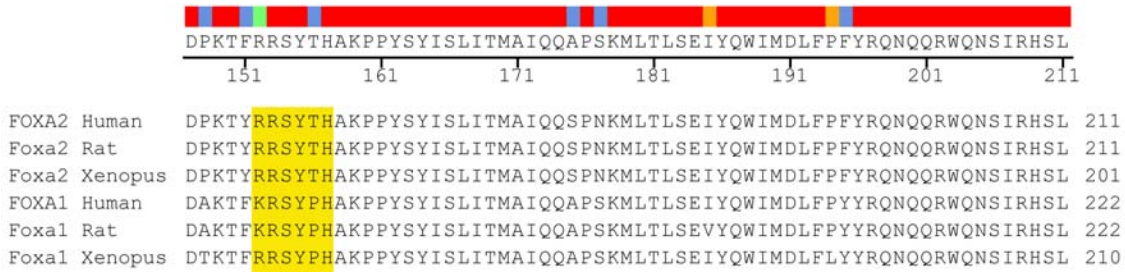

Figure 13. Partial sequence alignment of Foxa1 and Foxa2. The Foxa2 Akt phosphorylation site, is highlighted in yellow.

We therefore asked whether introduction of the Foxa2 Akt site into Foxa1 would be sufficient to induce its inactivation by insulin. This approach

Figure 14. Expression of Foxa1 mutants. Whole Cell extracts from HepG2 cells transfected with pcHAFoxa1 or pcHAFoxa2p3B, detected with an α-HA antibody

has been successfully used to identify a PGC1β-interaction domain in Foxa2, and has also been used to demonstrate the importance of a phosphorylation motif for shuttling of Foxo3 by domain swapping with Foxo6 (24, 56). Site directed mutagenesis was performed to clone the Foxa2 Akt site into a plasmid containing HA-tagged Foxa1 (Foxa1p3B), replacing the corresponding region in Foxa1, and its expression was confirmed by sequencing and western blot analysis (Figure 14).

To test whether introduction of the phosphorylation site was sufficient to induce Akt-dependent inhibition of Foxa1, expression vectors for Foxa1, Akt2, or dominant negative Akt (DN-Akt) were coexpressed with pGL2hGlucP, a luciferase reporter plasmid containing the human glucagon

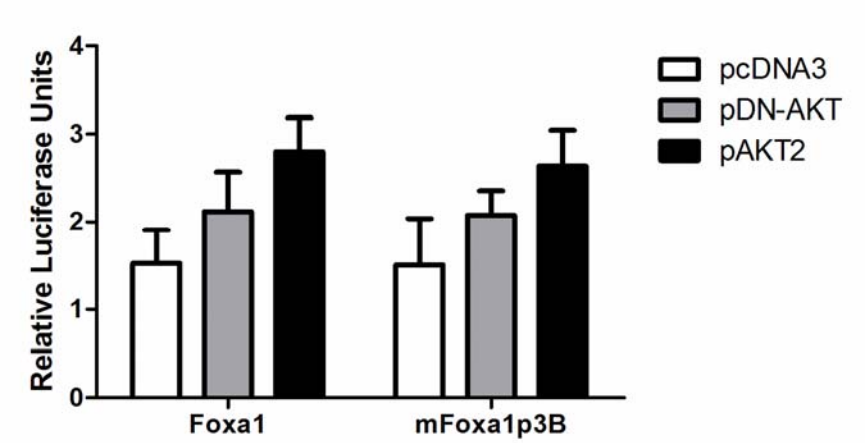

Figure 15. Transactivation by Foxa1 and Foxa1p3B. HepG2 cells were transfected with expression vectors containing Foxa1 constructs, alone or in combination with DN-Akt or Akt2. pGL2hGlucP was used as a reporter gene. Firefly luciferase activity was normalized to renilla luciferase, and shown relative to vector only controls. Experiments were performed in triplicate and shown as the average of 3 independent experiments ± SEM.

promoter (shown to preferentially bind Foxa1(57)) upstream of a minimal promoter and the firefly luciferase gene. Both Foxa1 variants only weakly transactivate the reporter, however there was no significant difference observed between them, with or without cotransfection of Akt or DN-Akt (Figure 15). If anything, transcriptional activity was stimulated by Akt, although this could be a general effect of increased transcription/translation caused by mimicking activation of a growth factor signaling pathway.

Foxa2 transactivation, as has been previously shown (36), was enhanced by co-expression with dominant negative Akt, and inhibited by overexpression of wild-type Akt2 in parallel experiments (Figure 16). These data suggest that the Foxa2 phosphorylation site alone is not sufficient to induce nuclear exclusion by Akt, and demonstrate that additional sequence elements might be necessary for the insulin-induced nuclear exclusion of Foxa2.

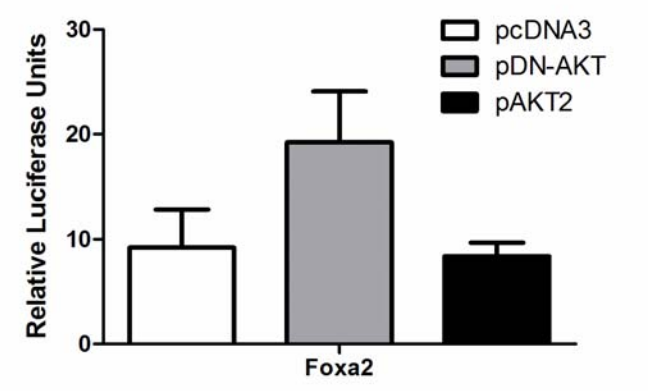

Figure 16. Foxa2 transactivation is inhibited by Akt. HepG2 cells were transfected with expression vectors containing Foxa2, alone or in combination with DN-Akt or Akt2. p6xCdx-TkLuc was used as a reporter gene. Firefly luciferase activity was normalized to renilla luciferase, and shown relative to vector only controls. Experiments were performed in triplicate and shown as the average of 3 independent experiments ± SEM.

2.2 Transient transfection inhibits shuttling of Foxa2

To further elucidate the sequence elements responsible for the insulin-induced nuclear exclusion of Foxa2 we generated N- and C-terminal Foxa2-GFP fusion constructs (GFPN1- and GFPC1-Foxa2, respectively). This is a useful approach for studying the intracellular localization of proteins in real time and in live cells, and has been previously used to visualize the intracellular localization of many different proteins, including members of the Foxo family, which also shuttle in response to external stimuli (56, 58-60). Western blot analysis confirmed the expression of a ~90 kDa band corresponding to the predicted size of GFP-Foxa2 fusions (Figure 17). However, fluorescence microscopy revealed that GFPC1-Foxa2 transfected into HepG2 cells was constitutively nuclear, despite cotransfection with Akt (Figure 18). Insulin was also unable to

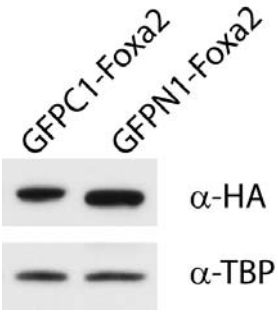

Figure 17. Expression of Foxa2-GFP fusion proteins. Whole cell lysates from HepG2 cells transfected with the indicated GFP-Foxa2 expression plasmids, separated by SDS-PAGE and subject to western blot analysis.

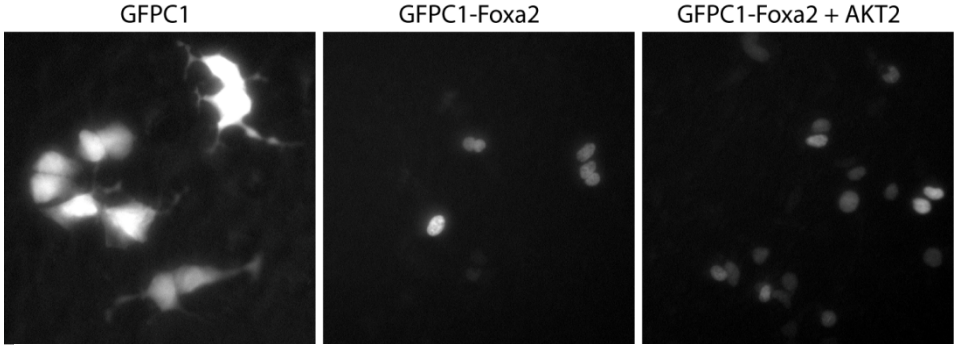

Figure 18. Immunofluorescent localization of GFPC1-Foxa2. HepG2 cells were transfected with 20ng of pEGFP-C1 (Clontech) or GFPC1-Foxa2, with or without cotransfection of Akt2 (40ng), and detected by fluorescence microscopy.

alter this nuclear localization, and GFPN1-Foxa2 gave similar results, with or without insulin or cotransfection of Akt (data not shown).

To determine whether this effect might be due to transient transfection, we analyzed the localization of HA and FLAG double-tagged wildtype rat Foxa2 (HA-Foxa2, which has previously been shown to shuttle in response to insulin signaling (36)) after transfection into HepG2 cells. Once again, even after stimulation with 500 nM insulin Foxa2 remained nuclear (Figure 19).

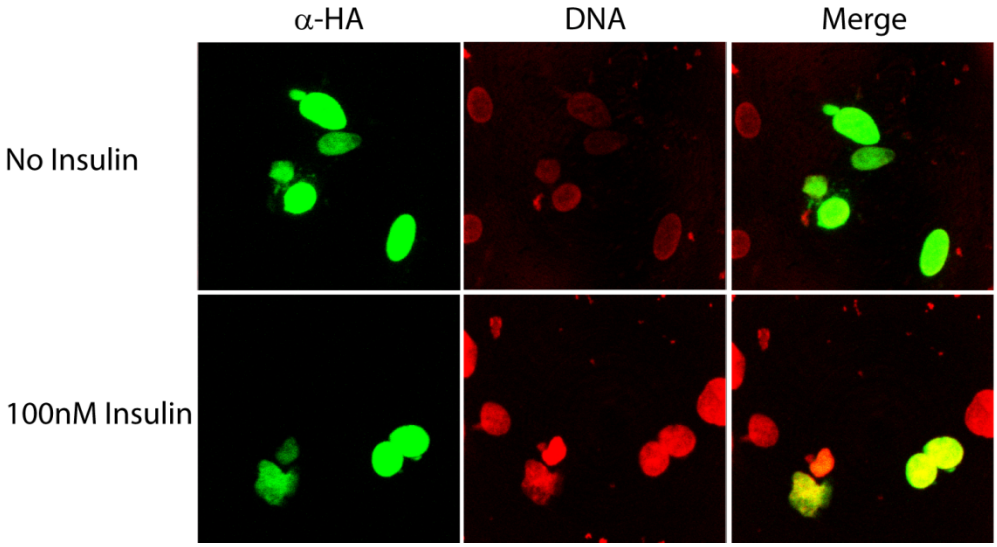

Figure 19. Immunofluorescence localization of transfected Foxa2. HepG2 cells were transiently transfected with 20ng of HA-Foxa2, serum starved for 18 hours and treated with or without 500nM insulin for 20minutes. Cells were fixed and stained with anti-HA antibody overnight at 4° and visualized with Alexa 480 Goat anti-mouse IgG using laser scanning micrsocopy. Nuclei were visualized by costaining with Topro3.

2.3 Cytoplasmic relocalization of endogenous Foxa2 by cellular fractionation

Given these unexpected *in vitro* results and the emerging controversy over Foxa2 shuttling, we decided to reconfirm nuclear exclusion of Foxa2 *in vivo*, using previously established methods. Nuclei were extracted from livers of fasted, random fed and *ob/ob* mice and assayed for the presence or absence of Foxa2 by western blotting. As shown in Figure 20, Foxa2 was found in the nuclear fractions of livers of fasted mice, but was excluded in the livers of random fed and *ob/ob* mice. Additionally, fasted mice injected with 150 ng of insulin 15 min prior to sacrifice showed nuclear exclusion of Foxa2, while PBS-injected mice did not (Figure 21).

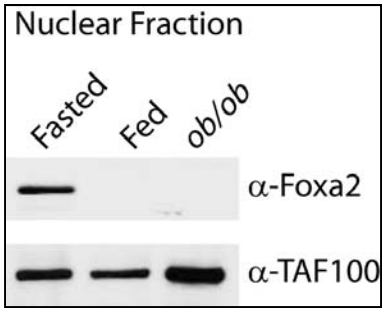

Figure 20. Nuclear exclusion of Foxa2 in livers of fed and hyperinsulinemic mice. Immunoblot analysis of Foxa2 in nuclear extracts from livers of C57BL/6 **and *ob/ob* mice, fasted for 24 h or *ad libitum* fed. Nuclear extracts were prepared by sucrose gradient fractionation and each lane represents livers pooled from 2 mice.**

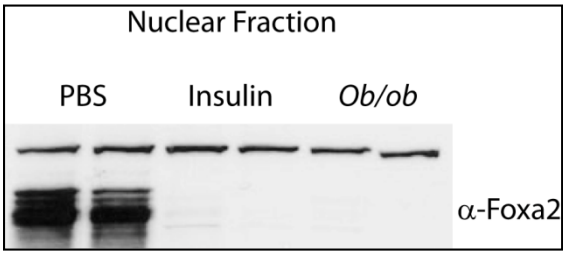

Figure 21. Nuclear exclusion of Foxa2 is induced by insulin *in vivo*. Immunoblot analysis of Foxa2 in nuclear extracts from livers of C57BL/6 **mice, fasted for 24 h and injected with PBS or 600 ng insulin via the tail vein. Nuclear extracts were prepared by sucrose gradient fractionation. The upper band is non-specific and serves as an internal loading control.**

While these data demonstrate robust nuclear exclusion of Foxa2, thereby confirming previous results, the experimental protocol did not allow for simultaneous analysis of cytoplasmic fractions, an ideal internal control. We therefore sought to develop a robust assay for determining the cellular localization of this factor both *in vitro* and *in vivo*. We subsequently used a gentle hypotonic lysis buffer to release cytoplasmic proteins, followed by brief centrifugation to pellet nuclei, which were ultimately extracted by addition of ammonium sulfate to 400 mM. This method of cellular fractionation yielded good resolution of nuclear and cytoplasmic fractions in liver tissue, as indicated by the predominantly nuclear localization of the TAF100 transcription factor (Figure 22). Moreover, it allowed us to visualize not only the nuclear exclusion of Foxa2, but the corresponding cytoplasmic relocalization upon stimulation with insulin (and in hyperinsulinemic *ob/ob* mice) by cellular fractionation and immunoblotting. This, in addition to the development of two new polyclonal Foxa2 antibodies, greatly improved our ability to accurately assay the cellular localization of Foxa2.

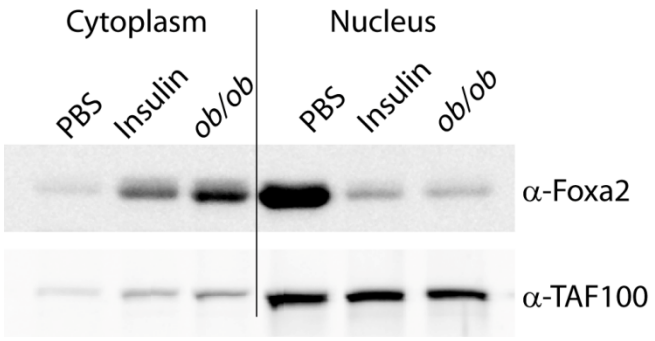

Figure 22. Cytoplasmic localization of Foxa2 in livers of insulin-injected and hyperinsulinemic mice. Nuclear/cytoplasmic fractionation of 50 mg of frozen liver from fasted mice injected with either PBS or insulin and subject to immunoblotting.

This new protocol allowed us to revisit the impaired shuttling of transfected Foxa2. Nuclear and cytoplasmic extracts confirmed shuttling of endogenous Foxa2 in untransfected HepG2 cells after stimulation with insulin, verifying that Foxa2 also shuttles *in vitro* (Figure 23, null). However, after transfection of the cells with either PCDNA3 vector and GFP, or HA-Foxa2 and GFP, neither transfected HA-Foxa2 nor endogenous Foxa2 shuttled in response to insulin (Figure 23).

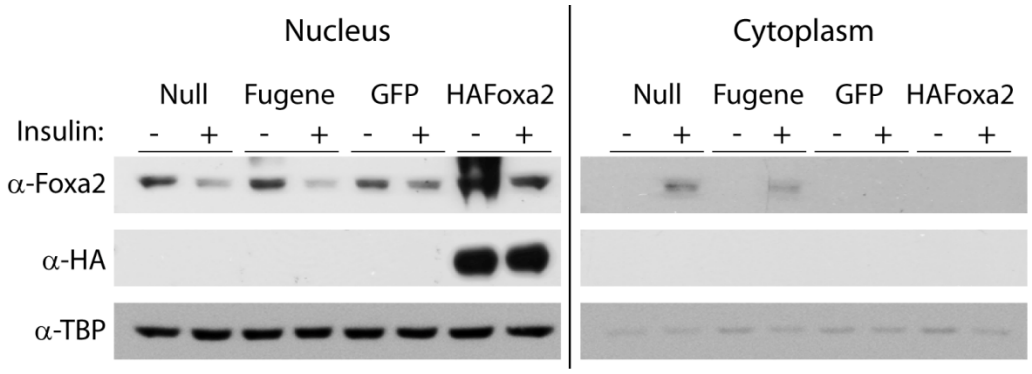

Figure 23. Endogenous and HA-Foxa2 are nuclear after transfection. HepG2 cells were transfected with either GFP and pcDNA3 (GFP), or GFP and HA-Foxa2 (HAFoxa2), not transfected (null) or mock transfected with Fugene only, serum starved for 19 h and treated with or without 500 nM insulin for 15 min. Cellular fractionation was followed by SDS-PAGE and immunoblot analysis using the indicated antibodies.

Mock transfection of the cells with Fugene transfection reagent did not alter the shuttling of endogenous Foxa2, demonstrating that this is not strictly an issue of toxicity caused by the transfection reagent. The same nuclear phenotype was observed when we transfected different concentrations of GFPC1-Foxa2 (Figure 24).

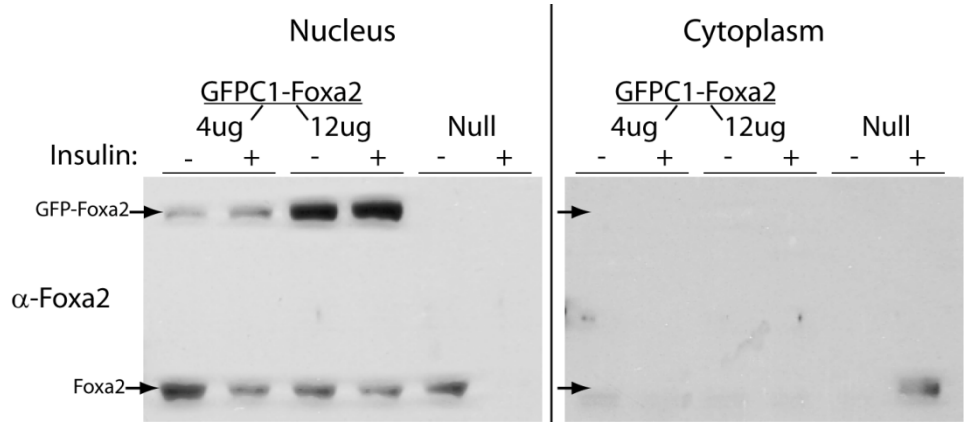

Figure 24. GFPC1-Foxa2 is nuclear after transfection. HepG2 cells were transfected with either 4 or 12 ug of GFPC1-Foxa2, or untransfected (null), serum starved for 19 h and treated with or without 500 nM insulin for 15 min. Cellular fractionation was followed by SDS-PAGE and immunoblot analysis with anti-Foxa2 antibody.

2.4 Nuclear/Cytoplasmic shuttling of tagged Foxa2

To avoid the issue of altered protein regulation after transfection, we generated stable cell lines expressing N- and C-terminal GFP-Foxa2 fusion plasmids in HepG2 cells. In the process of selecting stable cell lines we found that GFP-Foxa2 fusions occasionally integrated in such a way as to cause truncation of the fusion product. Clonal populations were selected based on fluorescence, and fusion constructs were detected by immunoblot analysis of whole cell extracts using an anti-HA antibody (Figure 25). Therefore, the truncations were generally predicted to have been shortened from the C-terminus, with the exception of GFPN1-Foxa2 clone #2, which is around 50 kDa and appears to have retained both the N-terminal HA-tag and C-terminal GFP.

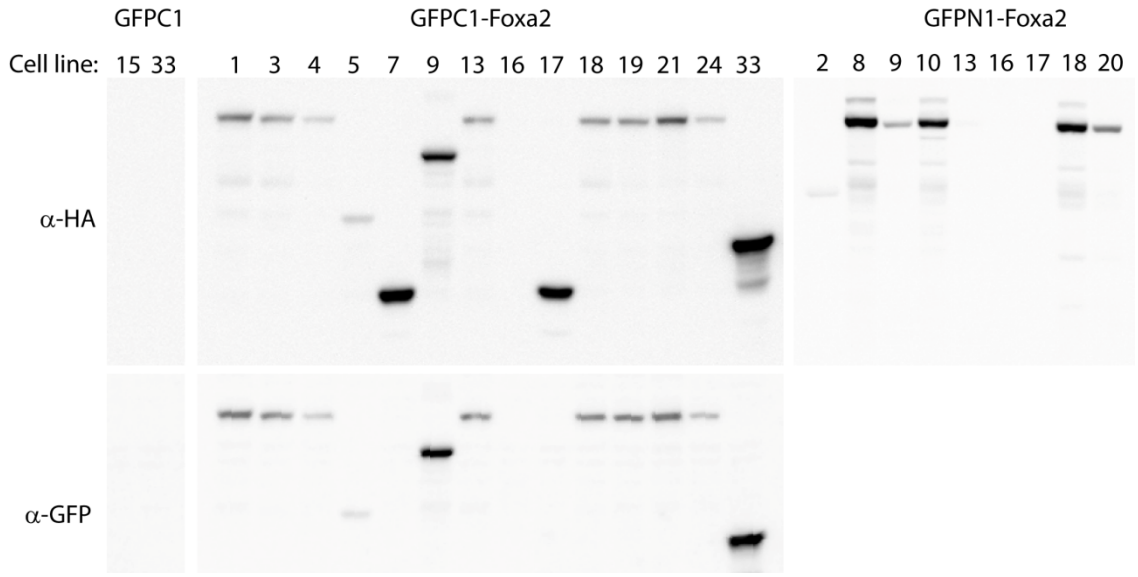

Figure 25. Stable expression of GFP-Foxa2 fusion constructs. Clonal populations of HepG2 cells were selected for G418 resistance and fluorescence, and screened for expression of GFP-Foxa2 fusion products in whole cell extracts by immunoblotting with anti-HA and anti-GFP antibodies

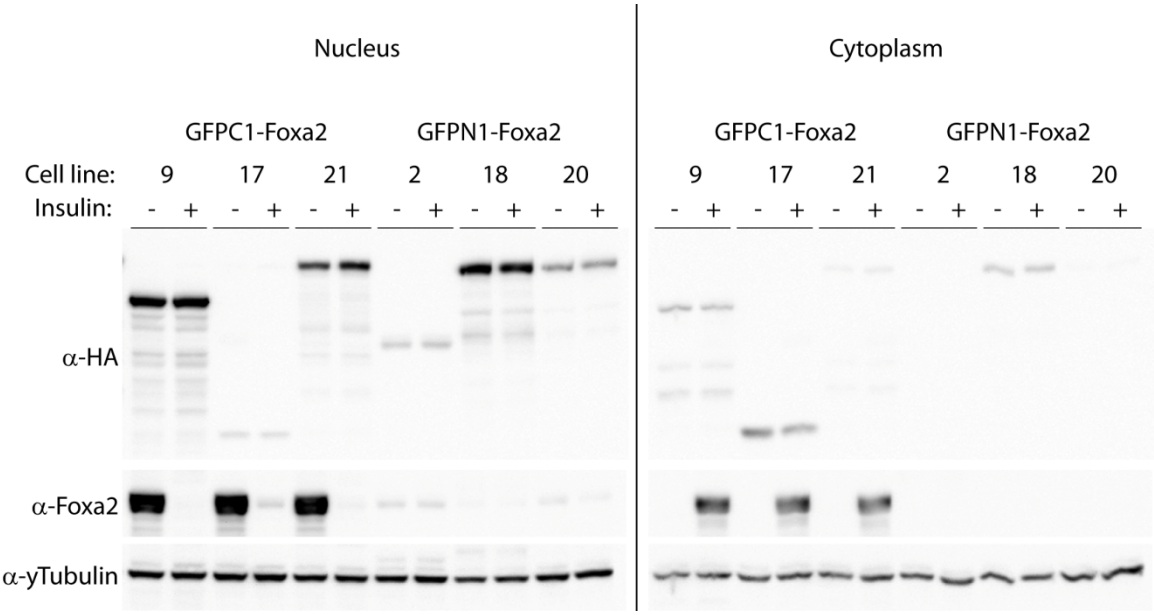

Figure 26. Impaired shuttling of GFP-Foxa2 in stable cell lines. Immunoblots of nuclear and cytoplasmic extracts from HepG2 cells stably expressing GFPC1-Foxa2, GFPN1-Foxa2, or truncations thereof, with and without stimulation with 500nM insulin for 15min. HA antibody was used to identify stably expressed Foxa2 variants, Foxa2 antibody was used to assay endogenous Foxa2, and γ-Tubulin was used as a loading control.

Although we did not sequence the constructs to determine exactly where truncations occurred, we took advantage of their size differences to investigate

the shuttling properties of shortened fusions alongside the full-length constructs. This allowed us to simultaneously assess whether stable expression and/or total size reduction could enable shuttling of GFP-Foxa2. GFPC1-Foxa2 #17, which is around 37 kDa and presumably contains less than 10 kDa of Foxa2, was the smallest fusion protein generated. While this one did show a general cytoplasmic shift in its distribution, the rest of the fusion constructs remained nuclear, and none were excluded from the nucleus after stimulation of the cells with insulin (Figure 26). Endogenous Foxa2, on the other hand, shuttled to the cytoplasm in all GFPC1-Foxa2 stable cell lines, suggesting that the loss of nuclear export observed with the GFP fusion constructs is not due to decreased insulin sensitivity, but rather is an artifact caused by fusion to GFP.

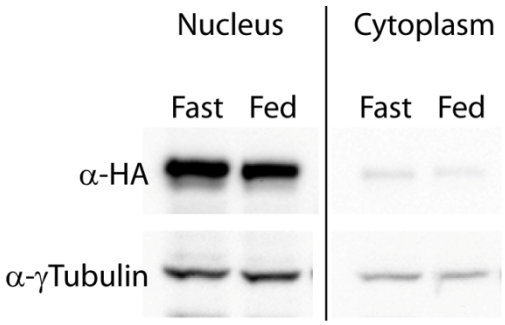

Figure 27. AdGFPC1-Foxa2 remains constitutively nuclear in fasted and fed mice. Immunoblots showing cellular fractionation of livers from fasted or *ad libitum* fed C57Bl/6 mice injected with GFPC1-Foxa2 adenovirus.

To further ensure that this was not an *in vitro* issue, we generated adenovirus from the GFPC1-Foxa2 construct and injected this into wildtype mice. Once again, the GFPC1-Foxa2 construct was clearly nuclear in livers from both fasted and fed mice (Figure 27). Taken together, these data demonstrate that both transfection and GFP-fusion inhibit insulin-induced nuclear exclusion of Foxa2.

As opposed to GFP, which encodes a protein of roughly 30 kDa, HA and FLAG peptides are hydrophilic and immunogenic fusion tags that are specifically designed to facilitate purification and detection using monoclonal antibodies. Due to their small size, they are less likely to interfere with protein function (61). We therefore established stable cell lines expressing N-terminal HA and FLAG double-tagged Foxa2 (HA-Foxa2) in HepG2 cells. Indeed, cellular fractionation showed that stably expressed HA-Foxa2 was almost completely excluded from the nucleus (and relocated to the cytoplasm) by 15 minutes after stimulation with insulin in each cell line (Figure 28).

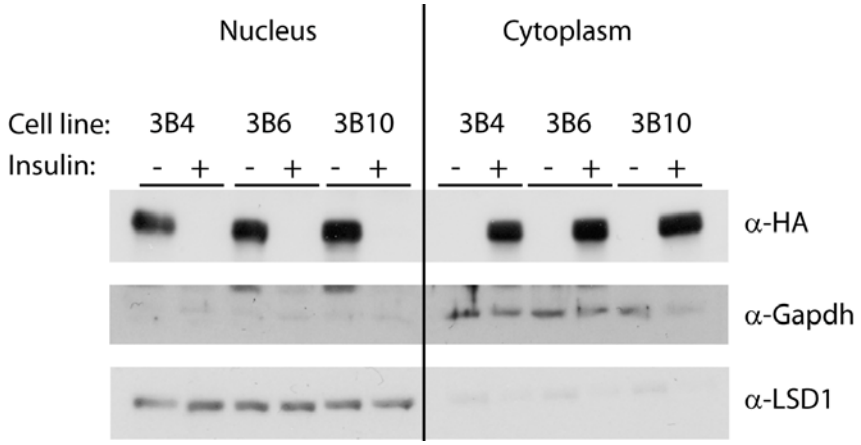

Figure 28. Nuclear-ctyosolic shuttling of HA-Foxa2 *in vitro*. Nuclear and cytoplasmic fractionation of HepG2 cells stably expressing HA-Foxa2 (3B4, 3B6, 3B10 denote individual clones), with and without stimulation with 500nM insulin for 15min. LSD1, and GAPDH were used as nuclear and cytoplasmic loading control markers, respectively.

2.5 Summary

Here we show that Foxa2 shuttling is disrupted by transient transfection in HepG2 cells *in vitro*. We have also tested shuttling in HEK293, and Huh7 cells, using various transfection methods with similar results (data not shown).

While we were not able to elucidate the cause of this impaired shuttling, our data suggest that it is a consequence of the transfection procedure. We have further shown that GFP fusion to Foxa2 ablates its nuclear export. This effect is independent of transfection, as we achieved the same results in stable cell lines, and by adenoviral expression *in vivo*.

Previously shuttling of Foxa2 had only been observed by its absence in nuclear extracts, or by immunofluorescent staining. Here we demonstrate the nuclear exclusion and cytoplasmic relocalization of Foxa2 by cellular fractionation, both *in vitro* and *in vivo*. Finally, we show that Foxa2 shuttling is not disturbed by HA/FLAG epitope tagging, thereby confirming previous data in the lab and establishing more robust assays for further mechanist analysis of its regulation.

CHAPTER 3: Nuclear export-independent inhibition of Foxa2

3.1 Foxa2 Contains a Nuclear Export Sequence

To identify possible mechanisms responsible for the nuclear export of Foxa2 we used a candidate approach focusing on CRM1 (also called exportin1/Xpo1) as the most common nuclear export factor. Since CRM1 mediated nuclear export can be potently inhibited by the pharmacological agent leptomycin B (LMB) (62, 63) we used this to analyze CRM1-dependent shuttling of Foxa2 in the 3B10 HepG2 cell line stably expressing HA-Foxa2 (3B10, Figure 31). Analysis of nuclear and cytoplasmic extracts showed that LMB prevents the export of Foxa2 from the nucleus after stimulation with insulin, while untreated control cells display normal export dynamics (Figure 29). This finding demonstrates that nuclear export of Foxa2 is mediated by CRM1.

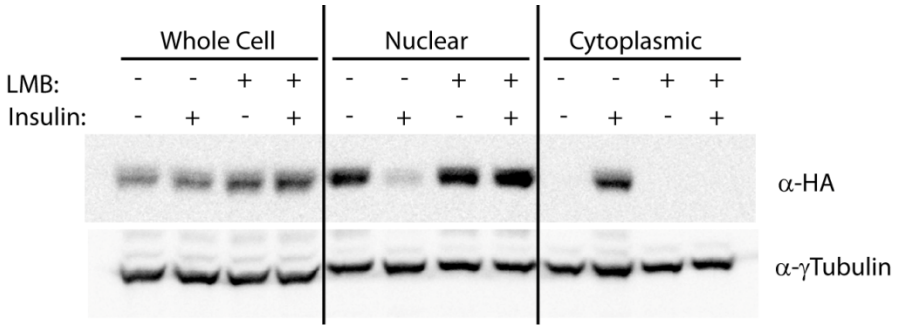

Figure 29. LMB inhibits nuclear export of Foxa2. Cellular fractionation of HepG2 cells stably expressing HA-tagged Foxa2, serum-starved overnight and stimulated with 500nM insulin, with or without pretreatment with 2.5ng/mL LMB. Foxa2 localization was determined by western blotting.

To identify possible regulatory sites in Foxa2 we performed a comparative analysis of the primary amino acid sequence using the generally accepted CRM1 consensus sequence, $LX_{(2,3)}[LIVFM]X_{(2,3)}LX[LI]$ (62, 64). Interestingly, Foxa2 contains one leucine-rich sequence that closely resembles this consensus nuclear export signal (NES) as shown in Figure 30, aligned to the prototypical HIV-REV NES. This region lies in the N-terminal half of Foxa2, about 40 amino acids upstream of the Akt phosphorylation site (T156), between the transactivation and DNA binding domains, and is evolutionarily well-conserved (Figure 30 and Figure 31).

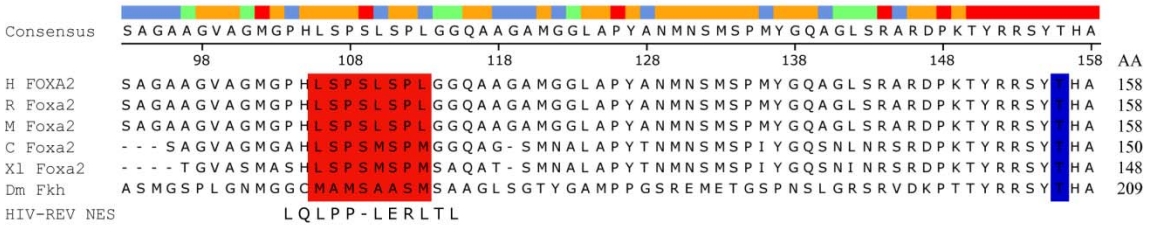

Figure 30. Partial sequence alignment of Foxa2 from six different species, and the HIV-REV NES. The putative NES (red) and phosphorylated threonine (blue) are highlighted. H, human; R, rat; M, mouse; C, chicken; Xl, *Xenopus laevis*; Dm, *Drosophila melanogaster.*

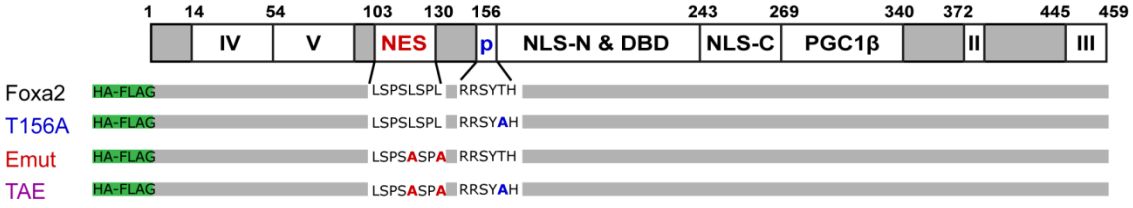

Figure 31. Schematic depiction of Foxa2 showing the putative NES in relation to other known domains, along with mutant constructs. II-V, transactivation domains; NES, nuclear export signal; p, phosphorylation site; NLS, nuclear localization signal (N- or C-terminal of the DNA binding domain); DBD, DNA binding domain; PGC1β, PGC1β interaction domain; Foxa2, rat wildtype Foxa2; T156A, mutated at residue T156A; Emut, mutated at residues L110A and L113A; TAE, mutated at residues T156A, L110A, and L113A.

3.2 Foxa2 NES is Necessary for Nuclear Export

To elucidate whether the putative CRM1 NES is responsible for nuclear export of Foxa2, and thus important for its regulation in different physiological states, we performed mutational analyses. Since the C-terminal hydrophobic residues of the CRM1 consensus sequence have been shown to be the most critical for nuclear export (65), we mutated both terminal leucines (L110 and L113) of the putative Foxa2 NES to determine whether this sequence is necessary for nuclear exclusion in response to insulin. L110A, L113A Foxa2 (Emut, Figure 31) was stably expressed in HepG2 cells, and analyzed for its ability to shuttle from the nucleus in response to insulin stimulation. Endogenous Foxa2 was used as an internal control. We show that while endogenous Foxa2 still shuttles in these cells in response to insulin stimulation, the export mutant remains nuclear, demonstrating that the NES is functional and necessary for export *in vitro* (Figure 32).

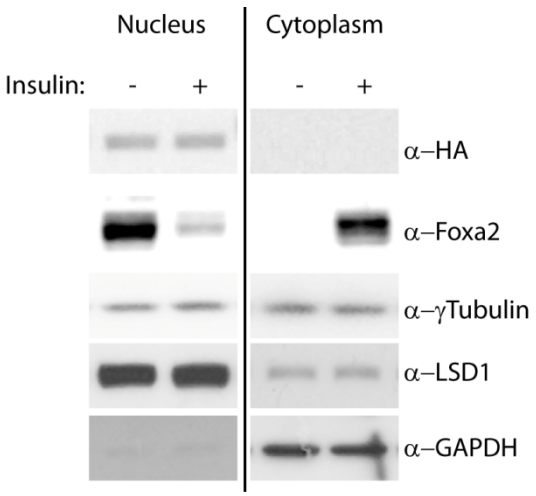

Figure 32. Nuclear/cytoplasmic shuttling of Foxa2 Emut *in vitro*. Immunoblots showing cellular fractionation of HepG2 cells stably expressing Emut Foxa2, serum-starved overnight and stimulated with 500nM insulin. γ-Tubulin was used as a general loading control, and LSD1 and GAPDH served as nuclear and cytoplasmic extraction controls, respectively.

To test whether this sequence is also necessary for export *in vivo* and thus might play an important role in the

hormonal regulation of Foxa2 activity we generated a recombinant adenovirus containing export mutant (Ad-Emut) Foxa2 and injected it into C57Bl/6 mice. As controls we treated mice with recombinant adenoviruses expressing wildtype (Ad-Foxa2) or phosphorylation-deficient, constitutively active Foxa2 (Ad-T156A), which have been previously characterized (10). All constructs were HA- and FLAG-tagged, and GFP adenovirus was used as an additional control. As shown in Figure 33, both endogenous and exogenous Foxa2 were nuclear in all fasted animals. However, while endogenous and Ad-Foxa2 were excluded from the nucleus in random fed animals, the export mutant (as well as the T156A control) remained nuclear. Thus, the newly identified NES in Foxa2 is responsible for the active nuclear export of Foxa2 in hepatotcytes both *in vitro* and *in vivo*.

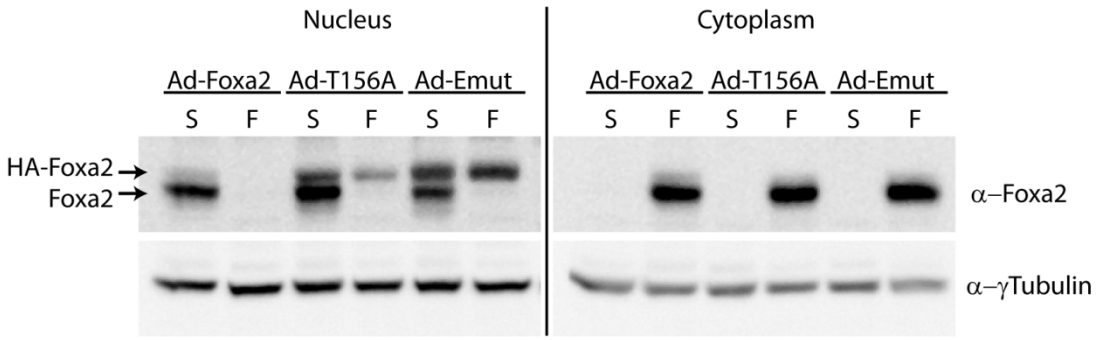

Figure 33. Ad-Emut is deficient in nuclear export *in vivo*. Immunoblots showing cellular fractionation of livers from C57BL/6 mice infected with GFP, Foxa2, T156A, or Emut adenovirus. Five days post-infection, mice were either fasted for 18 h (S) or *ad libitum* fed (F).

3.3 Emut Foxa2 is inhibited by insulin signaling

The ability to study the effect of phosphorylation uncoupled from subcellular localization of Foxa2 led us to ask whether regulation of Foxa2 activity by insulin is mainly controlled by nuclear export or by phosphorylation at T156. To explore this latter possibility, we first sought to determine if Emut Foxa2 could be efficiently phosphorylated through insulin signaling. Primary hepatocytes were isolated from C57Bl/6 mice, infected with the corresponding adenoviruses and serum starved overnight, followed by a 15 minute incubation with insulin. Exogenous Foxa2 was immunoprecipitated and subjected to western blot analysis with an anti-Foxa2T156-specific phosphopeptide antibody. Western blots show that Emut Foxa2 is phosphorylated to a similar extent as wildtype Foxa2, suggesting a segregation of postranslational modification and cellular localization.

To further clarify this point we generated recombinant adenovirus expressing a double Foxa2 mutant protein (TAE, Figure 31), containing both the Emut and T156A mutations. The T156A and TAE mutants, both of which lack the phosphorylation site and thus serve as negative controls, are not detected by the phospho-specific antibody (Figure 34).

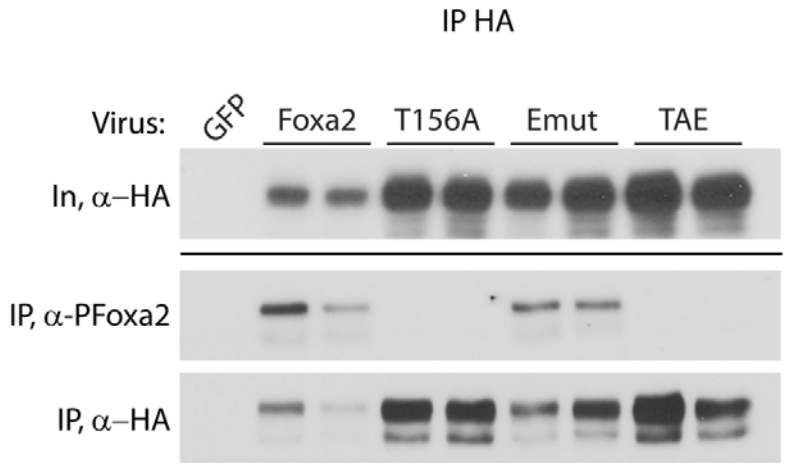

Figure 34. Insulin results in phosphorylation of Emut Foxa2. Primary hepatocytes isolated from C57BL/6 **mice were infected with the indicated adenovirus, serum starved overnight and stimulated with 100nM insulin. Whole cell extracts were subject to immunoprecipitation using an anti-HA antibody. Immunoblots of whole cell extracts and IPs were probed with antibodies against HA and phospho-Foxa2 (P-Foxa2).**

Since the export mutant is phosphorylated in response to insulin signaling, we hypothesized that, despite its nuclear localization, Foxa2 could still be inactivated by its Akt dependent phosphorylation. To test this hypothesis, we first expressed wildtype Foxa2, T156A, or Emut plasmids together with a reporter plasmid containing six Foxa binding sites of the murine *Cdx-2* gene upstream of firefly luciferase (6xCdx), with or without Akt2, in HepG2 cells. Reporter assays showed that while the export mutant retained transcriptional activity under basal conditions, cotransfection with Akt ablated this activity to a similar extent as wildtype (Figure 35). As a control, Foxa2T156A remained fully active with or without Akt coexpression. These data clearly demonstrate that on a functional level Foxa2 transcriptional activity is primarily regulated by posttranslational modification rather than by nuclear localization.

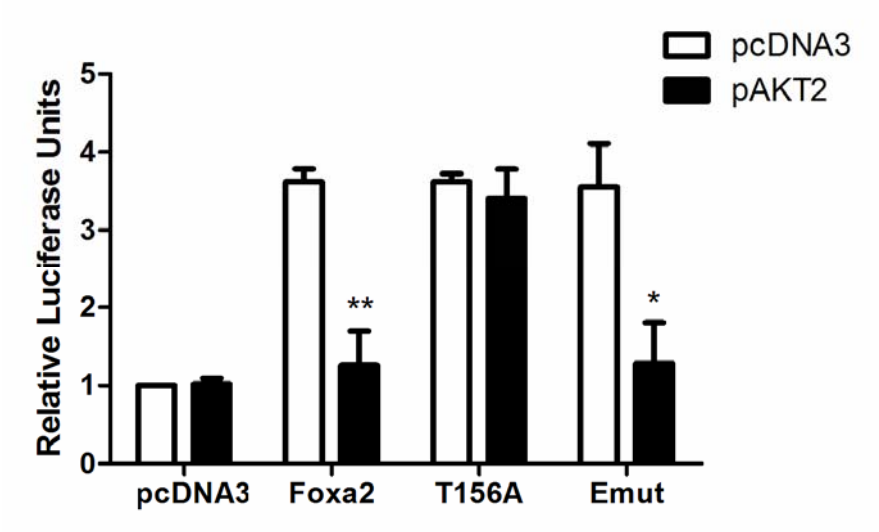

Figure 35. Akt inhibits transactiation by Emut Foxa2. HepG2 cells were transfected with expression vectors containing Foxa2 constructs, alone or in combination with Akt2. p6xCdx-TkLuc was used as a reporter gene. Luciferase activity was normalized to renilla luciferase, and shown relative to vector only controls. All experiments were performed in triplicate and values shown represent the mean of three independent experiments ± SEM. *, p< .05; **, p<.01 by unpaired t-test.

To test whether these functional changes translate to the binding of Foxa2 to its target promoter regions, we performed chromatin immunoprecipitations from C57Bl/6-derived primary hepatocytes infected with Ad-GFP, Ad-Foxa2, Ad-T156A, Ad-Emut and Ad-TAEmut. In a serum-starved state, all Foxa2 constructs were able to bind to known Foxa2 interaction sites in CPT1, HMGCS, and L-PK genes. However, after insulin stimulation, the wildtype and export mutant constructs were no longer found to bind the target sites, while binding of the T156A and TAE mutant Foxa2 proteins was unaffected by insulin (Figure 36). These data confirm the results obtained from the transactivation assays and show that phosphorylation determines binding of Foxa2 to its responsive promoter elements and that cellular localization is a secondary effect.

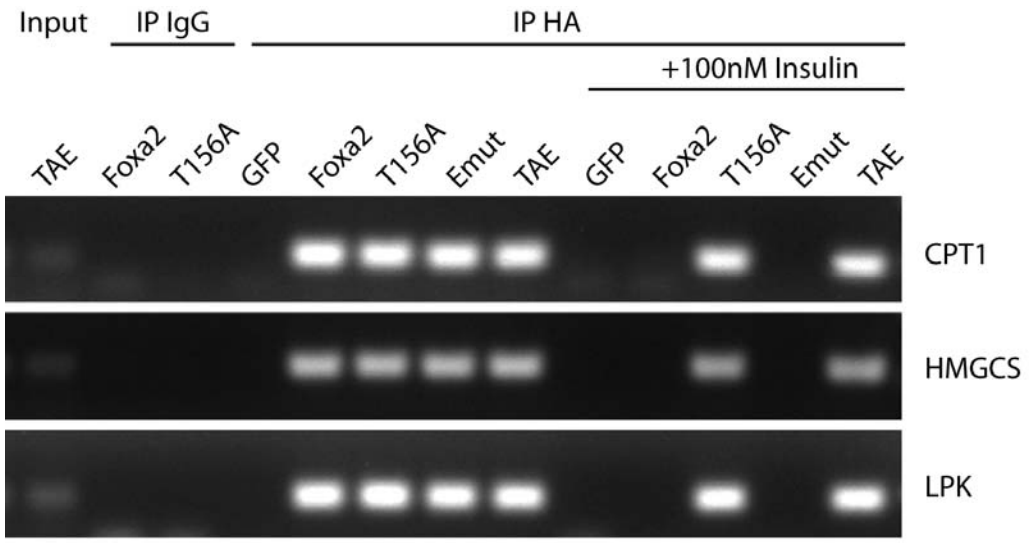

Figure 36. Insulin signaling disrupts promoter binding of Emut Foxa2. Chromatin immunoprecipitations from serum-starved or insulin-stimulated primary hepatocytes that were infected with the indicated adenoviruses. Chromatin was immunoprecipitated with HA or IgG (control) antibodies. Binding of Foxa2 and mutants to promoter sites in target genes was assayed by PCR. CPT1, carnitine palmitoyltransferase 1; HMGCS, HMG CoA synthase; L-PK, liver pyruvate kinase.

3.4 Emut is constitutively nuclear but inactive in hyperinsulinemic *ob/ob* mice

The effect of constitutive activation of Foxa2 is most striking in hyperinsulinemic mouse models that show constitutive inactivation of endogenous Foxa2 (10). Thus, to assess the importance of nuclear export on the physiological activity of Foxa2 in the context of metabolic disorders, and to elucidate whether the biological activities of Foxa2 mutants show the same regulation *in vivo*, we expressed Emut Foxa2 in the livers of *ob/ob* mice using recombinant adenoviruses. Transcriptional activity, and resulting metabolic and physiological consequences, were compared to age and sex-matched *ob/ob*

mice injected with either wildtype, T156A, or TAE Foxa2 adenoviruses. We previously demonstrated that endogenous and Ad-Foxa2 are constitutively cytoplasmic and inactive in hyperinsulinemic mouse models of type 2 diabetes, while Ad-T156A remains in the nucleus and is able to restore Foxa2 activity (10). Nuclear and cytoplasmic extracts from the livers of these mice confirmed that endogenous and Ad-Foxa2 are constitutively cytoplasmic, while the Ad-T156A, Ad-Emut and Ad-TAE Foxa2 constructs remain in the nucleus (Figure 37). Immuno-fluorescence microscopy was also used to confirm these results (Figure 38).

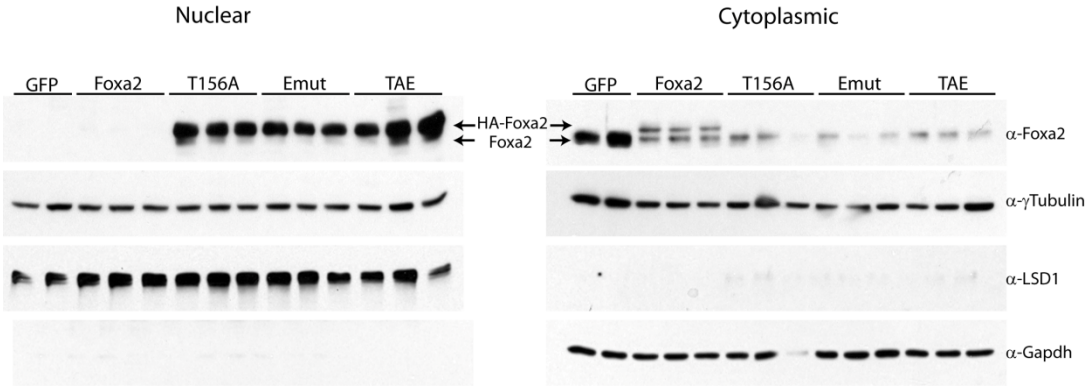

Figure 37. Emut is constitutively nuclear in *ob/ob* mice. *Ob/ob* mice were injected with the indicated adenovirus and livers were analyzed 10 days post-injection by cellular fractionation and immunoblotting. γ-Tubulin was used as a general loading control, and LSD1 (Lysine-specific demythlase 1) and GAPDH served as nuclear and cytoplasmic extraction controls, respectively.

To analyze the activity of the export mutant in these mice, which is the most important functional readout, we measured target gene activation by real-time PCR and assayed various metabolic parameters over 10 days. As expected, mRNA levels of Foxa2 target genes involved in mitochondrial fatty

acid oxidation and ketone body formation (MCAD, VLCAD, CPT1α, and HMGCS) were upregulated in livers of the T156A-injected mice, while no significant change was observed in mice injected with wildtype Foxa2. Consistent with our previous findings, Emut Foxa2 was unable to activate transcription of target genes in these hyperinsulinemic mice, while the double mutant TAE Foxa2 restored constitutive activation (Figure 39). As a control, we checked Foxa2 mRNA levels, which were upregulated roughly 2-fold in all mice, relative to Ad-GFP controls (Figure 40).

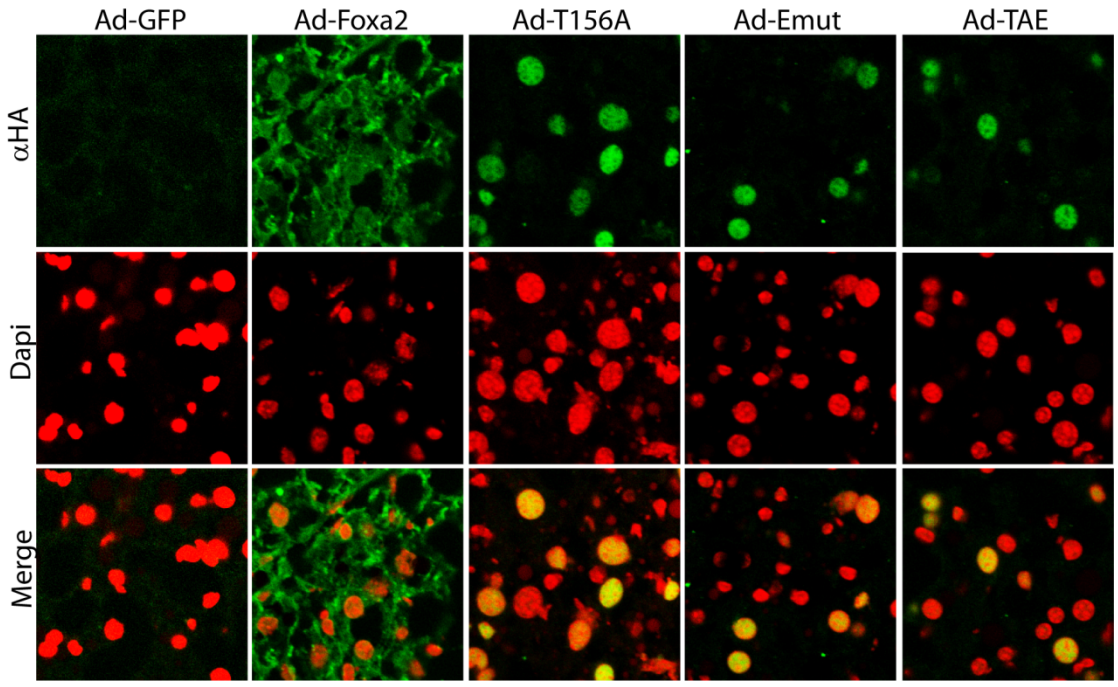

Figure 38. Immunofluorescence localization of Foxa2 variants in *ob/ob* liver. *Ob/ob* mice were injected with the indicated adenovirus and livers were frozen in OCT 10 days post-injection. Cryosections stained with anti-HA and Donkey anti-rabbit IgG Alexa Fluor 488 (Green) and Dapi (red) were visualized by fluorescence microscopy.

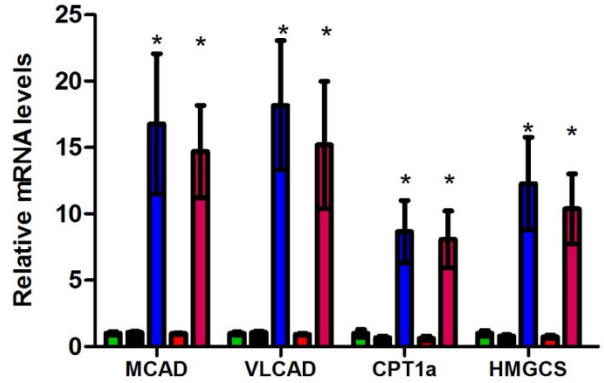

Figure 39. Mean mRNA levels of Foxa2 target genes in livers of *ob/ob* mice injected with the indicated adenovirus, n≥3. MCAD, medium chain acyl-CoA dehydrogenase; VLCAD, very long chain acyl-CoA dehydrogenase; CPT1α, carnitine palmitoyltransferase 1α; HMGCS, HMG CoA synthase. Colors as in Figure 40.

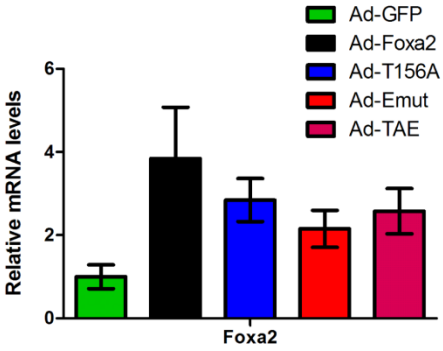

Figure 40. Foxa2 mRNA levels in adenovirus-injected *ob/ob* mice. Primers were designed to recognize both rat and mouse isoforms. Values shown represent the mean ± SEM, n≥3.

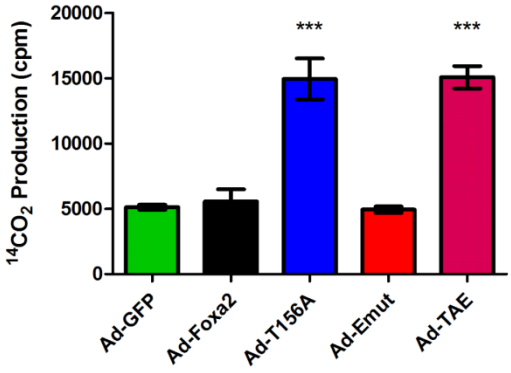

Figure 41. Emut does not activate mitochondrial β-oxidation in *ob/ob* livers. The formation of $^{14}CO_2$ from ^{14}C-palmitic acid was measured from liver mitochondrial extracts from *ob/ob* mice 10 days after injection with the indicated adenovirus. Values shown represent the mean ± SEM. *, p< 0.05; **, p<0.01; ***, p< 0.001 by unpaired t-test compared to Ad-GFP; n≥4.

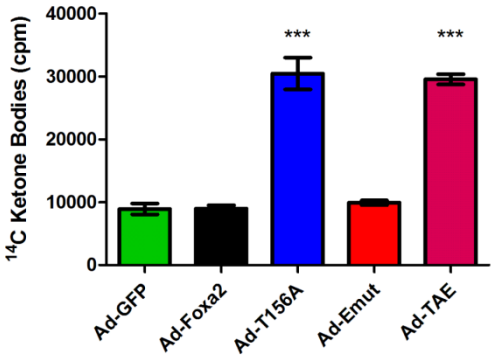

Figure 42. Emut does not activate liver ketone body production in *ob/ob* mice. The formation of ^{14}C-acid-soluble products from ^{14}C-palmitic acid was measured from liver mitochondrial extracts from *ob/ob* mice 10 days after injection with the indicated adenovirus. Values shown represent the mean ± SEM. *, p< 0.05; **, p<0.01; ***, p< 0.001 by unpaired t-test compared to Ad-GFP; n=4.

As a physiological readout, we measured hepatic mitochondrial fatty acid β-oxidation and ketone body production in the livers of hyperinsulinemic *ob/ob* mice that were infected with either Ad-GFP, Ad-Foxa2, Ad-T156A, Ad-Emut, or Ad-TAE. Consistent with the gene expression data, fatty acid oxidation and ketone body production remained unchanged in the Ad-Foxa2 and Ad-Emut injected mice, indicating that both are functionally inactive in hyperinsulinemic conditions. On the contrary, phosphorylation-deficient Ad-T156A and Ad-TAE groups were immune to inactivation by insulin and showed significant increases in fatty acid metabolism (Figure 41, Figure 42).

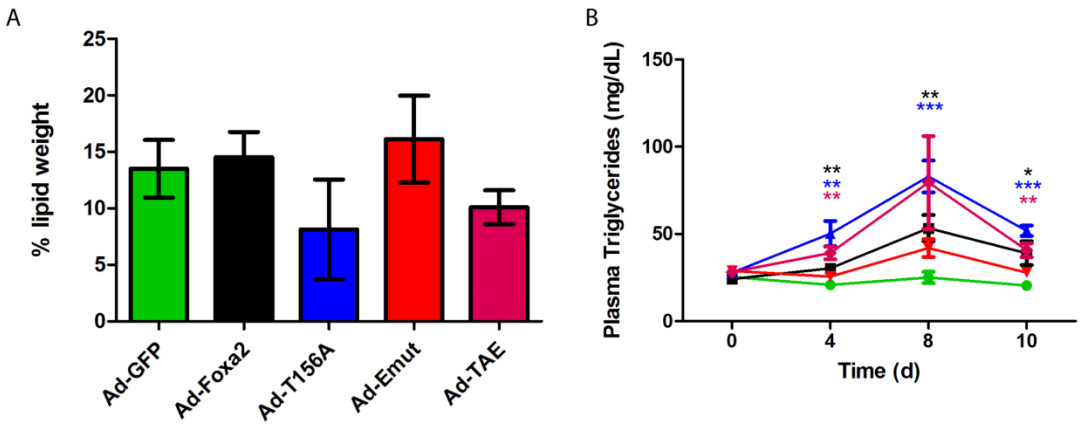

Figure 43. Liver and Plasma lipids in adenovirus-injected *ob/ob* mice. (A) Lipids were extracted from 50 mg of liver tissue by the Folch method, weighed and recorded as a percentage of the original tissue weight. (B) Triglycerides were measured from plasma samples taken after a moderate 6 hour fast over the course of the experiment. Values shown represent the mean ± SEM. *, p< 0.05; **, p<0.01; ***, p< 0.001 by unpaired t-test compared to Ad-GFP; n≥4.

As an additional readout of fatty acid metabolism we assayed liver lipids and plasma triglycerides. Hepatic lipid content (shown as percent wet weight) revealed a similar trend Figure 43A), with decreases observed only in Ad-

T156A and Ad-TAE groups. Plasma triglycerides showed an inverse trend (Figure 43B).

Blood glucose and plasma insulin levels were also measured in these mice, and both decreased significantly over 10 days in the T156A and TAE groups mice, whereas no decrease was seen in Ad-Foxa2 or Ad-Emut groups (Figure 44, Figure 45). In contrast to previous assumptions, these data demonstrate that nuclear exclusion is not necessary for insulin-induced transcriptional inactivation of Foxa2.

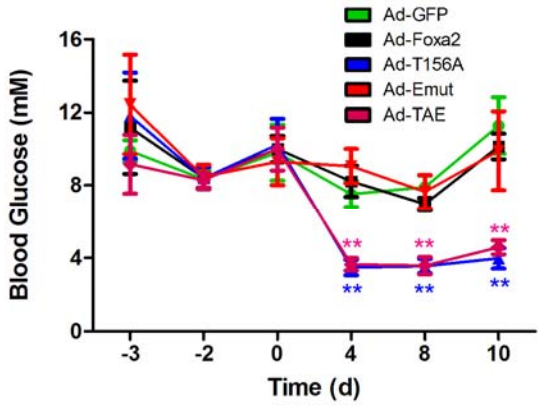

Figure 44. Emut is unable to normalize blood glucose in *ob/ob* mice. Blood glucose was measured from plasma samples taken after a moderate 6 hour fast over the course of the experiment. Values shown represent the mean ± SEM. *, p< 0.05; **, p<0.01; ***, p< 0.001 by unpaired t-test compared to Ad-GFP, n=5.

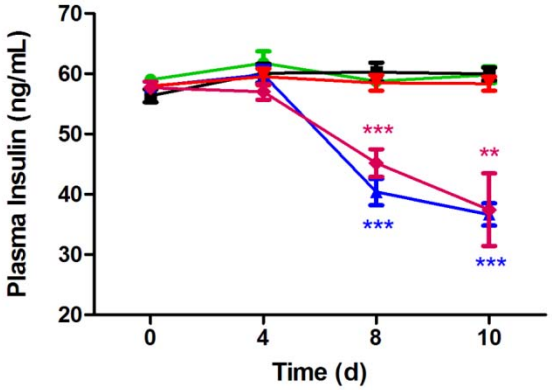

Figure 45. Emut is unable to decrease plasma insulin levels in *ob/ob* mice. Insulin was measured from plasma samples taken after a moderate 6 hour fast over the course of the experiment. Values shown represent the mean ± SEM. *, p< 0.05; **, p<0.01; ***, p< 0.001 by unpaired t-test compared to Ad-GFP; n=4.

3.5 Summary

Herein, we demonstrate that Foxa2 contains a functional CRM1-dependent (LMB-sensitive) nuclear export site, which is necessary for its nuclear exclusion in response to insulin stimulation. Our data clearly demonstrate that ablation of the nuclear export site, both *in vitro* and *in vivo*, results in constitutively nuclear Foxa2 that is still rendered transcriptionally inactive upon insulin stimulation. In addition, we have shown that phosphorylation at T156 is necessary for both nuclear export and transcriptional inactivation, since export mutants that are constitutively located in the nucleus are still phosphorylated by insulin signaling, and additional T156A mutation restores constitutive Foxa2 activity. Thus, we show here for the first time that intracellular relocation is a secondary effect and that Akt-dependent phosphorylation is a more direct determinant of Foxa2 activity and its physiological functions in maintaining hepatic lipid metabolism.

CHAPTER 4: Pulmonary Regulation of Foxa2 by insulin

4.1 Foxa2 expression in the lung

As previously mentioned, Foxa2 is expressed early in development in the node, notochord and floor plate, while in adult animals it is expressed in endodermally derived tissues such as the liver, pancreas, lung and gut (19, 31, 66, 67). While the lung is not generally considered an insulin-sensitive organ, it does play a role in metabolism. In addition to its respiratory functions, the lung has been demonstrated to act as a filter for certain metabolites, such as serotonin, and is the main source of angiotensin converting enzyme (ACE) (68). Perhaps the most well appreciated metabolic function of the lung, however, is the production and secretion of surfactant.

Pulmonary surfactant is an amphipathic lipoprotein complex composed of ~90% lipid and 10% protein (69). Its major function is to maintain low levels of surface tension at the air-liquid interface in lung alveoli, and thus allow for more efficient gas exchange, in addition to preventing lung collapse. For this reason, surfactant production is most critical for the transition to air breathing at birth, although it has also been linked to breathing disorders later in life. Both in mice and humans, mutations or deletions in the genes coding for surfactant protein B and C (SP-B and -C, two of the four major surfactant proteins), are associated with respiratory failure and interstitial lung diseases,

which can be lethal without lung transplantation (70, 71). More recently, additional proteins involved in surfactant production have been linked to respiratory diseases including proteins involved in lipid transport such as ABCA3 (ATP-binding cassette A3, a lipid transporter), as well as transcription factors regulating the expression of important surfanctant genes such as TTF-1 (thyroid transcription factor 1) and Foxa2 (72, 73).

In mice, Foxa2 is expressed in a subset of respiratory epithelial cells in the lung throughout development. In adult animals its pulmonary expression is restricted to epithelial cells of the bronchi, bronchioles, alveolar type II cells, and at lower levels in the trachea. Notably, its expression overlaps both temporally and spatially with the expression of key surfactant genes including SP-B, SP-C, CCSP and TTF-1, which have been shown to be Foxa2 targets (74-78). Furthermore, Wan and colleagues demonstrated that conditional deletion of Foxa2 in the lung impaired lung maturation and surfactant production, and resulted in respiratory failure and death, further emphasizing the crucial role of Foxa2 in lung development and surfactant production (79).

Despite the fact that the lung is not generally considered a metabolic organ, demonstration of such an important role for Foxa2 activation in the lung caused us to speculate as to whether insulin might also inhibit the activation of Foxa2 in the lung, and whether this might interfere with pulmonary function in hyperinsulinemic conditions. Indeed, Type 2 diabetes

has been suggested to be associated with certain chronic respiratory diseases such as asthma and COPD (80-82). While most of the genetic abnormalities discussed so far result in respiratory failure and lethality, chronic lung diseases are more common and less well understood (83). Additionally, there is known to be an increased risk of respiratory distress syndrome in newborns of diabetic mothers (84, 85). These mothers are generally hyperinsulinemic, but insulin resistant and therefore hyperglycemic. While insulin does not cross the placenta, glucose does, and an excess of blood glucose stimulates the fetal pancreas to produce more insulin, thus rendering the fetus hyperinsulinemic.

Taken toghether, these findings have led us to hypothesize that increased insulin levels may lead to nuclear exclusion and inactivation of Foxa2 in the lung, thus inhibiting transcription of important surfactant genes and providing a link between hyperinsulinemia and respiratory problems in type 2 diabetes.

4.2 Insulin induces nuclear exclusion of Foxa2 in the lung

To address whether insulin induces nuclear exclusion of Foxa2 in the lung, fasted C57Bl/6 mice were given injections of either PBS or PBS containing 600ng insulin. *Ob/ob* (leptin-deficient) mice were used as a model of hyperinsulinemia and were given no injections. 20 minutes post-injection the mice were sacrificed and nuclear extracts were made from whole lungs following a protocol previously established for the liver (10). Livers were

analyzed as a positive control and, as expected, livers derived from C57Bl/6 mice injected with insulin, as well as hyperinsulinemic *ob/ob* mice, showed nuclear exclusion of Foxa2 (Figure 21). Similarly, the lung showed clear nuclear exclusion of Foxa2 in response to insulin and in *ob/ob* mice, even with 25% more protein loaded in insulin and ob/ob lanes (Figure 46).

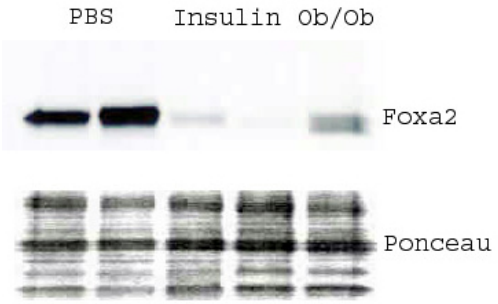

Figure 46. Nuclear exclusion of Foxa2 in lungs of insulin-treated and hyperinsulinemic mice. Western blots of nuclear extracts prepared from lungs and livers of fasted C57B6 and *ob/ob* mice injected with either PBS or 600 ng of insulin.

Though the predicted molecular weight of Foxa2 is 50 kDa, it generally runs around 55 kDa by SDS-PAGE. This is approximately the same mass as mouse IgG heavy chain, and the two polypeptides may comigrate in a gel. To ensure that the band we observed in the PBS lanes was not due to contaminating IgG (since a mouse monoclonal antibody was used to detect to Foxa2) we probed a control blot using only anti-mouse secondary antibody. After an hour long exposure (compared to a 4 minute exposure in Figure 46) we observed minimal IgG contamination, and the intensity of the

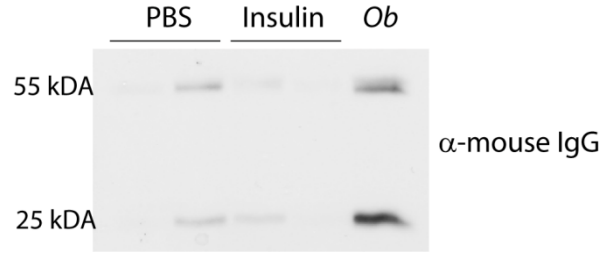

Figure 47. No effect of IgG contamination on shuttling of Foxa2. Blots from Figure 46 were preincubated with anti-mouse secondary antibody to control for background bands.

contaminating heavy chain species was higher in the ob/ob extracts than the PBS samples (Figure 47). Thus, detection of Foxa2 in these samples was not compromised by IgG contamination.

To determine whether this effect was relevant at physiological levels of insulin, we repeated the experiment in C57Bl/6 mice that were either fasted for 24 hours or allowed to eat normally, and again included *ob/ob* mice as a control. Nuclear extracts of lungs from these mice showed that postprandial insulin levels alone were enough to induce the nuclear exclusion of Foxa2 in fed mice (Figure 48). *Ob/ob* mice also showed clear nuclear exclusion of Foxa2. Ponceau staining or antibody against the generic TAF100 transcription factor were used as loading controls.

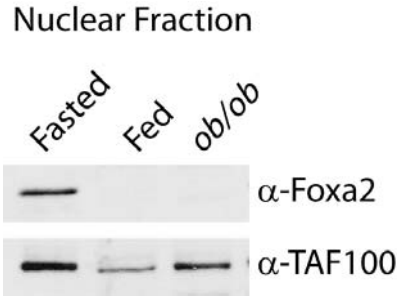

Figure 48. Nuclear exclusion of Foxa2 in lungs at physiological insulin levels. Immunoblot analysis of Foxa2 in nuclear extracts from livers of C57BL/6 **and *ob/ob* mice, fasted for 24 h or *ad libitum* fed. Nuclear extracts were prepared by sucrose gradient fractionation and each lane represents livers pooled from 2 mice.**

After development of the cellular fractionation protocol discussed in chapter 2, we repeated these experiments in triplicate in fasted, fed, insulin-injected C57Bl/6, and *ob/ob* mice. As expected, Foxa2 was once again found in the nucleus of lungs of fasted mice, but was excluded from the nuclear fractions in fed, insulin-injected and *ob/ob* mice (Figure 49). Accordingly, we

were able to see Foxa2 in the cytoplasmic fractions only in lungs from fed, insulin-injected and *ob/ob* mice.

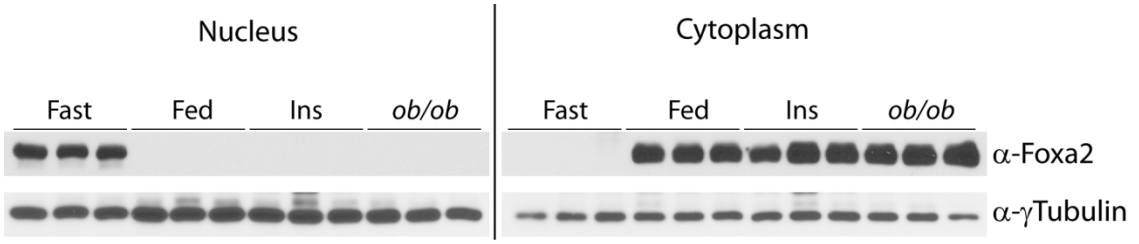

Figure 49. Foxa2 relocates to the cytoplasm in lungs of fed and hyperinsulinemic mice. Immunoblots of nuclear and cytoplasmic fractions from lungs of fasted, fed or insulin-injected C57Bl/6 mice, and fasted *ob/ob* mice.

4.3 Surfactant gene expression in adult lung

To determine whether the inhibition of Foxa2 in fed mice has an effect on surfactant gene expression we prepared RNA from lungs of fasted or *ad libitum* fed mice, and analyzed expression levels of candidate Foxa2 target genes by realtime PCR. While we did observe a slight decrease in SP-A , SP-B and Aqp3 (aquaporin 3, a water channel protein whose transcription is activated by Foxa2 in reporter assays (86)), only SP-A was significantly downregulated (Figure 50).

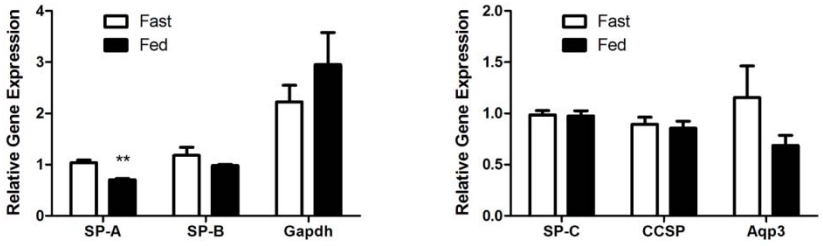

Figure 50. Surfactant gene expression in lungs of fasted and fed mice. RNA was prepared from lungs of C57Bl/6 mice that were fasted overnight or *ad libitum* fed. RNA was reverse transcribed and relative gene expression was measured by quantitative realtime PCR, normalized to either GAPDH (left panel) or 36B4 (right panel). Values represent the mean ± SEM; **, p<.01 by two-tailed students t-test relative to fasted controls, n≥3.

SP-A has been previously associated with Foxa2 due to its decreased expression in Foxa2$^{\Delta/\Delta}$ lungs, and there is evidence that insulin leads to inhibition of SP-A in a PI3-K-dependent manner (79, 87), suggesting that it could potentially be a direct target. However, this is debatable since reporter assays failed to show that Foxa2 can directly activate its transcription (79).

Since the expected downregulation of SP-B and CCSP in fed mice was not observed by realtime PCR we took a more unbiased approach to identify potential Foxa2 target genes that are regulated by nutritional status. mRNA was prepared from total lung RNA of fasted and fed C57Bl/6 mice, pooled, and compared by Affymetrix microarray hybridization. Table 2 shows the most downregulated and upregulated genes in the fed compared to the fasted state. Since Foxa2 generally acts as a transcriptional activator we consider the downregulated genes most likely to be direct targets of Foxa2.

Once again we saw no significant changes in surfactant genes, and no obvious target genes linking nutritional status to pulmonary function. It should be noted, however, that this experiment only compared lungs of adult, healthy, wildtype mice in fed and fasted states, and not more extreme hyperinsulinemic conditions. We therefore decided to investigate Foxa2 in a more demanding context.

Gene	Fold downregulation
chloride channel calcium activated 3	46.3
chitinase 3-like 4	23.6
eosinophil-associated, ribonuclease A family, member 11	6.9
resistin like alpha	6.6
cDNA sequence BC055107	4.7
serum amyloid A 3	4.4
solute carrier family 26, member 4	4.3
chloride channel calcium activated 1 ; chloride channel calcium activated 2	4.2
cDNA sequence BC055107	3.9
pyruvate dehydrogenase kinase, isoenzyme 4	3.9
anterior gradient 2 (Xenopus laevis)	3.5
angiopoietin-like 4	3.5
PREDICTED: zinc finger and BTB domain containing 16 mRNA	3.4
RIKEN cDNA 2210019G11 gene	3.4
Hexaribonucleotide binding protein 3 (Hrnbp3)	3.4
lysyl oxidase	3.3
Transcribed locus	3.3
UDP-N-acetyl-alpha-D-galactosamine:polypeptide N-	3.3
DNA-damage-inducible transcript 4	3.2
Gene	**Fold upregulation**
cathelicidin antimicrobial peptide	8.172
neutrophilic granule protein	3.838
major urinary protein 1 ; major urinary protein 2	3.704
lecithin-retinol acyltransferase (phosphatidylcholine-retinol-O-acyltransferase)	2.866
mannosidase 2, alpha B2	2.701
cytochrome P450, family 1, subfamily a, polypeptide 1	2.548
WNT1 inducible signaling pathway protein 1	2.479
Lecithin-retinol acyltransferase (Lrat), mRNA	2.455
chemokine (C-X-C motif) ligand 7	2.417
regulator of G-protein signaling 18	2.319
transmembrane protein 46	2.255
PREDICTED: Mus musculus RIKEN cDNA 9630020C08 gene	2.238
RIKEN cDNA 8430417A20 gene	2.221
DNA segment, human D4S114	2.217
checkpoint kinase 1 homolog (S. pombe)	2.201
limb-bud and heart	2.187
solute carrier family 7 (cationic amino acid transporter, y+ system),	2.174
tumor necrosis factor (ligand) superfamily, member 10	2.166
Insulin-like growth factor 1, mRNA (cDNA clone MGC:18617	2.165

Table 2. Highest down and upregulated genes in fed lung. Biotin-labelled cRNA samples from 5 fasted and 5 fed mice were pooled and hybridized to an Affymetrix GeneChip Mouse Genome 2.0 array. Shown are the 19 highest down and upregulated genes in fed compared to fasted mice.

4.4 Nuclear exclusion of Foxa2 in Fetal lungs

Since previous studies have demonstrated a critical role for Foxa2 in lung development and the transition to air breathing, we first investigated whether insulin also regulates the nuclear localization of Foxa2 in the fetus. Timed pregnancies were set up in wildtype C57Bl/6 mice and allowed to progress to embryonic day 19 (E19), at which point lung development is nearly complete (88). Pregnant females were either fasted, or allowed to feed freely for 16 hours prior to sacrifice, and cellular localization of Foxa2 was assessed in maternal and fetal liver and lung tissue. In accordance with previous data, Foxa2 is nuclear in maternal tissue from fasted mice, as well as in the lung and liver of fetuses from fasted mothers (Figure 51). This is in startk contrast to *ad libitum* fed pregnant females, where Foxa2 is excluded from the nucleus in maternal and fetal lung and liver (Figure 52). Here we demonstrate, for the first time, that Foxa2 shuttling also occurs in the fetus, and that its cellular localization is linked to the nutritional state of the mother.

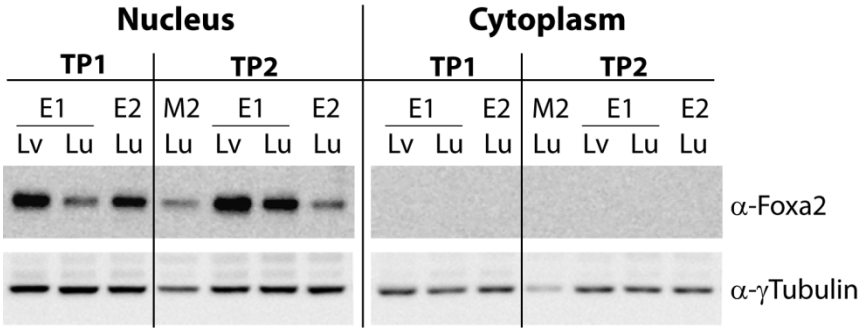

Figure 51. Foxa2 is nuclear in liver and lung of fasted fetuses. Nuclear and Cytoplasmic fractions from wildtype fasted maternal (M2) or E19 fetal (E1, E2) liver (Lv) and lung (Lu) were immunoblotted for Foxa2. TP1 and TP2 indicate individual timed pregnancies.

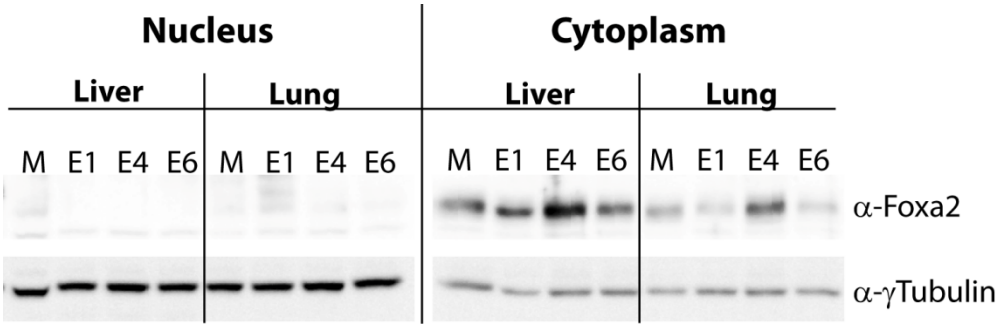

Figure 52. Foxa2 is cytoplasmic in fetal liver and lung of fed mice. Nuclear and Cytoplasmic fractions from wildtype *ad libitum* fed maternal (M) or E19 fetal (E1,4,6) liver and lung were immunoblotted for Foxa2.

Since insulin does not cross the placenta, we could not directly test the effect of insulin on the localization of Foxa2 in fetal tissues by injection. Instead, we took advantage of two mouse models of diabetes that are hyperglycemic and thus induce hyperinsulinemia in the fetus.

SREBP-1cAp2 (SREBP) transgenic mice, express nuclear Sterol regulatory element-binding protein (SREBP) 1c only in adipose tissue, but subsequently have a pronounced type 2 diabetic phenotype with marked hyperinsulinemia, insulin resistance and hyperglycemia (89). Previous data from the lab has shown that Foxa2 is constitutively cytoplasmic and inactivate in livers of these mice (10). We now show that Foxa2 is also constitutively cytoplasmic in lungs of these mice. Additionally, maternal hyperglycemia in these animals is able to signal a constant "fed" state even in these fasted mice, and thus triggers insulin secretion, as evidenced by nuclear exclusion of Foxa2 in fetal lungs of these mice (Figure 53).

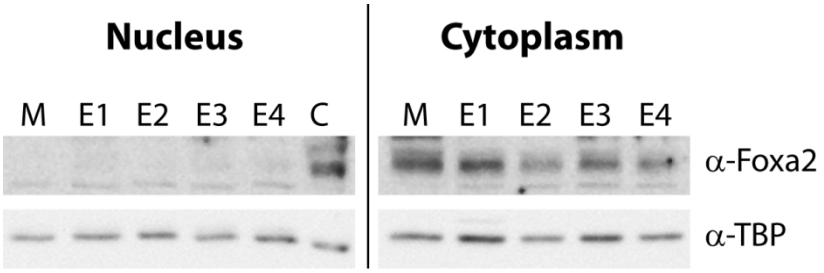

Figure 53. Nuclear exclusion of Foxa2 in fetal lungs of SREBP mice. Immunoblots of nuclear and cytoplasmic extracts from lungs of fasted SREBP mice. M, maternal lung; E1-4, E19 fetal lung; C, fasted lung whole cell lysate as a control; TBP, TATA binding protein.

The second mouse model we used to demonstrate the effect of aberrant insulin signaling on Foxa2 localization in fetal tissue is streptozotocin-induced diabetic mice, a model for Type I diabetes. Streptozotocin (stz) targets and kills pancreatic beta cells, inducing hypoinsulinemia and, consequently, hyperglycemia. Thus, these mice provide an elegant approach to studying the effects of maternal hyperglycemia on Foxa2 localization in wildtype fetuses. Fasted stz-treated mothers, in accordance with their hypoinsulinemic state, show Foxa2 localization in the nucleus in liver and lung (Figure 54).

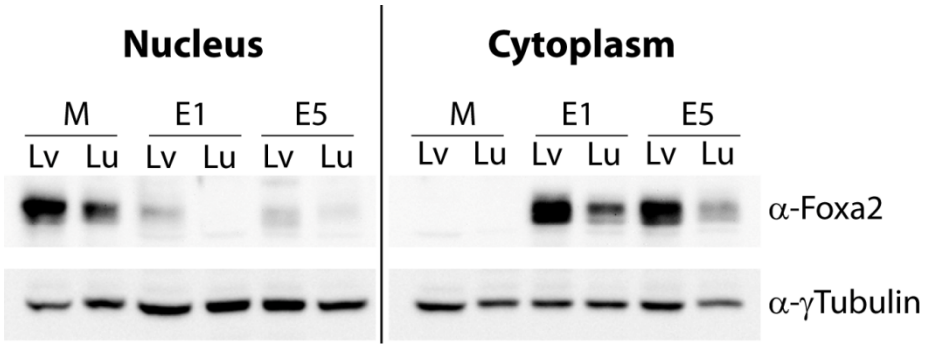

Figure 54. Differential Foxa2 localization in maternal and fetal livers and lungs of Stz mice. Pregnant C57Bl/6l mice were given injections of 3x75 mg/kg stz on E14-16. Mice were fasted on E18, sacced on E19 and nuclear and Cytoplasmic fractions maternal (M) or E19 fetal (E1, E5) liver (Lv) and lung (Lu) were subject to immunoblot analysis.

Conversely, fetuses of these hyperglycemic mothers retain beta cell function and secrete insulin, which results in cytoplasmic relocalization of Foxa2 only in fetal tissues (Figure 54).

To study the effect of hyperinsulinemia on gene regulation in fetal lungs we compared mRNA expression profiles from wildtype, fasted fetuses and stz-treated fetuses. Agilent microarray analysis revealed 37 genes which were found to be significantly downregulated and 103 genes significantly upregulated more than 2 fold in stz-lungs compared to fasted wildtype controls (Table 3).

While we have not yet verified any of these genes in the lung, preliminary cDNA analysis of fetal livers from stz and wildtype fasted fetuses by RTPCR shows a significant decrease in known Foxaa2 target genes including MCAD, VLCAD and CPT1 (Figure 55). This analysis was preliminary due to the limited n number, however it suggests that the model is sound. It is also reassuring to note that several of the top downregulated genes in the agilent list have already been linked to Foxa2 in the literature. Reg3g, has been shown to be a Foxa2 target gene *in vitro*, and is the highest downregulated in our list (90). Scgb3a1, the second most downregulated gene in stz-lungs is a homolog of CCSP, a secrotoglobulin also regulated by Foxa2 (91). Additionally, muc5b (mucin 5b) is a related to muc2, the main component of intestinal mucous which is regulated by Foxa1 and 2 in intestinal eplithelial cells (92).

Gene	Fold downregulation	Gene	Fold downregulation
Reg3g	78.98	A_52_P444116	3.77
Scgb3a1	31.79	Chst5	3.55
Muc5b	31.34	Krt5	3.31
Agr2	22.71	Klk10	3.26
Mfi2	16.90	Vip	3.23
1110017I16Rik	16.67	A_52_P686218	3.02
Matn3	14.50	A_52_P257026	2.95
Col9a1	11.89	B230303O12Rik	2.92
C1qtnf3	10.69	2310068J10Rik	2.91
Col9a3	9.74	AK163997	2.87
Lect1	8.63	Gzmb	2.85
3110079O15Rik	8.34	D130076A03Rik	2.69
Agc1	7.96	Mfsd2	2.64
Chac1	7.22	Abcg5	2.51
Adh7	5.65	Nr1i3	2.41
Cart	5.22	AK154840	2.37
A930038C07Rik	4.71	E430002D04Rik	2.03
BC006965	4.36	Nptxr	2.01
9030611K07Rik	4.05		
Gene	**Fold upregulation**	**Gene**	**Fold upregulation**
Pln	**169.7**	Akr1b7	**4.8**
Prap1	**71.3**	Serpina1e	**4.8**
Ckmt2	**65.3**	Agxt	**4.8**
Nppa	**25.5**	Cyp3a41	**4.7**
Ftcd	**21.5**	Kng1	**4.7**
Dhrs7c	**15.5**	F13b	**4.6**
C78409	**14.8**	Cps1	**4.5**
Xist	**14.4**	Fabp1	**4.4**
Apoa5	**10.1**	Abcb11	**4.3**
Nefh	**8.1**	Pck1	**4.1**
Pah	**7.6**	Slc10a1	**4.1**
9630020C08Rik	**5.9**	Apoa1	**4.0**
Cyp3a16	**5.8**	Sult1d1	**4.0**
Slco1b2	**5.7**	Bhmt2	**4.0**
Fthl17	**5.7**	Dmgdh	**4.0**
Ankrd1	**5.4**	Hsd17b13	**3.9**
Hfe2	**5.4**	Clec4f	**3.9**
Angptl3	**5.1**	Serpina1b	**3.7**
Bhmt	**5.0**	Spp2	**3.6**

Table 3. Genes altered in fetal lungs of stz-mothers. Highest up and downregulated genes in stz compared to fasted fetal lungs were identified using 4x44 Agilent whole mouse genome microarray service (miltenyi) and further analyzed using GenespringGX software.

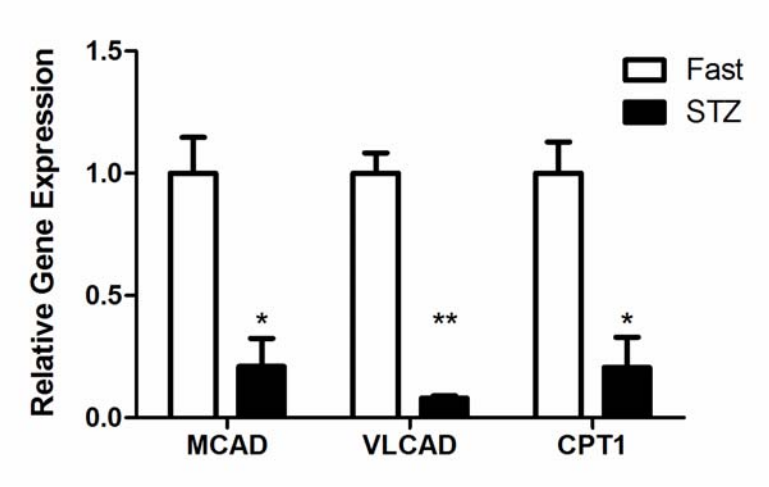

Figure 55. Foxa2 β-oxidation genes are inhibited in fetal livers of stz mothers. Realtime PCR analysis of Foxa2 target genes in cDNA made from livers of fetuses from C57Bl/6 fasted or stz-induced diabetic mothers. Values are means, normalized to GAPDH ± SEM shown relative to fasted fetal liver samples, which were sset to 1. *, p≤.05; **, p ≤ 0.01. MCAD, medium chain acyl-CoA dehydrogenase; VLCAD, very long chain acyl-CoA dehydrogenase; CPT1, carnitine palmitoyltransferase 1α. n≥2.

4.5 Summary

Though the lung is not considered a major metabolic organ, we have found that Foxa2 localization is regulated by insulin in the lung as it is in the liver. In lungs of adult mice Foxa2 is excluded from the nucleus following insulin injection, as well as by physiological levels of insulin experienced in the fed state. Furthermore it is constitutively cytoplasmic in lungs of hyperinsulinemic *ob/ob* mice. The increased incidence of lung disorders in babies of diabetic mothers, which are similar to that observed in Foxa2 lung conditional knockout mice, led us to search for a correlation between hyperinsulinemia, Foxa2 inactivation, and the production of surfactant proteins. In lungs of adult mice, RTPCR and microarray analysis failed to provide clear evidence that Foxa2 inactivation in the fed state links nutritional

status to pulmonary function. However, we did observe a slight but significant downregulation in SP-A gene expression by RTPCR.

While microarray analysis of gene expression in fetal lungs from stz-induced diabetic mothers was also unable to directly correlate Foxa2 regulation to surfactant production, we do clearly observe insulin-dependent inactivation of Foxa2 both in fetal liver and lung. In normal mice and in mouse models of diabetes, we find that Foxa2 in the embryonic lung (and liver) is excluded from the nucleus in conditions of high blood glucose. This sensitivity of Foxa2 to maternal glycemic state leaves open the possibility that there is a link between diabetic mothers and fetal lung development and function.

CHAPTER 5: Shuttling of Foxa2 in the Hypothalamus

5.1 Hypothalamic expression of Foxa2

In addition to aforementioned regions, Foxa2 is also expressed in the brain, including certain regions of the hypothalamus (19). Using Xgal knock-in mice (*Foxa2*$^{+/lacZ}$) in which one allele of Foxa2 is replaced by the LacZ gene, we have further mapped the expression of Foxa2 in the central nervous system. X-gal staining was observed in the lateral hypothalamic area, paraventricular hypothalamic area, zona incerta, and substantia nigra (Silva J, unpublished data). However, the function of Foxa2 in these cells is not well understood. Given the newly emerging view of Foxa2 as an important sensor and regulator of metabolic genes, we found its expression in the lateral hypothalamus (considered to be the feeding center of the brain) to be of particular interest (93).

While the hypothalamic role of Foxa2 has not yet been appreciated, the anorectic effects of insulin and its subsequent activation of the phospatidylinositol 3 kinase (PI3K)/IRS/Akt signaling pathway in the hypothalamus are well documented (94-96). In the arcuate nucleus, these effects have been shown to be mediated in part by suppression of orexigenic neuropeptides such as neuoropeptide Y (Npy) and *Agouti*-related protein (Agrp), while activating the expression of anorexigenic Pomc

(proopiomelanocortin) at the same time (97). Inactivation of Foxo1 by insulin and leptin has been shown to play a key role in these regulatory events (98).

Neurons in the lateral hypothalamus also respond to feeding and fasting, and control food intake as well as spontaneous physical activity due in large part to the effects of orexin and MCH (99, 100). However, the mechanism and metabolic stimuli controlling their regulation in response to feeding and fasting is unknown. Dual immunofluorescence labeling with Foxa2 and MCH or orexin reveals that all MCH and orexin positive neurons also express Foxa2 (Silva J, unpublished data). Thus we hypothesized that insulin-induced nuclear exclusion of Foxa2 could mediate feeding-induced inhibition of MCH and orexin, and thus appetite and food seeking behavior.

5.2 Insulin induces nuclear exclusion and inactivation of Foxa2 in the hypothalamus

To begin to address the role of Foxa2 in the hypothalamus, we first sought to determine whether it is inactivated by insulin signaling in this portion of the brain. Hypothalami were dissected from fasted or *ad libitum* fed wild type mice, subjected to cellular fractionation and assayed for nuclear exclusion. As shown in Figure 56, Foxa2 is nuclear in hypothalami from fasted mice, but cytoplasmic in fed mice.

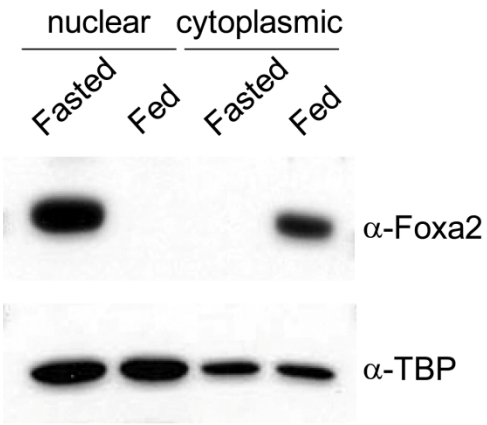

Figure 56. Insulin induces nuclear exclusion of hypothalamic Foxa2. Immunoblot analysis of nuclear and cytoplasmic extracts prepared from pooled hypothalami from 3 mice each that were either fasted overnight or ad libitum fed. TBP, TATA binding protein.

To demonstrate that this regulation is due specifically to increased postprandial insulin levels and not blood glucose concentrations, we isolated hypothalami from fasted wildtype mice and incubated them *ex vivo* in basal media with low glucose, high glucose, or low glucose plus insulin. Neither low nor high glucose concentrations are sufficient to induce nuclear export of Foxa2, however Foxa2 did shuttle when insulin was added to the low glucose media (Figure 57)

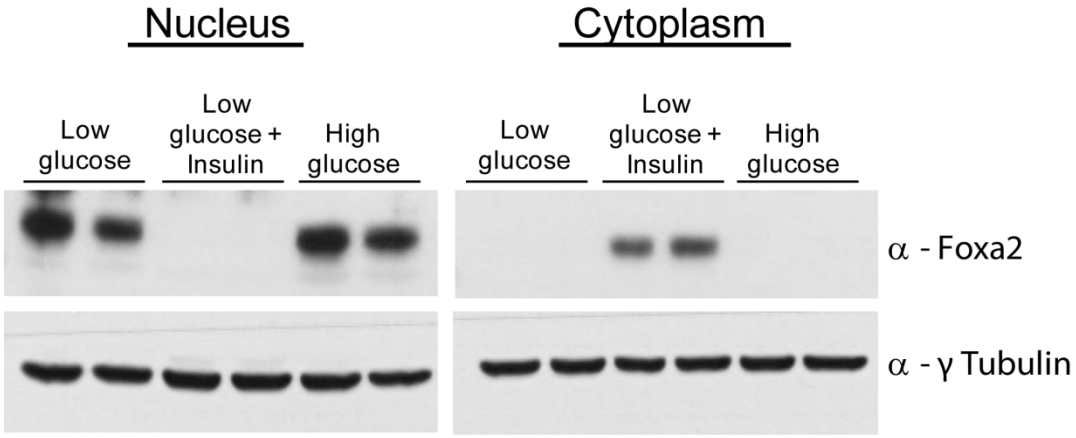

Figure 57. Hypothalamic nuclear exclusion of Foxa2 is insulin and not glucose-dependent. Immunoblot analysis of nuclear and cytoplasmic extracts prepared from hypothalami incubated *ex vivo* in DMEM with either low (5 mM) or high (16 mM) glucose, in the absence or presence of 10 ng/mL of human recombinant insulin.

In order to study the effects of constitutive inactivation of Foxa2 in the hypothalamus, we analyzed high fat diet-induced obese mice, which provide a hyperinsulinemic model of type 2 diabetes. As expected, high fat diet-induced

obesity and the corresponding increases in plasma insulin result in constitutive nuclear exclusion of Foxa2 in the hypothalami of these mice. While Foxa2 is completely nuclear in fasted chow fed mice, cytoplasmic levels of Foxa2 in hypothalmi from high fat diet-fed mice are similar to those of *ad libitum* fed controls (Figure 58).

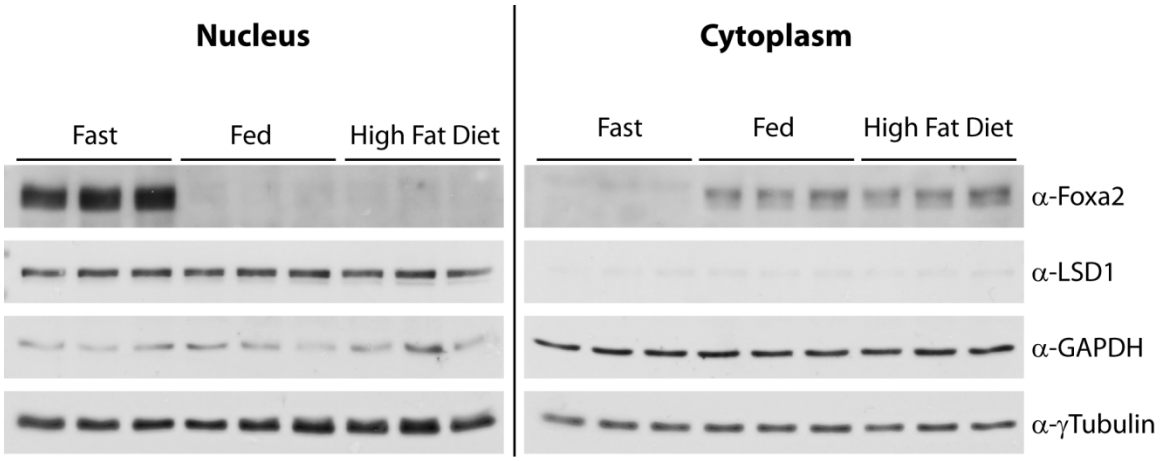

Figure 58. Foxa2 is constitutively cytoplasmic in hypothalami from high fat diet-fed mice. Immunoblot analysis of nuclear and cytoplasmic extracts prepared from hypothalami of fasted, fed or fasted high fat diet-fed mice. Each lane represents hypothalami pooled from 2 mice. γ-Tubulin was used as a general loading control, and LSD1 (Lysine-specific demythlase 1) and GAPDH served as nuclear and cytoplasmic extraction controls, respectively.

Correspondingly, expression of both MCH and orexin was decreased by ~60% in hypothalami of fed and high fat diet-fed mice, compared to fasted controls (Figure 59). Further work in the lab has shown that MCH and orexin are direct targets of Foxa2 in transactivation and chromatin immunoprecipitation experiments.

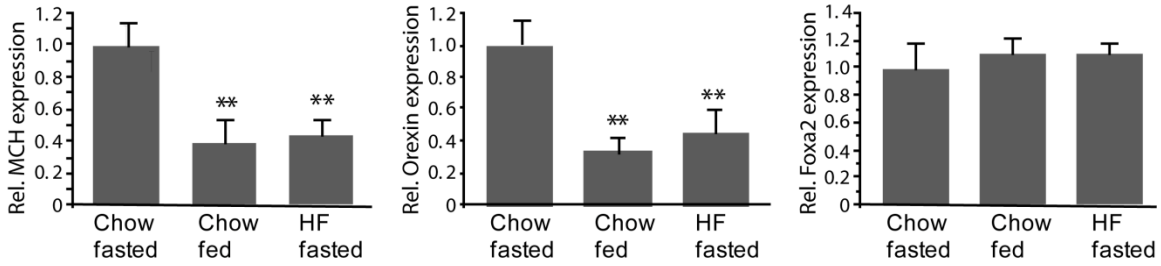

Figure 59. Real-time RT-PCR analysis of MCH and orexin in fasted, chow fed and fasted, high fat diet-fed (HF) mice. Results are expressed as amount of cDNA normalized to GSPDH cDNA. The values represent the mean ± sem (n=5 in all groups; *, P<0.05; **, P<0.01).

5.3 Constitutive activation of Foxa2 in the hypothalamus

In order to show that Foxa2 activation is sufficient to induce metabolic changes associated with MCH and orexin we constitutively activated Foxa2 in hypothalamic nuclei by 3 different means. First, conditional mutant mice with a constitutively active Foxa2-T156A allele were generated by introducing loxP sites upstream and downstream of exon 3, which encodes most of the open reading frame of Foxa2 as well as the 3' untranslated region. An exon 3 duplication, harboring the T156A mutation, was introduced downstream of the floxed wildtype exon 3 and neuron specific recombination was obtained by breeding to nestin-Cre mice. These mice show significantly increased expression of MCH and orexin, as well as CPT1, MCAD and VLCAD, Foxa2 target genes involved in mitochondrial β-oxidation (Figure 60).

Accordingly, these mice show a significant enhancement of metabolic function. Serum glucose levels, plasma insulin levels and serum free fatty acid concentrations are all decreased in the fed state in Nes-Cre/Foxa2T156A$^{fl/fl}$

mice compared to control littermates (Figure 61). Glucose clearance from the circulation following an insulin tolerance test is modestly increased in Nes-Cre/Foxa2T156A$^{fl/fl}$ mice, indicating increased insulin sensitivity (Figure 61).

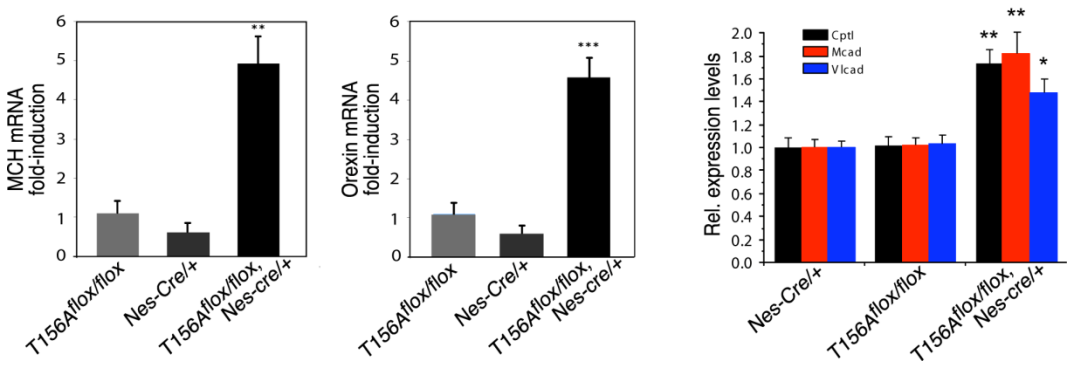

Figure 60. Real-time RT-PCR analysis of gene expression in mice with neuron-specific activation of Foxa2. cDNA was prepared from hypothalami of fed *Nescre/+, Foxa2T156A*$^{fl/fl}$ mice, fed *Foxa2T156A*$^{fl/fl}$ mice and fed *Nescre/+* mice. Relative expression of MCH, Orexin, CPT1, Mcad, and Vlcad was normalized to β-actin or GAPDH housekeeping genes. The results are expressed as fold-induction over fed *Foxa2T156A*$^{fl/fl}$ mice and represent the mean ± SEM.

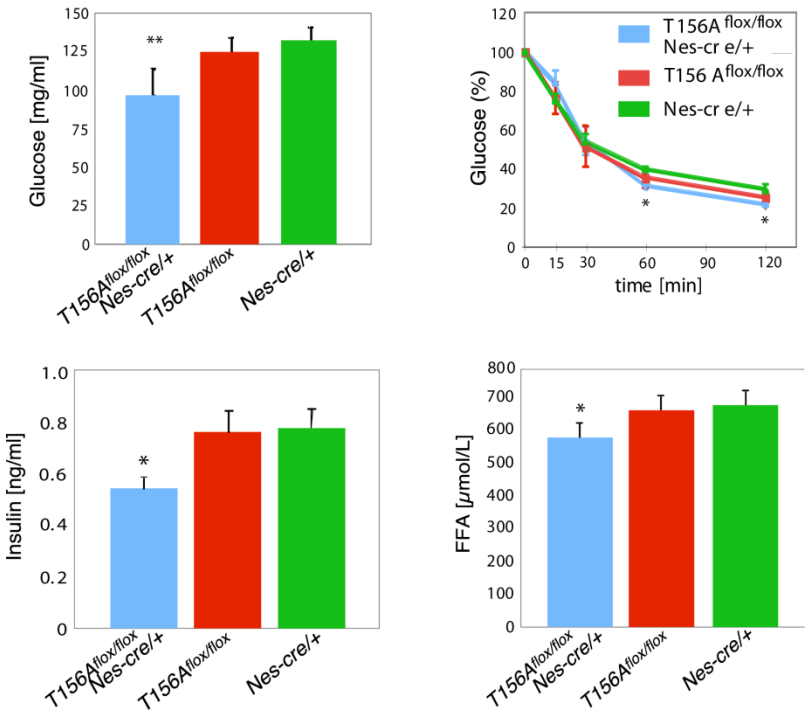

Figure 61. Altered serum parameters in Nes-Cre/Foxa2T156A$^{fl/fl}$ mice. Blood glucose, percentage of starting plasma glucose concentration during an insulin tolerance test, plasma insulin and plasma Free fatty acids were measured in in *Nescre/+, Foxa2T156A*$^{fl/fl}$ mice, *Nescre/+* mice, and *Foxa2T156A*$^{fl/fl}$ mice.

Measurements of metabolic rates reveal that Nes-Cre/Foxa2T156A fl/fl mice have increased O_2 consumption and CO_2 production, and exhibit dramatic increases in spontaneous physical activity over 24 hours compared to Nes-Cre/+ and Foxa2T156A fl/fl control mice (Figure 62). Food consumption and drinking volume are also increased in Nes-Cre/Foxa2T156A fl/fl animals (Data not shown).

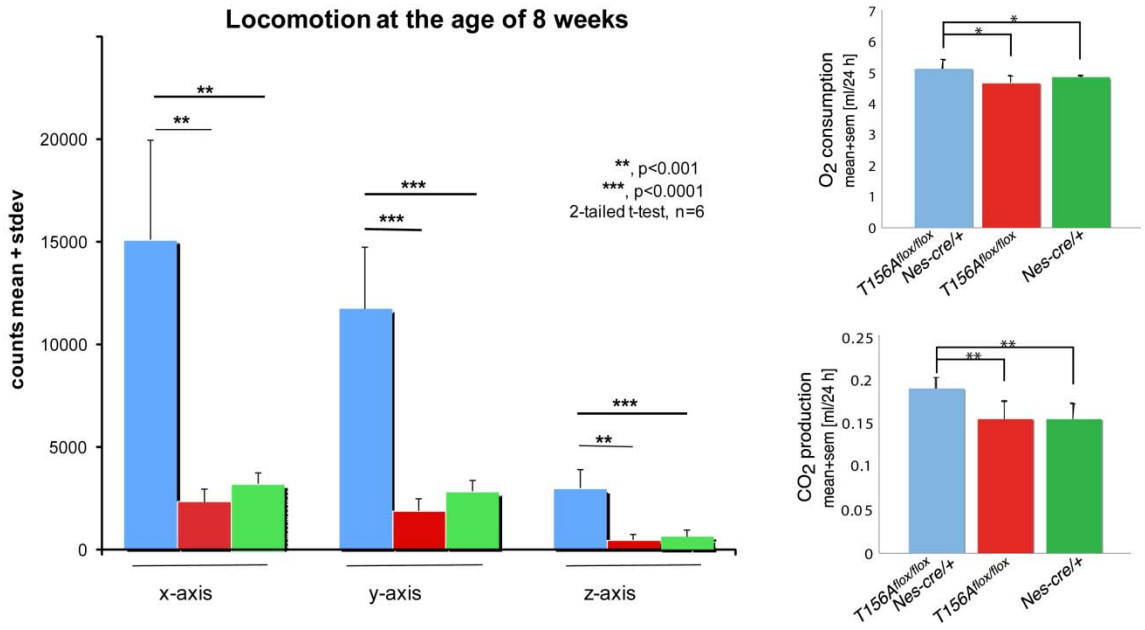

Figure 62. Altered metabolic parameters in Nes-Cre/Foxa2T156A fl/fl mice. Spontaneous physical activity during a light phase 12 hr interval, oxygen consumption and CO_2 production were determined simultaneously during a 24-h period in individual mice using an oxymax metabolic chamber system.

To ensure that these effects were not due to activation of Foxa2 in neurons outside of the hypothalamus we used two alternate methods to express constitutively active Foxa2 specifically in the hypothalamus: injection of constitutive Foxa2-T156A adenovirus into the hypothalamus of wildtype mice,

and direct injection of adenovirus CRE into hypothalami of Foxa2T156A fl/fl mice. Cellular fractionation confirmed the expression and constitutively nuclear localization of Foxa2-T156A in fed mice injected with either Ad-T156A or Ad-Cre, while endogenous Foxa2 is cytoplasmic (Figure 63, Figure 64). Both of these methods achieved similar results to the Nes-Cre/Foxa2T156A fl/fl experiments, demonstrating that the metabolic phenotypes are due to constitutive activation of Foxa2 in the hypothalamus.

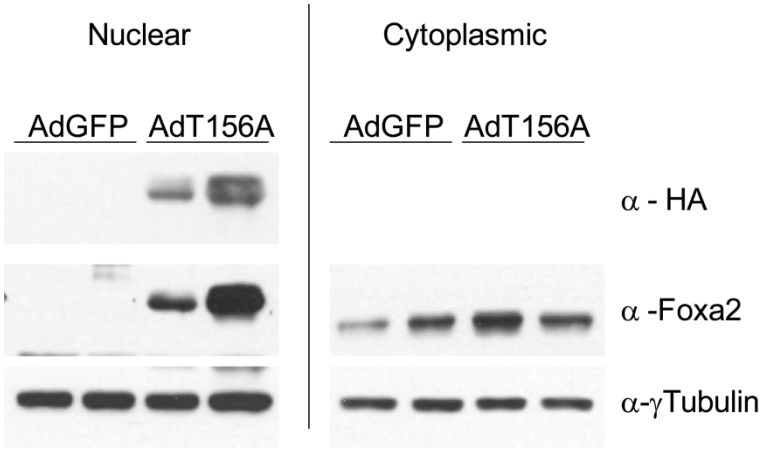

Figure 63. Hypothalamic expression and localization of Foxa2 after AdT156A injection. C57Bl/6 mice were given hypothalamic injections of adenovirus expressing GFP or Foxa2-T156A. Immunoblots of cellular fractionation experiments are shown.

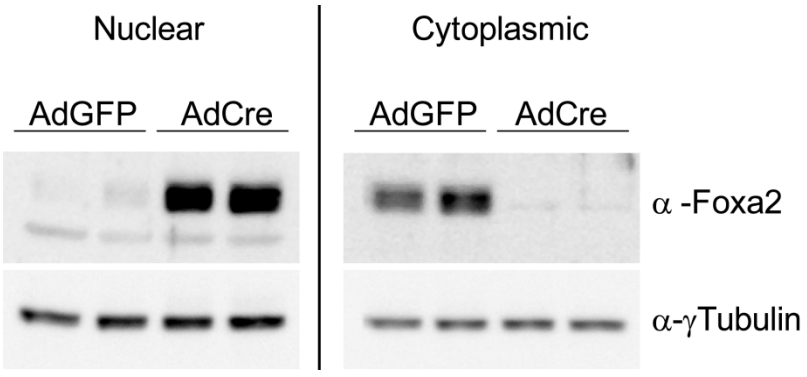

Figure 64. Hypothalamic expression and localization of Foxa2 after AdCre injection in Nes-Cre/Foxa2T156A fl/fl mice. Nes-Cre/Foxa2T156A fl/fl mice given hypothalamic injections of either GFP or Cre adenovirus. Immunoblot analysis of nuclear and cytoplasmic fractions are shown.

5.4 Summary

These studies reveal a molecular mechanism by which insulin controls the feeding/fasting response of the lateral hypothalamus. In fasting conditions, Foxa2 acts as a direct transcriptional activator of MCH and orexin genes, thereby stimulating classical fasting responses such as feeding, behavioral arousal and spontaneous physical activity. In the fed state, Foxa2 is phosphorylated by insulin/PI3K/Akt signaling, which leads to Foxa2 inactivation and nuclear exclusion. Interestingly, MCH and orexin expression is regulated by the same metabolic stimuli and molecular signaling pathway, thereby integrating metabolic and adaptive behavioral responses. Similar to what we have shown for the liver and lung, Foxa2 is permanently inactive in MCH and orexin neurons in hyperinsulinemic states such as type 2 diabetes, resulting in reduced MCH and orexin expression. Conditional constitutive activation of Foxa2 in the hypothalami of these mice leads to increased physical and metabolic activity, improved glucose homeostasis, and increased insulin sensitivity.

DISCUSSION

Affect of genetic variation on Foxa2 regulation and associated metabolic activity

While data support a role for Foxa2 as a metabolic transcription factor, there is conflicting evidence regarding its inactivation, particularly its nuclear exclusion by insulin. Our studies confirm that Foxa2 can be inactivated through insulin-induced nuclear exclusion in all mouse strains tested. However, marked differences exist in the modulation of metabolic pathways by insulin signaling with respect to background genetic strain differences. The inherent metabolic differences in the strains studied are exemplified by their responses to high fat diets. C57Bl/6 mice are generally more obese, glucose intolerant, and hyperinsulinemic on high fat diets and exhibit higher levels of liver triglycerides, increased hepatic steatosis, and insulin sensitivity than their 129 counterparts (101) (102). These findings are in line with our observations, which demonstrate that in addition or due to having lower insulin levels, Sv129 mice have higher rates of β-oxidation and increased oxygen consumption in comparison to C57/B6 mice. Accordingly, only in C57Bl/6 and dba mice were the postprandial levels of insulin high enough to effect nuclear exclusion of Foxa2 under physiological circumstances. These data provide a plausible

explanation for the observed discrepancies in nuclear exclusion of Foxa2 reported by Zhang et al (11).

We also demonstrate that primary hepatocytes from hyperinsulinemic insulin resistant mice (*ob/ob*, *db/db* and HF-diet induced obese mice) are capable of shuttling Foxa2 back into and out of the nucleus in culture, while Foxa2 is always cytoplasmic in livers of these mice *in vivo*. These data demonstrate that hepatocytes from these mice are not defective, but accurately reflect the insulin concentrations to which they are exposed.

Not only do our data demonstrate the importance of genetic background on metabolism and Foxa2 regulation, but we also find the inverse to be true: the activation state of Foxa2 is sufficient to account for some of these observed metabolic alterations. While constitutive activation of Foxa2 in Sv129 mice has little effect (Foxa2 is already active), constitutive activation in C57Bl/6 mice normalizes β-oxidation between fasting and feeding states by increasing β-oxidation in the fed state, corresponding with Foxa2-dependent activation of target genes such as Mcad, Vlcad and CPT1.

The increased insulin levels in "obesity-prone" C57Bl/6 inbred mice (in the fed state) result in the translocation of insulin-dependent hepatic factors Foxo1 and Foxa2 from the nucleus, which leads to the inhibition of downstream target genes involved in glucose and lipid metabolism. This could also serve to set up a negative feedback loop whereby genetic factors in certain

strains lead to decreased Foxa2 activity (or to increased insulin and thereby decreased Foxa2 activity) , which in turn leads to decreased metabolism and enhanced metabolic differences between strains. In such a case, with the addition of a high fat diet or additional environmental stresses, this negative feedback could be even further exacerbated in the "obesity-prone" mice, resulting in this exaggerated phenotype.

The development of diabetes and the associated metabolic syndrome in humans is also dramatically affected by background genes. In mice, this was first reported for the *ob/ob* and *db/db* traits (53) and has been shown subsequently in mice with genetically induced lipodystrophy (103), and diet-induced obesity (104). Furthermore, a recent study showed that in the insulin receptor/IRS-1 double-heterozygous knockout, the background genes of C57/B6 mice caused severe hyperinsulinemia and diabetes, whereas background genes of the Sv129 strain protected against diabetes (105). This "thrifty" phenotype displayed by the C57/B6 mice as shown by weight gain, hyperinsulinemia, and increased hepatic lipid content is similar to that observed in various human populations that exhibit an increased susceptibility to obesity and diabetes, given an average caloric intake (106, 107). Even though the causes of increased release of insulin are unclear, it may be possible to counteract some of the pathophysiological conditions that are a direct result of the metabolic syndrome. Thus, it is of the utmost interest to elucidate ways to

modulate Foxa2 activity through dephosphorylation and nuclear reactivation, with the goal of influencing hepatic lipid metabolism and thereby alleviating symptoms such as hepatic steatosis and insulin resistance.

Inhibition of Foxa2 occurs independently of nuclear exclusion

Previous data from our lab provide evidence for a strong correlation between insulin signaling, T156 phosphorylation, nuclear exclusion and inactivation of Foxa2 (10, 36). While nuclear exclusion certainly leads to inhibition of transcriptional activity, there was previously no means to differentiate between these correlative observations. The novel identification of a functional NES in Foxa2 has now allowed us to uncouple these events.

Interestingly, alignment of the Foxa2 NES shows that it is well-conserved throughout vertebrate homologues of Foxa2. Minor variations within the sequence occur from *Xenopus* to human (methionines instead of leucines at amino acids 110 and 113), but these changes conserve the overall character of the export sequence and are not likely to hinder nuclear export capability. Indeed, it has been shown that hydrophobic residues other than leucine (including isoleucine, valine, methionine, and phenylalanine) may constitute a functional CRM1 NES (62, 108). By contrast, this sequence conservation does not extend to Fork head, the *Drosophila* homolog of Foxa2.

Consequently, *Drosophila* Fork head may not be capable of shuttling in response to insulin stimulation, suggesting that the nuclear export capability may have arisen later in evolution. Notably, the T156 phosphorylation site (T207 in *Drosophila*) is conserved (36). It will therefore be interesting to see whether the same mechanism of insulin-induced phosphorylation exists in flies, and whether this also results in Fork head inactivation.

Mechanisms to this effect have also been reported for the Foxo family of transcription factors. Phosphorylation of three critical residues in Foxo1 has been shown to contribute to nuclear export and subsequent loss of transcriptional activity in response to insulin/IGF signaling (46, 47, 58). *In vitro* data suggest that Serine 256 acts as a "gatekeeper" to subsequent regulatory events, with phosphorylation at this residue resulting in transcriptional inhibition of nuclear Foxo1 (50, 109). However, additional posttranscriptional modifications have also been shown to contribute to the regulation of FoxO family members, including acetylation, ubiquitination and methylation (reviewed in (110, 111). The relative contribution and exact mechanisms of these modifications are still being worked out.

Our data support a model whereby phosphorylation of Foxa2 acts as the dominant signal for transcriptional inactivation; however we cannot exclude the possibility that additional post-translational modifications exist. Since we generally observe that Foxa2 runs about 9 kDa above its predicted molecular

weight, we asked whether it might be sumoylated or ubiquitinated. Running the rat Foxa2 amino acid sequence through a sumoylation site predicting program identified several sites with high probability, and several with low probability (Figure 65). Intriguingly, one of the high probability sites is very close to the Akt phosphorylation site.

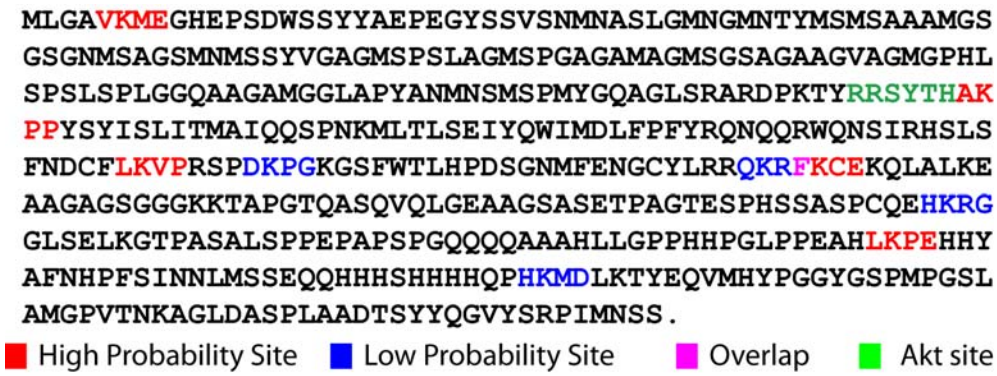

Figure 65. Sumoylation site prediction. The amino acid sequence for rat Foxa2 was put into SumoPlot, a sumoylation prediction program. The following high and low probability sites were predicted. The Foxa2 Akt phosphorylation site is shown in green, for reference.

To test whether Foxa2 is sumoylated we used whole cell lysates from insulin-treated primary hepatocytes infected with the four Foxa2 variant viruses. Surprisingly, we observe a very strong sumoylation signal in immunoprecipitates, and even in whole cell lysates of all insulin-stimulated primary hepatocytes, except GFP controls (Figure 66). There did not seem to be any difference in sumoylation state between the viruses however, and more data will need to be acquired to determine the function of Foxa2 sumoylation, and whether it is regulated by insulin.

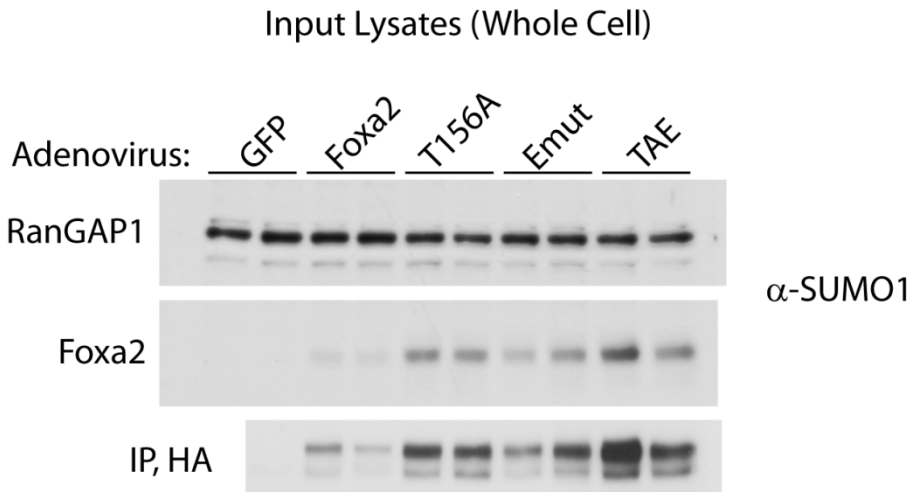

Figure 66. Foxa2 is sumoylated. Primary hepatocytes were infected with the indicated adenovirus, serum starved overnight and stimulated with 100nM insulin for 15 min. Whole cell lysates were then saved as input, or immunoprecipitated (IP) with an anti-HA antibody. Immunoblots of input and IPs were probed with an antibody against SUMO1.

In an attempt to determine whether the phosphorylation site is sufficient to induce inactivation of Foxa2 we generated Foxa2-T156E or -T156D phosphomimetic variants. These both appear to result in constitutively nuclear Foxa2 when stably expressed in HepG2 cells, although further studies are needed to sufficiently assay its activation state (data not shown). Thus, whether this single phosphorylation event is sufficient for inactivation of Foxa2 remains to be determined.

One plausible hypothesis for the regulation of Foxa2 by phosphorylation, is that T156 phosphorylation, which occurs N-terminal of the DNA binding domain, directly decreases the DNA binding affinity of Foxa2. While EMSA data suggest that this is not the case, it was not possible to monitor the phosphorylation state of Foxa2 in these assays (36). Alternatively,

or additionally, phosphorylation (or other modifications) could affect coactivator or histone binding.

Our data thus provide a novel perspective on the regulation of Foxa2 by insulin, which can potentially be applied to the hormonal regulation of other transcription factors. Additionally, the discovery of an essential NES controlling insulin-induced nuclear export of Foxa2 lays a strong foundation for the identification of additional signaling pathways and/or post-translational modifications involved in the regulation of Foxa2 activity.

The constitutive inactivation of Foxa2 by insulin, in addition to the beneficial effects of constitutively active Foxa2 in mouse models of obesity make understanding the molecular mechanisms of its regulation of great scientific, and potentially therapeutic interest. Taken together, our data show that Foxa2 is subject to active nuclear export in response to insulin signaling, that this export is not prerequisite for transcriptional inactivation and that Foxa2 phosphorylation is the most direct readout of Foxa2 activity.

Pulmonary and embryonic regulation of Foxa2 by insulin

We clearly observe insulin-induced nuclear exclusion of Foxa2 in lung cells, just as has been previously described for hepatocytes. Expression of Foxa2 is enriched in lung, as it is in liver, so to some degree it is not surprising

that it behaves similarly in both tissues. Curiously, though, there is no well established metabolic reason for gene expression in lung tissue to be regulated by the routine insulin fluctuations that accompany fasted and fed states.

We hypothesize that an indirect connection between insulin and metabolism may be found in the production of lung surfactant proteins. Lung surfactant maximizes the surface area of the lung available for gas exchange, and therefore expression of surfactant genes may increase the efficiency of respiration. Efficient respiration, in turn, may permit more efficient use of energy during periods of activity, and studies have shown that caloric restriction stimulates locomotion. Indeed, in chapter 5 we report the novel regulation of Foxa2 by insulin in the hypothalamus, where nuclear Foxa2 (induced by fasting), increases locomotion and food-seeking behavior. In this way, insulin-dependent regulation of Foxa2 in the lung may correlate with the overall metabolic state of the organism. This model would also implicate Foxa2 in one of the developmental disorders associated with type 2 diabetes: impaired lung function in infants of mothers with uncontrolled gestational diabetes (84, 85). These mothers are generally hyperinsulinemic, but insulin resistant and therefore hyperglycemic. While insulin does not cross the placenta, glucose does, and an excess of blood glucose stimulates the fetal pancreas to produce more insulin, thus rendering the fetus hyperinsulinemic. We hypothesize that this results in the cytoplasmic localization and inactivation

of Foxa2 in the lungs of fetuses developing in insulin resistant mothers, leading to reduced surfactant production just prior to their transition to air breathing at birth. There is also some evidence for an associated risk of respiratory diseases like asthma and chronic obstructive pulmonary disease in adults with obesity and type II diabetes (80-82).

The most obvious way for Foxa2 to regulate surfactant production is through transcriptional control of surfactant genes. Surfactant protein B (SP-B) and clara cell secretory protein (CCSP) are both reported Foxa2 target genes in the lung (76, 112), however our initial realtime PCR analysis for fasted and fed adult lung show very minor, if any, changes in these genes. Interestingly, a different surfactant protein, SP-A, was significantly decreased. Furthermore, several genes from our microarray analysis on embryonic lung look promising in terms of being potential Foxa2 targets that are also implicated in lung function: Reg3g, Scgb3a1, and muc5b. While these genes do not encode surfactant proteins *per se*, they are all implicated in host defense, suggesting a possible alternative or additive function for insulin sensitivity in the lung.

Our observations do not preclude the possibility of surfactant regulation by Foxa2 in a more indirect manner or on a longer timescale. Indeed, the fact that Foxa2 is expressed in lung and is regulated by insulin strongly suggests that it mediates some metabolic regulation of this organ. Further study is required to more fully investigate the possibility of insulin-dependent regulation in lung

tissue, and to understand the molecular mechanisms responsible for diabetes-associated lung disorders.

Finally, our studies demonstrate that Foxa2 target genes in the liver can be disregulated by insulin signaling during development, as early as E19. The long term effects of this early disregulation are not known, however it is possible that it starts the negative feedback loop discussed earlier, and so sets the stage for insulin resistance or obesity later in life. If so, this would be relevant to human forms of the disease which can be "inherited" but are not always directly linked to genetics.

Regulation of Foxa2 in the Hypothalamus

A well established connection has been noted between the neurons of the lateral hypothalamus and feeding behavior or arousal (113-116). For instance, trauma to the LHA may result in decreased arousal, failure to meet metabolic challenges by modifications in behavior, and ultimately death by starvation (117, 118). Our studies elucidate a molecular mechanism through which metabolic state may influence behavioral responses: insuilin-dependent signaling in the lateral hypothalamus inhibits Foxa2-dependent expression of MCH and orexin neuropeptides.

As observed in the liver, Foxa2 in MCH and orexin neurons is nuclear and active in fasted C57Bl/6 mice, but inactive in fed C57Bl/6 mice and fasted,

hyperinsulinemic obese mice. We have identified MCH and orexin as novel targets of Foxa2, and show that their expression is reduced when Foxa2 is inactivated through insulin signaling. MCH and orexin are known to regulate food intake and movement, respectively (114, 116, 119, 120). MCH increases food consumption, and gene deletion causes hypophagia. Interestingly, increased expression of MCH on its own results in obesity in susceptible mice; however increased expression of MCH in Nescre/+,Foxa2T156A$^{fl/fl}$ mice did not have this effect. This can be attributed to the coregulation of orexin, which mediates wakefulness and results in increased activity. Orexin gene deletion is associated with narcolepsy and obesity. As MCH and orexin signaling are associated with activity and feeding behavior, their downregulation in this hyperinsulemic model may constitute a system of negative feedback, which exacerbates the phenotype. Indeed, decreased activity is a common phenomenon overweight individuals, in humans and in mice, and is now recognized as a major factor contributing to the continuing rise in obesity.

Interestingly, introduction of constitutively active Foxa2-T156A in these mice leads to improved metabolic properties, including ameliorated glucose homeostasis, decreased fat and lean body mass, and increased physical activity. These observations suggest that Foxa2 activation in the hypothalamus may be a novel therapeutic approach to overcome the metabolic pathologies in diabetic individuals.

EXPERIMENTAL PROCEDURES

Materials. Human recombinant insulin (I9278), Collagen (Type I, C3867), phosphate-buffered saline pH 7.4 (PBS) and Leptomycin B (L2913) were purchased from Sigma. HALT phosphatase inhibitor cocktail was from Pierce, and Complete protease inhibitor cocktail was from Roche. Antibodies to: HA (Covance and Santa Cruz), Foxa1 (a gift from J. Darnell, Rockefeller University; or from Abcam, ab23738), rabbit or goat polyclonal to Foxa2 (Abcam), phosphorylated Foxa2 (T156) antibody was generated and described previously (Cell Signaling) (10), LSD1 (Cell Signaling), GAPDH (Abcam), Orexin A (Abcam, ab35337), pro-MCH (Santa Cruz, sc-14509) gamma tubulin (Sigma), AKT (Cell Signaling), Foxo1 (Santa Cruz), TAF100 (a gift from R.G. Roeder, Rockefeller University), SUMO-1 (Zymed, 38-1900).

Animal Models. C57BL/6 and *ob/ob* mice were purchased from Charles River. All animals were maintained on a normal chow diet and a 12 h light/dark cycle. All mutant animals were crossed to a *C57Bl/6* background. Diet induced obese animals were fed a high fat diet (Harland Teklad) containing 50% fat for 12 weeks. Gestation was dated by detection of the vaginal plug, which was considered gestational/embryonic day 1.

Sreptozotocin-induced diabetes was initiated on gestational day 14; mice were given 3 injections of 75 mg/kg stz over 3 days.

Generation of FOXA2 T156A knock-in mice. *FOXA2T156A*$^{flflox/flox}$ mice were generated using a targeting construct. The short arm spanning exon 1 and 2 (3.4 kb in length) from bp position -2517 to +919, relative to the translation start site (+1). The long arm, which contained exon 3 with the T156A mutation was 4.7 kb in length from bp position +1034 to +5782, relative to the translation start site. Wild type exon 3 was located between the long and short arm and flanked by a lox*P* sequence. A neo/tk cassette, flanked by lox*P* sites, was inserted upstream of wild type exon 3. An outside probe was used to visualize homologous recombination and Cre recombination events. The targeting vector was electroporated into R1 ES cells from mouse strain 129 (Nagy et al., 1993) and neomycin-resistant colonies were recovered. The colonies were screened by Southern blotting using probe 1 and positive colonies were confirmed by Southern blotting with a probe located downstream of the 3' homology arm. To delete the neo/tk-cassette from the targeted allele, recombinant ES clones were transiently transfected with a plasmid expressing Cre-recombinase. ES clones with partial recombination and deletion of the neo/tk cassette were injected into B6(D2B6F1) blastocysts to produce chimeric mice. Germline transmission was confirmed by Southern

blotting. *FOXA2T156A*$^{flox/flox}$ mice were first backcrossed for 7 generations to *C57Bl/6J* mice. To obtain brain-specific *FOXA2T156A* knock-in mice, *FOXA2T156A*$^{flox/flox}$ mice were bred to *Nestin-Cre* mice **(**B6.Cg-Tg(Nes-cre)1Kln/J, Jackson Laboratories) (14), which had been backcrossed to *C57Bl/6J* for at least 6 generations. To confirm expression of the *Foxa2T156A* allele, *Foxa2T156A* transcripts were amplified from brain and liver using primers spanning one intron of the mouse *Foxa2* gene (AGCGGCCAGCGAGTTAAAGTATGC and CTGCCGGTAGAAAGGGAAGAGGTC). RT-PCR products were cloned into the TOPO3 vector (Invitrogen) and sequenced.

Plasmids and Adenovirus. HA-tagged Foxa2, Foxa2-T156A, and Akt2 were in PCDNA3 expression vectors as previously described (36). Emut (L110A, L113A) and TAE (L110A, L113A, T156A) constructs were generated by site-directed mutagenesis using overlap extension PCR. Adenoviruses were generated using the Rapid Adenovirus Production System (Viraquest). With the exception of Ad-GFP-C1Foxa2, GFP was coexpressed from an independent promoter in addition to HA-Foxa2 or Foxa2 variants. Ad-GFP, Ad–Foxa2 and Ad–T156A were described previously (10). For *in vivo* experiments, mice were injected with $8x10^8$ PFU of adenovirus through the tail vein.

Cell culture. HepG2 cells and primary hepatocytes were maintained on collagen-coated plates in DMEM (Gibco, containing 4.5 g/L glucose, 110 mg/L sodium pyruvate, 4 mM L-glutamine) supplemented with 10% fetal bovine serum (Sigma) and 100 U/mL penicillin/ streptomycin, in a humidified incubator at 37°C and 5% CO_2. Serum starvation was carried out for 18 h in DMEM without FBS and Pen/Strep. Stable cell lines were generated by transfection of $4.5x10^6$ HepG2 cells with 6 μg of plasmid DNA using Fugene6 transfection reagent (Roche), and selection with 1 mg/mL of G418 (Calbiochem) over 2-3 weeks. Clonal populations were isolated and analyzed for expression of Foxa2 constructs by western blotting using an anti-HA antibody (MMS-101P, Covance).

Primary Hepatocytes. Mice were anesthetized with pentobarbital. A catheter (24 gauge) was inserted into the portal vein, and the liver was perfused with a buffer containing 10 mM HEPES (pH 7.4), 143 mM NaCl, 7 mM KCl, and 0.2 mM EDTA at a flow rate of 1 ml/min. Effluent exited via the vena cava inferior. After 10 ml of perfusion, the buffer was switched to a collagenase buffer (50 mM HEPES (pH 7.4), 100 mM NaCl, 7mM KCl, 5mM CaCl2, and 0.2% collagenase type IV (Sigma)). After 6 ml of perfusion, the liver was cut out and minced in Dulbecco's modified Eagle's medium (with 10% fetal bovine

serum) containing 4.5 g/liter glucose. Hepatocytes were released from the liver during 15 min of light shaking at 37 °C. The cell suspension was filtered through a 40 μm nylon mesh cell strainer (BD Falcon) and centrifuged at 80 x *g* to pellet the hepatocytes. The cell pellet was washed three times with warm media, and the cells were plated onto collagenized plates. Cells were allowed to attach for 6 h after which cells were washed and medium was changed.

Whole Cell Extracts. From HepG2 cells: Cells were washed, scraped and centrifuged at 500 x g for 5 m at 4°C in cold 0.01 M PBS. The cell pellet was then resuspended in whole cell extract buffer (150 mM NaCl, 50 mM Tris pH 7.4, 5 mM EDTA, 0.1% SDS, and complete protease inhibitor (Roche)). The soluble fraction was collected after centrifugation at 13,000 rpm for 5 m at 4°C. A two-step lysis was used for tissue whole cell extracts: tissues were dounced 10-15x with a tight pestle in cold buffer A (10 mM HEPES pH 7.9, 1.5 mM $MgCl_2$, 10 mM KCl, 0.6% NP40) containing 1.67x phosphatase inhibitor cocktail (Pierece HALT) and 1.67x protease inhibitor cocktail (Complete mixture Roche Applied Science) and incubated on ice for 10 m. Lysates were then vortexed for 5 s, followed by dropwise addition of 140 μL of buffer B (1.2 M NaCl, 20 mM Hepes pH 7.9, 0.2 mM EDTA, 1.5 mM MgCl2, 25% glycerol;without additives) and overhead rotation for 40 m at 4°C to ensure

lysis. Insoluble cellular components were removed by centrifugation at 16,000 x g for 30 m at 4°C, and the supernatant was collected.

Protein measurement. In all cases, protein concentrations were determined bicinchoninic acid (BCA) assay using a bovine serum albumin standard curve prepared in the cell lysate buffer. (In the case of buffers containing DTT the standard curves were always made fresh for most accurate quantitation).

Nuclear Fractionation. Initial nuclear extraction experiments were by sucrose gradient fractionation. Tissues were dounced 20x in homogenization buffer (10 mM Hepes pH 7.9, 25 mM KCl, 2 M Sucrose, 10% glycerol, 1 mM EDTA) containing protease inhibitor cocktail (added fresh). Homogenates were carefully layered over a 1 cm cushion of homogenization buffer in SW55 ultracentrifugation tubes (Beckman) and centrifuged at 100,000 x g (29,000 RPM in SW55) for 40 minutes at 4°C. Supernatant was carefully removed by pipetting and discarded, and nuclear pellets were resuspended in 2 mL of nuclear lysis buffer (10 mM Hepes pH 7.9, 100 mM KCl, 3 mM MgCl2, 0.1 mM EDTA) containing 1 mM DTT and protease inhibitor cocktail (added fresh). Nuclear lysates were incubated on ice for 20 minutes, followed by the addition of 0.1 volume $(NH_4)_2SO_4$ over 30 m to precipitate chromatin, and

centrifuged at 100,000xg (29,000 RPM) for 60 min at 4°C. The supernatant was collected and 0.66 g of $(NH_4)_2SO_4$ was added over 15 m to precipitate protein, which was pelletted by centrifugation for 30 minutes at 100,000g at 4°C and resuspended in nuclear resuspension buffer (25 mM Hepes pH 7.4, 40 mM KCl, 0.1 mM EDTA, 10% (v/v) glycerol) containing 1mM dTT (added fresh). Protein was dialyzed overnight against 3 x 2 L of nuclear resuspension buffer.

Nuclear/Cytosoplasmic Extracts. HepG2 cells were grown in 10 cm plates to 80% confluency and serum-starved for 18 h, followed by the indicated treatments (LMB: 2 h with 2.5 ng/mL leptomycin B, Insulin: 500 nM human recombinant insulin for 15 min at 37°C). Nuclear and cytoplasmic extracts were prepared as previously described (23). Briefly, cells were swollen on ice in hypotonic lysis buffer (10 mM HEPES pH 7.9, 1.5 mM $MgCl_2$, 10 mM KCl) containing 1 mM dithiothreitol and protease inhibitors (Complete mixture, Roche Applied Science), and permeabilized by the addition of NP40 to 0.6%. After centrifugation at 10,400xg for 30 sec at 4°C, the supernatants (cytoplasmic extracts) were collected, and nuclear pellets were resuspended in nuclear lysis buffer (10 mM HEPES pH 7.9, 100 mM KCl, 3 mM $MgCl_2$, 0.1 mM EDTA) containing 1 mM dithiothreitol and protease inhibitors. Nuclei

were lysed by the gradual addition of one-tenth volume of 4 M $(NH_4)_2SO_4$ over 30 min. For liver experiments, ~50 mg of liver was dounced directly in hypotonic lysis buffer on ice, 10x with a tight pestle.

Quantification of Cytosolic and Nuclear Foxa2. Western blots were scanned and band intensity quantified by densitometry using Kodak imaging software. Each value was normalized to the corresponding γ-tubulin value. To account for differences in blotting and exposure, each blot contained the same standard, and all values were adjusted to the intensity measured for this standard.

Transfection and Transactivation assays. HepG2 cells were plated at 70,000 cells per well in 24-well plates and transfected the following day with 25 ng p6xCdx-TkLuc reporter gene (36), 10 ng pRL-Tk, and 25 ng of Foxa2 expression vectors alone or in combination with 5 ng of a human Akt2 expression vector using Lipofectamine 2000 (Invitrogen). Cells were harvested 40 h post-transfection and luciferase was measured using the Dual Luciferase System (Promega) according to manufacturer's protocol on a Promega GloMax luminometer.

Immunofluorescence Microscopy. Liver pieces were frozen directly in OCT (optimal cutting temperature) compound at –80°C. 9 μM cryosections were fixed in 4% paraformaldehyde in 0.01 M PBS at 4°C for 30 min, permeabilized in 0.2% NP40 in PBS, blocked in 5% NDS, 1% BSA, 0.1% NP40 in PBS, and incubated with anti-HA antibody (1:25, Santa Cruz Biotechnology, *sc-805*) overnight at 4°C in a humidified chamber. Donkey anti-rabbit IgG Alexa Fluor 488 (Molecular Probes) was used as a secondary antibody, and mounted with VECTASHIELD mounting media with Dapi (Vector Labs) to visualize nuclei. For hypothalamus staining, mice were CO_2-anesthesized and intracardially perfused with 5 ml of phosphate-buffered 2% paraformaldehyde (pH 7.4). Brains were postfixed in phosphate-buffered 2% paraformaldehyde (pH 7.4) for 10 minutes at room temperature, equilibrated in phosphate-buffered 30% sucrose at + 4O C for 24 hours and frozen in tissue-tek OCT compound (Sakura). Brains were cryo-sectioned into 12μm thick coronal sections, which were stored at -20 °C until further use. Cryosections were permeabilized for 1 h at room temperature in 10mM PBST (10 mM PBS, pH 7.4, 0.1%-Triton X-100), blocked with 1% BSA, 5% serum in PBST for 1 h at room temperature and incubated overnight at 4 °C with the primary antibody at a 1:50 - 1:300 dilution in 1% BSA, 5% serum in PBST. After three washes, sections were incubated for 1 h at room temperature with secondary antibodies (Alexa Fluor

488 or Alexa Fluor 568 conjugated; Molecular Probes, Invitrogen) diluted 1:500 in 1% BSA, PBST. Immunofluorescent staining was visualized with a Leica confocal microscope at 40x magnification.

Immunoprecipitation. Primary hepatocytes from three wildtype C57Bl/6 mice were pooled and plated onto ten 10 cm collagen-treated plates. Cells were washed extensively and allowed to recover over 48 h, after which they were infected with $2.5x10^7$ PFU of the indicated virus. After an additional 24 h, cells were serum-starved overnight, followed by 15 min stimulation in the absence or presence of 100 nM insulin. Cells were washed twice in cold 0.01 M PBS (containing 10mM NaF, and 0.5X HALT phosphatase inhibitor cocktail from Pierce) and moved directly to ice, scraped and centrifuged at 500 x g for 5 m at 4°C. Cell pellet was resuspended in 200 µL of buffer A (10 mM HEPES pH 7.9, 1.5 mM $MgCl_2$, 10 mM KCl, 0.6% NP40) containing 1.67x phosphatase inhibitor cocktail (Pierece HALT) and 1.67x protease inhibitor cocktail (Complete mixture Roche Applied Science). Incubated cells on ice for 10 m, vortexed 5 s, followed by dropwise addition of 140 µL buffer B (1.2 M NaCl, 20 mM Hepes pH 7.9, 0.2 mM EDTA, 1.5 mM $MgCl_2$, 25% glycerol) without additives. Rotated (overhead) 40 m at 4°C to ensure lysis. Centrifuged at 16,000 x g for 30 m at 4°C to pellet chromatin and debris, and collected supernatant as whole cell lysate. Brought 120ug of protein lysate up to 276 µL

with A/B lysis buffer (mixed 1.5:1), added 600 μL IP buffer (0.01 M PBS pH 7.4, .01 mM EDTA, 0.02% NP40) containing phoshpatase and protease inhibitor) to each and subjected all to immunoprecipitation overnight at 4°C with monoclonal HA agarose (Sigma A2095) in SigmaPrep spin columns. Washed 5 x 800 μL with IP buffer containing 10 mM NaF. Centrifuged 1 m at 1000xg to remove excess liquid, plugged columns and added 60 μL 1X laemli buffer (50 mM Tris pH 6.8, 2% SDS, 10% glycerol, 1 mM bromophenol blue) to elute.

Chromatin Immunoprecipitation. Primary hepatocytes from three wildtype C57Bl/6 mice were pooled and plated onto ten 10 cm collagen-treated plates. Cells were washed extensively and allowed to recover over 48 h, after which they were infected with $2.5x10^7$ PFU of the indicated virus. After an additional 24 h, cells were serum-starved overnight, followed by 15 min stimulation in the absence or presence of 100 nM insulin. 11X fixing solution (50mM Hepes-KOH pH 7.5, 100mM NaCl, 1mM EDTA pH 8.0, 0.5mM EGTA p H8.0, 11% formaldehyde) was added to the cells to a final concentration of 1X and incubated for 10 min at 37°C. Cells were then moved to ice, washed twice with ice cold 0.01 M PBS and scraped in 1 mL ChIP cell lysis buffer (10 mM Tris–Cl, pH 8.0, 10 mM NaCl, 1.5 mM $MgCl_2$, 0.2% NP-40, with protease

inhibitors). Lysates were centrifuged for 5 min at 5400xg at 4°C. Pellets were resuspended in 450 µL of SDS Lysis buffer (Upstate Biotechnology) and sonicated 4x20 sec on, 30 sec off, at amplitude 16 on a Misonix Sonicator 4000. Lysates were further processed according to the manufacturers protocol (Chromatin immunoprecipitation assay kit, Upstate Biotechnology). DNA complexes were immunoprecipitated overnight using 2.6 µg of HA-antibody (Santa Cruz Biotechnology, *sc-805*) or rabbit IgG (ChromPure, Jackson ImmunoResearch). Primer sequences are given in Table 5.

Table 4. Primer Sequences and annealing temperatures for ChIP.

Primer Name	Forward Sequence	Reverse Sequence	Ta (°C)
CPT1α	AAGGCATACATCACCACAACCAGT	TTCACAACAACACTGTGGTGTGC	57
Gck	TCTCCACACCAGCTTGGAACC	TTTCACCACCATCAGTATGCAC	57
HMGCS1	TGCACTGTTCCTGGCTGGTATCTA	TGATTGTTGGATGTGTTAGAAGGA	57
LPK	TCTCTATTGAAGCTGATGGACTG	AGTCCCCACATCTTCCCTTCC	57
PEPCK	ATACGTACATACTGACCCCTGCTC	GATCATCAGAGTTCCATTTCAAGA	57

Gene Chip. Adult lung RNA was prepared from 5 fasted and 5 fed mice by Trizol extraction, pooled and purified using RNEasy columns (Qiagen). RNA was then submitted to the functional genomics center (ETH Zurich) for labeling and hybridization. Whole snap-frozen embryonic lungs from two fetuses of stz-induced diabetic mothers, and two from fasted mothers were submitted to Miltenyi for RNA extraction, labeling, and hybridization onto a one-color 4x44K Agilent genechip. Data was analyzed using Genespring software.

Gene Expression. Total RNA was extracted from lung tissue using TRIzol reagents following the manufacturer's instructions (Invitrogen). Contaminating genomic DNA was removed by a 3 hour DNase I treatment (Ambion). RNA quality was confirmed by denaturing gel electrophoresis stained with ethidium bromide. cDNA was synthesized using Superscript III with random hexamer primers and oligo dT according to the manufacturer's protocol (Invitrogen). Combined extraction of mRNA and cDNA synthesis were performed from 50 mg of liver tissue with the μMACS One-step cDNA Kit (Miltenyi Biotec) following the manufacturer's protocol, with an additional 10 minute RNase-free DNase I treatment (NEB). Gene expression was measured quantitatively as a function of SYBR green incorporation during PCR using gene-specific exon-spanning primers, LightCycler 480 SYBR Green I Master mix (Roche) and the Mx3005P Real-Time QPCR Detection System (Stratagene). Values shown are given in arbitrary units based on a standard curve, and normalized to GAPDH. Primer sequences are given in Table 5.

Table 5. Primer sequences and annealing temperatures for real-time PCR.

Primer Name	Forward Sequence	Reverse Sequence	T_a °C
Apq3	GCTGGGATTGTTTTTGGGCTGTAC	GCGGCTGTGCCTATGAACTGATC	63
CCSP	TCACTGTGGTCATGCTGTCCATCT	TGAAAGGCTTCAGGGATGCCACAT	63
CPT1α	AGCGACTCTTCAATACTTCCCGCA	TCTGTGGTACACGACAATGTGCCT	63
Foxa2	AAGTATGCTGGGAGCCGTGAAGAT	CGCGGACATGCTCATGTATGTGTT	60
GAPDH	CTGACGTGCCGCCTGGAGAAA	CCGGCATCGAAGGTGGAAGA	63
HMGCS1	AATCCAGCTCTTGGGATGGACGAT	ACCTGTAGGTCTGGCATTTCCTGT	63
MCAD	AGTACCCGTTCCCTCTCATCAA	TACACCCATACGCCAACTCTTC	60
SP-A	TGCACCTGGAGAACATGGAGACAA	ATGGATCCTTGCAAGCTGAGGACT	63
SP-B	CCTGCCCCTGGTTATTGACTACTTC	GCAGCACAGGGAGGACCAG	63
SP-C	CGCCTTCTCATCGTGGTTGT	AGGAGCCGCTGGTAGTCATA	63
VLCAD	GGTTACCCATGGGCTCCCTGAAAAG	TTGAAGCCATCTCCCACCTCTCCTA	60
Orexin	CTGCCGTCTCTACGAACTGTTG	CGCTTTCCCAGAGTCAGGATA	60
MCH	TTCAGAAGGAAGATACTGCAGAAAGA	CGCTCTCGTCGTTTTTGTATTG	60
β-actin	GAGAAGCTGTGCTATGTTGCTC	AGGAAGAGGATGCGGCA	60

Immunoblotting. Protein extracts were separated by SDS-PAGE (10%) and transferred onto nitrocellulose membranes (Perkin Elmer) by electroblotting. Membranes were immunoblotted according to standard protocols using 5% non-fat dry milk in TBST. Blots were stained with Ponceau S to ensure equal loading and incubated with primary antibodies overnight at 4 °C (rabbit anti-HA 1:500; rabbit anti-Foxa2 (Abcam) 1:10,000; all others were at 1:1000). Secondary antibody was added for 1 h at room temperature (1:10,000; Calbiochem).

Antibody Production. Rabbit polyclonal antibody to Foxa2 was generated by injection of GST-purified Foxa2 (Bethyl) and affinity purified over a GST-Foxa2 column.

Physiological measurements. Retro-orbital blood samples were taken into non-heparinized capillary tubes. Blood glucose was measured using a standard glucometer (Ascensia Contour, Bayer). Plasma insulin was measured with the Sensitive Rat Insulin RIA kit (Linco Research). Liver triglycerides were extracted by the Folch method and quantitated by colorimetric assay (Roche). Plasma cholesterol and plasma triglycerides were measured by colorometric assay (Roche).

Metabolic Measurements. Locomotion (x-, y- and z-axis), food and water intake, oxygen consumption, CO_2 and heat production were simultaneously determined for four mice in separate cages per experiment during a 24 h period in an Oxymax metabolic chamber system (Columbus Instruments) at the ages of 4 and 8 weeks.

Mitochondrial isolation. Mitochondria were isolated as previously described (121). 200 mg of PBS-perfused mouse livers were dounced in 4 volumes of MSM buffer (220 mM mannitol, 70 mM sucrose, 5 mM Mops pH 7.4) 4 x with a loose pestle. The homogenate was diluted with MSM buffer to a final tissue concentration of 10% , and EDTA was added to 2 mM. Nuclei, unbroken cells, and cell debris were removed by differential centrifugation at 400 x g for 10 m. Mitochondria were isolated from the supernatant by additional

centrifugation at 7000 x g for 10 m and washed once with MSM buffer. Mitochondrial pellets were resuspended in a small volume (20 μL) MSM buffer, and normalized to protein concentration.

Beta Oxidation/Ketone Body Formation. We assessed the β-oxidation of and ketone body production from [1-^{14}C]palmitic acid by liver mitochondria in samples normalized to mitochondrial protein, as described (122). 1 mg of mitochondrial protein was brought up to 360 μL with preincubation medium (70 mM sucrose, 43 mM KCl, 3.6 mM $MgCl_2$, 7.2 mM KH_2PO_4, 36 mM Tris-HCl pH 7.4, 0.2 mM adenosine triphosphate, 50 μM L-carnitine, 15 μM CoASH) and incubated for 5 m at 37 °C. 40 μL of incubation media (400 μM [1-^{14}C]palmitic acid (0.4 μCi/40 μL), 2.5 mg/mL BSA) was then added and tubes were closed with Whatman paper-lined caps soaked in 100 mM NaOH and incubated for 30 m at 37 °C with in a water bath shaking at 85 RPM. The reaction was stopped by adding 100 μL of 5% perchloric acid to the incubation mixture, and further incubated for 60 m at 37 °C with gentle shaking. CO_2 trapped on the filter papers was counted for ^{14}C activity by scintillation counter. To measure ketone body formation, the incubation mixture was centrifuged at 4,000xg for 10min, and ^{14}C acid-soluble products of mitochondrial palmitate metabolism were counted from an aliquot (200 μL) of the supernatant.

Statistical Analysis. Results are given as mean ± SEM, if not otherwise indicated. Statistical analyses were carried out by using a two-tailed Student's unpaired *t* test, and the null hypothesis was rejected at the 0.05 level. *, $p < .05$; **, $p < .01$, ***, $p < .001$

REFERENCES

1. Gojka R*, et al.* (2005) The Burden of Mortality Attributable to Diabetes. *Diabetes Care* 28:2130-2135.

2. Anonymous (2003) International Diabetes Federation: Diabetes Atlas 2003 *Brussels, International Diabetes Federation*.

3. Jemal A, Ward E, Hao Y, & Thun. M (2005) Trends in the Leading Causes of Death in the United States, 1970-2002. *JAMA* 294:1255-1259.

4. Reaven GM, Bernstein R, Davis B, & Olefsky JM (1975) Nonketotic diabetes mellitus: Insulin deficiency or insulin resistance? *American Journal of Medical Sciences* 60(1):80-88.

5. Perry IJ*, et al.* (1995) Prospective study of risk factors for development of non-insulin dependent diabetes in middle aged British men. *BMJ* 310(6979):560-564.

6. Bjorntorp P (1988) The associations between obesity, adipose tissue distribution and disease. *Acta Med Scand Suppl* 723:121-134.

7. Nussey SSaW, S.A. (2001) Endocrinology: An Integrated Approach. (Taylor & Francis, London).

8. Guignot L & Mithieux G (1999) Mechanisms by which insulin, associated or not with glucose, may inhibit hepatic glucose production in the rat. *Am J Physiol Endocrinol Metab* 277(6):E984-989.

9. Barthel A & Schmoll D (2003) Novel concepts in insulin regulation of hepatic gluconeogenesis. *Am J Physiol Endocrinol Metab* 285(4):E685-692.

10. Wolfrum C, Asilmaz E, Luca E, Friedman JM, & Stoffel M (2004) Foxa2 regulates lipid metabolism and ketogenesis in the liver during fasting and in diabetes. *Nature* 432(7020):1027-1032.

11. Zhang L, Rubins NE, Ahima RS, Greenbaum LE, & Kaestner KH (2005) Foxa2 integrates the transcriptional response of the hepatocyte to fasting. *Cell Metabolism* 2(2):141-148.

12. Kaestner KH, Knochel W, & Martinez DE (2000) Unified nomenclature for the winged helix/forkhead transcription factors. *Genes Dev.* 14(2):142-146.

13. Lai E, Clark KL, Burley SK, & Darnell JE, Jr. (1993) Hepatocyte Nuclear Factor 3/Fork Head or "Winged Helix" Proteins: A Family of Transcription Factors of Diverse Biologic Function. *PNAS* 90(22):10421-10423.

14. Lai E, Prezioso VR, Tao WF, Chen WS, & Darnell JE, Jr. (1991) Hepatocyte nuclear factor 3 alpha belongs to a gene family in mammals that is homologous to the Drosophila homeotic gene fork head. *Genes Dev.* 5(3):416-427.

15. Kim I-M*, et al.* (2005) The Forkhead Box M1 Transcription Factor Is Essential for Embryonic Development of Pulmonary Vasculature. *J. Biol. Chem.* 280(23):22278-22286.

16. Isaac Brownell MDMJ (2000) Forkhead Foxe3 maps to the dysgenetic lens locus and is critical in lens development and differentiation. *genesis* 27(2):81-93.

17. Tran H*, et al.* (2002) DNA Repair Pathway Stimulated by the Forkhead Transcription Factor FOXO3a Through the Gadd45 Protein. *Science* 296(5567):530-534.

18. Brunet A*, et al.* (1999) Akt Promotes Cell Survival by Phosphorylating and Inhibiting a Forkhead Transcription Factor. *Cell* 96(6):857-868.

19. Besnard V, Wert SE, Hull WM, & Whitsett JA (2004) Immunohistochemical localization of Foxa1 and Foxa2 in mouse embryos and adult tissues. *Gene Expression Patterns* 5(2):193-208.

20. Costa RH, Grayson DR, & J E Darnell J (1989) Multiple hepatocyte-enriched nuclear factors function in the regulation of transthyretin and alpha 1-antitrypsin genes. *Mol Cell Biol* 9(4):1415-1425.

21. Chen D & Riddle D (2008) Function of the PHA-4/FOXA transcription factor during C. elegans post-embryonic development. *BMC Developmental Biology* 8(1):26.

22. Panowski SH, Wolff S, Aguilaniu H, Durieux J, & Dillin A (2007) PHA-4/Foxa mediates diet-restriction-induced longevity of C. elegans. *Nature* 447(7144):550-555.

23. Wolfrum C, Howell JJ, Ndungo E, & Stoffel M (2008) Foxa2 Activity Increases Plasma High Density Lipoprotein Levels by Regulating Apolipoprotein M. *J. Biol. Chem.* 283(24):16940-16949.

24. Wolfrum C & Stoffel M (2006) Coactivation of Foxa2 through Pgc-1[beta] promotes liver fatty acid oxidation and triglyceride/VLDL secretion. *Cell Metabolism* 3(2):99-110.

25. Clark KL, Halay ED, Lai E, & Burley SK (1993) Co-crystal structure of the HNF-3/fork head DNA-recognition motif resembles histone H5. *Nature* 364(6436):412-420.

26. Cirillo LA*, et al.* (2002) Opening of Compacted Chromatin by Early Developmental Transcription Factors HNF3 (FoxA) and GATA-4. *Molecular Cell* 9(2):279-289.

27. Cirillo L*, et al.* (1998) Binding of the winged-helix transcription factor HNF3 to a linker histone site on the nucleosome. *EMBO J* 17(1):244-254.

28. Overdier DG, Porcella A, & Costa RH (1994) The DNA-binding specificity of the hepatocyte nuclear factor 3/forkhead domain is influenced by amino-acid residues adjacent to the recognition helix. *Mol. Cell. Biol.* 14(4):2755-2766.

29. Kaestner KH, Hiemisch H, & Schutz G (1998) Targeted Disruption of the Gene Encoding Hepatocyte Nuclear Factor 3gamma Results in Reduced Transcription of Hepatocyte-Specific Genes. *Mol. Cell. Biol.* 18(7):4245-4251.

30. Weinstein DC*, et al.* (1994) The winged-helix transcription factor HNF-3[beta] is required for notochord development in the mouse embryo. *Cell* 78(4):575-588.

31. Ang S-L & Rossant J (1994) HNF-3[beta] is essential for node and notochord formation in mouse development. *Cell* 78(4):561-574.

32. Shih DQ, Navas MA, Kuwajima S, Duncan SA, & Stoffel M (1999) Impaired glucose homeostasis and neonatal mortality in hepatocyte nuclear factor 3Î±-deficient mice. *Proceedings of the National Academy of Sciences of the United States of America* 96(18):10152-10157.

33. Kaestner KH, Katz J, Liu Y, Drucker DJ, & Schütz G (1999) Inactivation of the winged helix transcription factor HNF3α affects glucose homeostasis and islet glucagon gene expression in vivo. *Genes & Development* 13(4):495-504.

34. Qian X & Costa RH (1994) Analysis of hepatocyte nuclear factor-3δ protein domains required for transcriptional activation and nuclear targeting. *Nucleic Acids Res.* 23(7):1184-1191.

35. George S*, et al.* (2004) A Family with Severe Insulin Resistance and Diabetes Due to a Mutation in AKT2. *Science* 304(5675):1325-1328.

36. Wolfrum C, Besser D, Luca E, & Stoffel M (2003) From the Cover: Insulin regulates the activity of forkhead transcription factor Hnf-3{beta}/Foxa-2 by Akt-mediated phosphorylation and nuclear/cytosolic localization. *PNAS* 100(20):11624-11629.

37. Matsuzaka T*, et al.* (2007) Crucial role of a long-chain fatty acid elongase, Elovl6, in obesity-induced insulin resistance. *Nat Med* 13(10):1193-1202.

38. Pani L*, et al.* (1992) Hepatocyte nuclear factor 3 beta contains two transcriptional activation domains, one of which is novel and conserved with the Drosophila fork head protein. *Mol Cell Biol* 12:3723-3732.

39. Shimomura I*, et al.* (2000) Decreased IRS-2 and Increased SREBP-1c Lead to Mixed Insulin Resistance and Sensitivity in Livers of Lipodystrophic and ob/ob Mice. *Molecular Cell* 6(1):77-86.

40. Ogg S*, et al.* (1997) The Fork head transcription factor DAF-16 transduces insulin-like metabolic and longevity signals in C. elegans. *Nature* 389(6654):994-999.

41. Kenyon C, Chang J, Gensch E, Rudner A, & Tabtiang R (1993) A C. elegans mutant that lives twice as long as wild type. *Nature* 366(6454):461-464.

42. Gottlieb S & Ruvkun G (1994) daf-2, daf-16 and daf-23: Genetically Interacting Genes Controlling Dauer Formation in Caenorhabditis elegans. *Genetics* 137(1):107-120.

43. Morris JZ, Tissenbaum HA, & Ruvkun G (1996) A phosphatidylinositol-3-OH kinase family member regulating longevity and diapause in Caenorhabditis elegans. *Nature* 382(6591):536-539.

44. Paradis S & Ruvkun G (1998) Caenorhabditis elegans Akt/PKB transduces insulin receptor-like signals from AGE-1 PI3 kinase to the DAF-16 transcription factor. *Genes & Development* 12(16):2488-2498.

45. Kops GJPL*, et al.* (1999) Direct control of the Forkhead transcription factor AFX by protein kinase B. *Nature* 398(6728):630-634.

46. Tang ED, Nunez G, Barr FG, & Guan K-L (1999) Negative Regulation of the Forkhead Transcription Factor FKHR by Akt. *J. Biol. Chem.* 274(24):16741-16746.

47. Rena G, Guo S, Cichy SC, Unterman TG, & Cohen P (1999) Phosphorylation of the Transcription Factor Forkhead Family Member FKHR by Protein Kinase B. *J. Biol. Chem.* 274(24):17179-17183.

48. Durham SK*, et al.* (1999) FKHR Binds the Insulin Response Element in the Insulin-Like Growth Factor Binding Protein-1 Promoter. *Endocrinology* 140(7):3140-3146.

49. Ayala JE*, et al.* (1999) Conservation of an insulin response unit between mouse and human glucose-6-phosphatase catalytic subunit gene promoters: transcription factor FKHR binds the insulin response sequence. *Diabetes* 48(9):1885-1889.

50. Tsai W-C, Bhattacharyya N, Han L-Y, Hanover JA, & Rechler MM (2003) Insulin Inhibition of Transcription Stimulated by the Forkhead Protein Foxo1 Is Not Solely due to Nuclear Exclusion. *Endocrinology* 144(12):5615-5622.

51. Kulkarni RN*, et al.* (2003) Impact of Genetic Background on Development of Hyperinsulinemia and Diabetes in Insulin Receptor/Insulin Receptor Substrate-1 Double Heterozygous Mice. *Diabetes* 52(6):1528-1534.

52. Biddinger SB*, et al.* (2005) Effects of Diet and Genetic Background on Sterol Regulatory Element-Binding Protein-1c, Stearoyl-CoA Desaturase 1, and the Development of the Metabolic Syndrome. *Diabetes* 54(5):1314-1323.

53. Coleman DL & Hummel KP (1973) The influence of genetic background on the expression of the obese (Ob) gene in the mouse. *Diabetologia* 9(4):287-293.

54. Almind K, Manieri M, Sivitz WI, Cinti S, & Kahn CR (2007) Ectopic brown adipose tissue in muscle provides a mechanism for differences in risk of metabolic syndrome in mice. *Proceedings of the National Academy of Sciences* 104(7):2366-2371.

55. Frescas D, Valenti L, & Accili D (2005) Nuclear Trapping of the Forkhead Transcription Factor FoxO1 via Sirt-dependent Deacetylation Promotes Expression of Glucogenetic Genes. *J. Biol. Chem.* 280(21):20589-20595.

56. Jacobs FMJ*, et al.* (2003) FoxO6, a Novel Member of the FoxO Class of Transcription Factors with Distinct Shuttling Dynamics. *J. Biol. Chem.* 278(38):35959-35967.

57. Sharma SK*, et al.* (2005) Characterization of a novel Foxa (hepatocyte nuclear factor-3) site in the glucagon promoter that is conserved between rodents and humans. *Biochem J* 389(3):831-841.

58. Biggs WH, Meisenhelder J, Hunter T, Cavenee WK, & Arden KC (1999) Protein kinase B/Akt-mediated phosphorylation promotes nuclear exclusion of the winged helix transcription factor FKHR1. *Proceedings of the National Academy of Sciences of the United States of America* 96(13):7421-7426.

59. Scheimann AO, Durham SK, Suwanichkul A, Snuggs MB, & Powell DR (2001) Role of Three FKHR Phosphorylation Sites in Insulin Inhibition of FKHR Action in Hepatocytes. *Horm Metab Res* 33(11):631-638.

60. Ogawa H, Inouye S, Tsuji FI, Yasuda K, & Umesono K (1995) Localization, trafficking, and temperature-dependence of the Aequorea green fluorescent protein in cultured vertebrate cells. *Proceedings of the National Academy of Sciences of the United States of America* 92(25):11899-11903.

61. Terpe K (2003) Overview of tag protein fusions: from molecular and biochemical fundamentals to commercial systems. (Translated from eng) *Appl Microbiol Biotechnol* 60(5):523-533 (in eng).

62. la Cour T*, et al.* (2003) NESbase version 1.0: a database of nuclear export signals.), pp 393-396.

63. Fukuda M*, et al.* (1997) CRM1 is responsible for intracellular transport mediated by the nuclear export signal. *Nature* 390(6657):308-311.

64. Kudo N*, et al.* (1998) Leptomycin B Inhibition of Signal-Mediated Nuclear Export by Direct Binding to CRM1. *Experimental Cell Research* 242(2):540-547.

65. Wen W, Meinkotht JL, Tsien RY, & Taylor SS (1995) Identification of a signal for rapid export of proteins from the nucleus. *Cell* 82(3):463-473.

66. Monaghan A, Kaestner K, Grau E, & Schutz G (1993) Postimplantation expression patterns indicate a role for the mouse forkhead/HNF-3 alpha, beta and gamma genes in determination of the definitive endoderm, chordamesoderm and neuroectoderm. *Development* 119(3):567-578.

67. Sasaki H & Hogan B (1993) Differential expression of multiple fork head related genes during gastrulation and axial pattern formation in the mouse embryo. *Development* 118(1):47-59.

68. de Wet C & Moss J (1998) METABOLIC FUNCTIONS OF THE LUNG. *Anesthesiology Clinics of North America* 16(1):181-199.

69. Fisher AB (1976) Normal and pathologic biochemistry of the lung. (Translated from eng) *Environ Health Perspect* 16:3-9 (in eng).

70. Nogee LM, de Mello DE, Dehner LP, & Colten HR (1993) Brief report: deficiency of pulmonary surfactant protein B in congenital alveolar proteinosis. (Translated from eng) *N Engl J Med* 328(6):406-410 (in eng).

71. Whitsett JA & Weaver TE (2002) Hydrophobic surfactant proteins in lung function and disease. (Translated from eng) *N Engl J Med* 347(26):2141-2148 (in eng).

72. Hartl D & Griese M (2005) Interstitial lung disease in children - genetic background and associated phenotypes. *Respiratory Research* 6(1):32.

73. Epaud R, Feldmann D, Guillot L, & Clément A (2008) Pathologies respiratoires associées à des anomalies héréditaires du métabolisme du surfactant. *Archives de Pédiatrie* 15(10):1560-1567.

74. Ikeda K, Shaw-White J, Wert S, & Whitsett J (1996) Hepatocyte nuclear factor 3 activates transcription of thyroid transcription factor 1 in respiratory epithelial cells. *Mol. Cell. Biol.* 16(7):3626-3636.

75. Zhou L, Lim L, Costa R, & Whitsett J (1996) Thyroid transcription factor-1, hepatocyte nuclear factor-3beta, surfactant protein B, C, and Clara cell secretory protein in developing mouse lung. *J. Histochem. Cytochem.* 44(10):1183-1193.

76. Bohinski RJ, Di Lauro R, & Whitsett JA (1994) The lung-specific surfactant protein B gene promoter is a target for thyroid transcription factor 1 and hepatocyte nuclear factor 3, indicating common factors for organ-specific gene expression along the foregut axis. *Mol. Cell. Biol.* 14(9):5671-5681.

77. Clevidence DE*, et al.* (1994) Members of the HNF-3/forkhead Family of Transcription Factors Exhibit Distinct Cellular Expression Patterns in Lung and Regulate the Surfactant Protein B Promoter. *Developmental Biology* 166(1):195-209.

78. Bingle CaG, JD (1993) Identification of hepatocyte nuclear factor-3 binding sites in the Clara cell secretory protein gene. *Biochemical Journal* 295:227-232.

79. Wan H*, et al.* (2004) Foxa2 is required for transition to air breathing at birth. *PNAS* 101(40):14449-14454.

80. Movahed M-R, Hashemzadeh M, & Jamal MM (2006) Increased Prevalence of Asthma in Patients with Type II Diabetes Mellitus. *Chest* 130(4):160S-c-.

81. Carroll P & Matz R (1982) Adult respiratory distress syndrome complicating severely uncontrolled diabetes mellitus: report of nine cases and a review of the literature. *Diabetes Care* 5(6):574-580.

82. Davis TME, Knuiman M, Kendall P, Vu H, & Davis WA (2000) Reduced pulmonary function and its associations in type 2 diabetes: the Fremantle Diabetes Study. *Diabetes Research and Clinical Practice* 50(2):153-159.

83. Costa RH, Kalinichenko VV, & Lim L (2001) Transcription factors in mouse lung development and function. *Am J Physiol Lung Cell Mol Physiol* 280(5):L823-838.

84. Livingston EG, Herbert WN, Hage ML, Chapman JF, & Stubbs TM (1995) Use of the TDx-FLM assay in evaluating fetal lung maturity in an insulin-dependent diabetic population. The Diabetes and Fetal Maturity Study Group. *Obstet Gynecol* 86(5):826-829.

85. Piazze JJ*, et al.* (1999) Fetal lung maturity in pregnancies complicated by insulin-dependent and gestational diabetes: a matched cohort study. *European Journal of Obstetrics & Gynecology and Reproductive Biology* 83(2):145-150.

86. Shota Higuchi MK, Kazuhiro Iguchi, Shigeyuki Usui, Tadashi Kiho, Kazuyuki Hirano, (2007) Transcriptional regulation of aquaporin 3 by insulin. *Journal of Cellular Biochemistry* 102(4):1051-1058.

87. Miakotina O, Goss K, & Snyder J (2002) Insulin utilizes the PI 3-kinase pathway to inhibit SP-A gene expression in lung epithelial cells. *Respiratory Research* 3(1):27.

88. Warburton D*, et al.* (2000) The molecular basis of lung morphogenesis. *Mechanisms of Development* 92(1):55-81.

89. Shimomura I*, et al.* (1998) Insulin resistance and diabetes mellitus in transgenic mice expressing nuclear SREBP-1c in adipose tissue: model for congenital generalized lipodystrophy. *Genes & Development* 12(20):3182-3194.

90. De Leon DD*, et al.* (2006) Identification of transcriptional targets during pancreatic growth after partial pancreatectomy and exendin-4 treatment. *Physiol. Genomics* 24(2):133-143.

91. Reynolds SD, Reynolds PR, Pryhuber GS, Finder JD, & Stripp BR (2002) Secretoglobins SCGB3A1 and SCGB3A2 define secretory cell subsets in mouse and human airways. (Translated from eng) *Am J Respir Crit Care Med* 166(11):1498-1509 (in eng).

92. van der Sluis M*, et al.* (2008) Forkhead box transcription factors Foxa1 and Foxa2 are important regulators of Muc2 mucin expression in intestinal epithelial cells. (Translated from eng) *Biochem Biophys Res Commun* 369(4):1108-1113 (in eng).

93. Theologides A (1976) Anorexia-producing intermediary metabolites. *Am J Clin Nutr* 29(5):552-558.

94. Bruning JC*, et al.* (2000) Role of Brain Insulin Receptor in Control of Body Weight and Reproduction. *Science* 289(5487):2122-2125.

95. Burks DJ*, et al.* (2000) IRS-2 pathways integrate female reproduction and energy homeostasis. *Nature* 407(6802):377-382.

96. Niswender KD*, et al.* (2003) Insulin Activation of Phosphatidylinositol 3-Kinase in the Hypothalamic Arcuate Nucleus: A Key Mediator of Insulin-Induced Anorexia. *Diabetes* 52(2):227-231.

97. Schwartz MW, Woods SC, Porte D, Jr., Seeley RJ, & Baskin DG (2000) Central nervous system control of food intake. (Translated from eng) *Nature* 404(6778):661-671 (in eng).

98. Kim M-S*, et al.* (2006) Role of hypothalamic Foxo1 in the regulation of food intake and energy homeostasis. *Nat Neurosci* 9(7):901-906.

99. Rodgers RJ, Ishii Y, Halford JCG, & Blundell JE (2002) Orexins and appetite regulation. *Neuropeptides* 36(5):303-325.

100. Hisayuki Funahashi FT, Jian-Lian Guan, Haruaki Kageyama, Toshihiko Yada, Seiji Shioda, (2003) Hypothalamic neuronal networks and feeding-related peptides involved in the regulation of feeding. *Anatomical Science International* 78(3):123-138.

101. Almind K & Kahn CR (2004) Genetic determinants of energy expenditure and insulin resistance in diet-induced obesity in mice. *Diabetes* 53(12):3274-3285.

102. Biddinger SB*, et al.* (2005) Effects of diet and genetic background on sterol regulatory element-binding protein-1c, stearoyl-CoA desaturase 1, and the development of the metabolic syndrome. *Diabetes* 54(5):1314-1323.

103. Colombo C*, et al.* (2003) Opposite effects of background genotype on muscle and liver insulin sensitivity of lipoatrophic mice. Role of triglyceride clearance. *J Biol Chem* 278(6):3992-3999.

104. Rossmeisl M, Rim JS, Koza RA, & Kozak LP (2003) Variation in type 2 diabetes--related traits in mouse strains susceptible to diet-induced obesity. *Diabetes* 52(8):1958-1966.

105. Kulkarni RN*, et al.* (2003) Impact of genetic background on development of hyperinsulinemia and diabetes in insulin receptor/insulin receptor substrate-1 double heterozygous mice. *Diabetes* 52(6):1528-1534.

106. Baier LJ & Hanson RL (2004) Genetic studies of the etiology of type 2 diabetes in Pima Indians: hunting for pieces to a complicated puzzle. *Diabetes* 53(5):1181-1186.

107. Ravussin E & Bogardus C (2000) Energy balance and weight regulation: genetics versus environment. *Br J Nutr* 83 Suppl 1:S17-20.

108. Yanai H*, et al.* (2006) A Methionine-Rich Domain Mediates CRM1-Dependent Nuclear Export Activity of Borna Disease Virus Phosphoprotein.), pp 1121-1129.

109. Zhang X*, et al.* (2002) Phosphorylation of Serine 256 Suppresses Transactivation by FKHR (FOXO1) by Multiple Mechanisms. DIRECT AND INDIRECT EFFECTS ON NUCLEAR/CYTOPLASMIC SHUTTLING AND DNA BINDING. *J. Biol. Chem.* 277(47):45276-45284.

110. Vogt PK, Jiang H, & Aoki M (2005) Triple layer control: phosphorylation, acetylation and ubiquitination of FOXO proteins. (Translated from eng) *Cell Cycle* 4(7):908-913 (in eng).

111. Calnan DR & Brunet A (The FoxO code. *Oncogene* 27(16):2276-2288.

112. Bingle CD, Hackett BP, Moxley M, Longmore W, & Gitlin JD (1995) Role of hepatocyte nuclear factor-3 alpha and hepatocyte nuclear factor-3 beta in Clara cell secretory protein gene expression in the bronchiolar epithelium. *Biochem J* 308 (Pt 1):197-202.

113. Salton SR, Hahm S, & Mizuno TM (2000) Of mice and MEN: what transgenic models tell us about hypothalamic control of energy balance. (Translated from eng) *Neuron* 25(2):265-268 (in eng).

114. Willie JT, Chemelli RM, Sinton CM, & Yanagisawa M (2001) To eat or to sleep? Orexin in the regulation of feeding and wakefulness. (Translated from eng) *Annu Rev Neurosci* 24:429-458 (in eng).

115. Shimada M, Tritos NA, Lowell BB, Flier JS, & Maratos-Flier E (1998) Mice lacking melanin-concentrating hormone are hypophagic and lean. (Translated from eng) *Nature* 396(6712):670-674 (in eng).

116. Sakurai T*, et al.* (1998) Orexins and orexin receptors: a family of hypothalamic neuropeptides and G protein-coupled receptors that regulate feeding behavior. (Translated from eng) *Cell* 92(5):1 page following 696 (in eng).

117. Bernardis LL & Bellinger LL (1993) The lateral hypothalamic area revisited: neuroanatomy, body weight regulation, neuroendocrinology and metabolism. (Translated from eng) *Neurosci Biobehav Rev* 17(2):141-193 (in eng).

118. Hara J*, et al.* (2001) Genetic ablation of orexin neurons in mice results in narcolepsy, hypophagia, and obesity. (Translated from eng) *Neuron* 30(2):345-354 (in eng).

119. Gomori A*, et al.* (2003) Chronic intracerebroventricular infusion of MCH causes obesity in mice. Melanin-concentrating hormone. (Translated from eng) *Am J Physiol Endocrinol Metab* 284(3):E583-588 (in eng).

120. Ludwig DS*, et al.* (2001) Melanin-concentrating hormone overexpression in transgenic mice leads to obesity and insulin resistance. (Translated from eng) *J Clin Invest* 107(3):379-386 (in eng).

121. Hoppel C, DiMarco JP, & Tandler B (1979) Riboflavin and rat hepatic cell structure and function. Mitochondrial oxidative metabolism in deficiency states. *J. Biol. Chem.* 254(10):4164-4170.

122. Fréneaux E*, et al.* (1988) Inhibition of the mitochondrial oxidation of fatty acids by tetracycline in mice and in man: possible role in microvesicular steatosis induced by this antibiotic. *Hepatology* 8(5):1056-1062.